Cummulative Dissertation

Implications of local and regional processes on the stability of metacommunities in diverse ecosystems

Author:
Markus Stark

A thesis submitted in fulfillment of the requirements
for the degree of Dr. rer. nat. in "Theoretical Ecology"

Group for Ecology and Ecological Modeling
Institute for Biochemistry and Biology
Department of Mathematic and Science
University of Potsdam

Supervisor:
Prof. Dr. Ursula Gaedke
Dr. Christian Guill

Mentor:
Ph.D. Ulrike Schlägel

Examiner:
Prof Dr. Ursula Gaedke
Ph.D. Sonia Kéfi
Prof. Dr. Volker Grimm

Potsdam, October 22, 2021

"My big thesis is that although the world looks messy and chaotic, if you translate it into the world of numbers and shapes, patterns emerge and you start to understand why things are the way they are."

Marcus du Sautoy

"There are only two days in the year that nothing can be done. One is called yesterday and the other is called tomorrow, so today is the right day to love, believe, do and mostly live."

The Dalai Lama

https://doi.org/10.25932/publishup-52639
https://nbn-resolving.org/urn:nbn:de:kobv:517-opus4-526399

Abstract

Anthropogenic activities such as continuous landscape changes threaten biodiversity at both local and regional scales. Metacommunity models attempt to combine these two scales and continuously contribute to a better mechanistic understanding of how spatial processes and constraints, such as fragmentation, affect biodiversity. There is a strong consensus that such structural changes of the landscape tend to negatively effect the stability of metacommunities. However, in particular the interplay of complex trophic communities and landscape structure is not yet fully understood.

In this present dissertation, a metacommunity approach is used based on a dynamic and spatially explicit model that integrates population dynamics at the local scale and dispersal dynamics at the regional scale. This approach allows the assessment of complex spatial landscape components such as habitat clustering on complex species communities, as well as the analysis of population dynamics of a single species. In addition to the impact of a fixed landscape structure, periodic environmental disturbances are also considered, where a periodical change of habitat availability, temporally alters landscape structure, such as the seasonal drying of a water body.

On the local scale, the model results suggest that large-bodied animal species, such as predator species at high trophic positions, are more prone to extinction in a state of large patch isolation than smaller species at lower trophic levels. Increased metabolic losses for species with a lower body mass lead to increased energy limitation for species on higher trophic levels and serves as an explanation for a predominant loss of these species. This effect is particularly pronounced for food webs, where species are more sensitive to increased metabolic losses through dispersal and a change in landscape structure. In addition to the impact of species composition in a food web for diversity, the strength of local foraging interactions likewise affect the synchronization of population dynamics. A reduced predation pressure leads to more asynchronous population dynamics, beneficial for the stability of population dynamics as it reduces the risk of correlated extinction events among habitats. On the regional scale, two landscape aspects, which are the mean patch isolation and the formation of local clusters of two patches, promote an increase in β-diversity. Yet, the individual composition and robustness of the local species community equally explain a large proportion of the observed diversity patterns. A combination of periodic environmental disturbance and patch isolation has a particular impact on population dynamics of a species. While the periodic disturbance has a synchronizing effect, it can even superimpose emerging asynchronous dynamics in a state of large patch isolation and unifies trends in synchronization between different species communities.

In summary, the findings underline a large local impact of species composition and interactions on local diversity patterns of a metacommunity. In comparison, landscape structures such as fragmentation have a negligible effect on local diversity patterns, but increase their impact for regional diversity patterns. In contrast, at the level of population dynamics, regional characteristics such as periodic environmental disturbance and patch isolation have a particularly strong impact and contribute substantially to the understanding of the stability of population dynamics in a metacommunity. These studies demonstrate once again the complexity of our ecosystems and the need for further analysis for a better understanding of our surrounding environment and more targeted conservation of biodiversity.

Zusammenfassung

Folgen von lokalen und regionalen Prozessen auf die Stabilität von Metagemeinschaften

Seit geraumer Zeit prägt der Mensch seine Umwelt und greift in die Struktur von Landschaften ein. In den letzten Jahrzehnten wurde die Landschaftsnutzung intensiviert und Ökosyteme weltweit anthropogen überprägt. Solche Veränderungen der Landschaft sind mit Verantwortlich für den derzeit rapiden Verlust an Biodiversität auf lokaler wie regionaler Ebene. Metagemeinschafts-Modelle versuchen diese beiden Ebenen zu kombinieren und kontinuierlich zu einem besseren mechanistischen Verständnis beizutragen, wie räumliche Prozesse, so z. B. Fragmentierung von Biotopen, die Biodiversität beeinflussen. Es besteht dabei ein großer Konsens, dass sich solche Änderungen der Landschaft tendenziell negativ auf die Stabilität von Metagemeinschaften auswirken. Jedoch ist insbesondere das Zusammenspiel von komplexen trophischen Gemeinschaften und räumlichen Prozessen längst nicht vollständig verstanden.

In der vorliegenden Arbeit wird ein Metagemeinschafts-Modellansatz verwendet, der auf einem dynamischen und räumlich expliziten Modell basiert, das Populationsdynamiken auf der lokalen Ebene und Migrationsdynamiken auf der regionalen Ebene integriert. Dieser Ansatz erlaubt die Bewertung komplexer räumlicher Landschaftskomponenten wie z. B. die Auswirkung von Habitatsclustern auf Populationsdynamiken einzelner Arten bis hin zur Diversität komplexer Artengemeinschaften. Zusätzlich zum Einfluss von einzelner konstanter räumlicher Strukturen werden auch periodische Umweltstörungen berücksichtigt, bei der ein Wechsel der Habitatverfügbarkeit, die räumliche Struktur der Landschaft temporär verändert, wie z. B. die Austrocknung eines Gewässers.

Auf der lokalen Ebene deuten die Modellergebnisse darauf hin, dass Tierarten mit einer großen Körpermasse, wie z. B. Raubtierarten in höheren trophischen Positionen, in einem Zustand großer Habitat-Isolation stärker vom Aussterben bedroht sind, als Arten mit geringer Körpermasse auf unteren trophischen Ebenen. Arten mit einer geringerer Körpermasse haben einen erhöhten metabolischen Verlust, der zu einer Energielimitierung auf den höheren trophischen Ebenen führt. Dies kann eine Erklärung dafür sein, dass Arten mit großer Körpermasse ein höheres Aussterberisiko

in den Modellergebnissen aufweisen. Dieser Effekt ist vor allem in Nahrungsnetzen ausgeprägt, bei denen Arten empfindlicher auf metabolische Verluste durch Migration und eine Veränderung der Habitat Struktur reagieren. Neben der Bedeutung der Zusammensetzung der Arten eines Nahrungsnetzes für die Diversität, haben lokale Fraßinteraktionen ebenfalls Auswirkungen auf die Synchronisierung von Populationsdynamiken. Ein geringerer Fraßdruck führt zu mehr asynchronen Populationsdynamiken, die diese Dynamiken einer Metapopulation stabilisiert, sodass das Risiko von Aussterbeereignissen einzelner Arten sinkt. Auf der regionalen Ebene führen als landschaftliche Aspekte, neben der mittleren Habitat-Isolation, ebenso die Bildung von lokalen Clustern aus zwei Habitaten zu einer Zunahme der Beta-Diversität. Jedoch erklären die individuelle Zusammensetzung und Robustheit der lokalen Arten- gemeinschaft gleichermaßen einen großen Anteil der zu beobachteten Diversitätsmuster. Eine Kombination aus periodischen Umweltstörungen und Habitat-Isolation hat insbesondere einen Einfluss auf die Populationsdynamiken einzelner Arten. Populationsdynamiken können durch periodische Umweltstörungen synchronisiert werden, und dabei die sonst auftauchende asynchronen Populationsdynamiken bei einer größeren Habitat-Isolation überlagern. Die dadurch vereinheitlichen Trends in der Synchronisierung erhöhen das Risiko korrelierter Aussterbeereignisse einer Art.

Zusammenfassend lassen sich zwei große Einflussfaktoren auf die lokalen Diversitätsmuster der Metagemeinschaften feststellen. Zum Einen die lokale Artenzusammensetzung und zum Anderen die Interaktionen der Arten. Im Vergleich dazu, haben räumliche Komponenten wie die Fragmentierung der Landschaft einen vernachlässigbaren Einfluss auf die lokalen Diversitätsmuster und gewinnen erst für regionale Diversitätsmuster an Gewicht. Im Gegensatz dazu spielen auf der Ebene der Populationsdynamik besonders regionale Eigenschaften, wie die periodische Umweltstörung und Habitat-Isolation, eine Rolle und tragen wesentlich zum Verständnis der Stabilität von Populationsdynamiken der Metagemeinschaft bei. Diese Untersuchungen zeigen einmal mehr die Komplexität unserer Ökosysteme und die Notwendigkeit weiterer Analysen für ein besseres Verständnis unserer umgebenen Umwelt und gezielteren Schutz der Biodiversität.

Acknowledgements

A huge thanks for all those who supported me and most importantly made me laugh during these now almost four years of dissertation.

First and foremost, I would like to express my sincere gratitude to my supervisor Christian Guill for his guidance, support and coordination of the project. In professional and also private conversations you were a good interlocutor and advisor and with your patience I got through the time well.

This doctoral thesis was written in the research group Networks on Networks, where I got to know a great network of scientists, from my co-authors Remo, Johanna, Björn Rall and Ulrich Brose, to all the participants of the research group, to the invited guests of our joint meetings. I already miss the Waldschlösschen, the beer and wine rounds and especially Korinna's Hacky Sack.

This dissertation wouldn't have been possible without the support of the Ecology and Ecosystem Modeling Group and I would like to thank Prof. Ursula Gaedke for her support and encouraging attitude. There are many great and beautiful first acquaintances I remember, some of which developed into wonderful friendships. I miss the rounds of Doppelkopf, exciting Kicker matches and evenings of games and beer together. Special thanks to Ruben, Sarah B., Claudia, Victor, Moritz and Pierluigi for a terrific office atmosphere. Another thanks to Stefan for his technical support and patience. And a big thanks to many more people at the institute: Toni, Ellen, Elias, Michael & Larissa, Jasmina, Julia, Janne, Dominique, Xenia, Vanessa and more.

A grateful thank you to everyone who helped me proofread this paper - especially Remo and Martin.

Great gratitude to my whole family including aunts and cousins for their encouragements and motivation. Thanks to the Eppelheim crew and cheers to more great races together.

A big hug to my dear Benni and Lisa, I love your direct and warm way. Sporty greetings to Max and Jens in Schöneberg you two Schnuckel. Thanks to Slawa, Christof and Kelsey for your great and musical-sporty way. A big hug to Daniel and Momo for being such lovely and artful people and to Ruben and Charlotte for wonderful shared moments and getting new perspectives.

And kisses to my Darling Sarah who makes my life a happier place - you charm me!

Contents

Abstract **iii**

Acknowledgements **vii**

1 General Introduction **1**

1.1 Metacommunities in Ecology 1

1.2 Regional complexity 3

1.3 Local complexity 6

1.4 Modelling species interactions 8

1.5 Thesis overview 10

2 Effects of number of patches and patch isolation on diversity patterns **21**

3 Interplay of temporal patch availability and patch isolation on population dynamics **45**

4 Comparison of local and regional scale processes on observed trends in $\bar{\alpha}$- and β-diversity **73**

5 General Discussion **101**

5.1 From metacommunities to meta-food webs 101

5.1.1 Local trophic interactions form metacommunities 102

5.1.2 Few landscape characteristics matter for metacommunities 105

5.2 Metacommunities in temporal changing landscape structures 108

5.3 Perspectives - metacommunities in a globally changing world 111

A Supplementary material to Chapter 2 **117**

B Supplementary material to Chapter 3 **143**

C Supplementary material to Chapter 4 **151**

Declaration of Authorship **167**

Chapter 1

General Introduction

A serious biodiversity decline threatens species communities worldwide (Pimm et al., 2014). The Millennium Report (Assessment, 2005) identified major causes for this ongoing decline including habitat change, climate change, invasive species, over-exploitation and pollution. While each of these causes contribute to the biodiversity decline, the magnitude of their impact varies depending on the ecosystem and local conditions. By assessing the impact of individual causes on the coexistence of species communities, on both local and regional scales, we gain a better understanding of critical metacommunity processes and can develop more targeted biodiversity conservation strategies in the future.

1.1 Metacommunities in Ecology

In ecology, metacommunities refer to species communities that interact with each other on a local and a regional scale (Figure 1.1), with a variety of processes influencing species composition and distribution. At the local scale, ecological processes such as intra- and interspecific competition or trophic interactions are known to play a key role in structuring the composition of a local community (Connell, 1971, 1978; Tilman, 1982). These processes are the local basis for the coexistence of a diverse species community. At the regional scale, landscape-level processes such as landscape fragmentation, seasonality of environmental conditions, or habitat loss affect the distribution and interaction between different species and thus structure metacommunities (Cuesta et al., 2017). The interaction between local and regional scales can be illustrated based on the example of dispersal limitation. Empirical experiments (e.g. Burke and Nol (1998); Tilman (1997)) demonstrate that species local diversity (local species richness) increases if dispersal rates are high (less dispersal limitation), but there is still a strong selection pressure on the local scale due to interspecific competition and soil conditions. Therefore, an approach considering both scales is needed to understand which regional and local processes support the persistence and diversity of species communities (Leibold and Chase, 2017).

Dispersal in metacommunities

Dispersal is a complex process, linking the local and regional scale of a metacommunity. Causes and effects of dispersal are species-specific ranging from the individual behavioral level to synchronized passive wind dispersal and act on the two different scales (Bowler and Benton, 2005; Schlägel et al., 2020). Local interactions between species, such as predation pressure or competition within a habitat, are drivers for species to leave or stay in a patch (Bowler and Benton, 2005). At the regional scale, species have further developed capabilities to adapt to e.g. changing resource availability of a landscape and adjust their dispersal accordingly (García et al., 2011). As a result, a tremendous variety of dispersal strategies have evolved based on individual species properties in response to changing local and regional conditions.

Despite this, there are successful theoretical approaches trying to predict a general relationship between dispersal rate (used here as a proxy for patch isolation or distance among patches) and species local diversity, which assume a unimodal pattern (Cadotte et al., 2006). The latter is based on the following reasoning: If the rate of dispersal for a species is limited, then the species is more isolated and can be restricted to fewer resources or cannot be rescued through recolonization (Gotelli, 1991). This explains the differences in the local diversity of plant communities between mainland and isolated islands (Kreft et al., 2008). Yet, when dispersal rates are high, the synchronization of population dynamics between habitat patches increases the risk of correlated extinctions for a species in multiple patches (Gouhier et al., 2010), or may enhance regional competition and decrease diversity (Matthiessen et al., 2010). Consequently, intermediate dispersal rates are supposed to be the most beneficial for species local diversity (Mouquet and Loreau, 2002). However, the difficulty of empirical measurements and a lack of empirical examples make it challenging to verify this hypothesis (LeCraw et al., 2014).

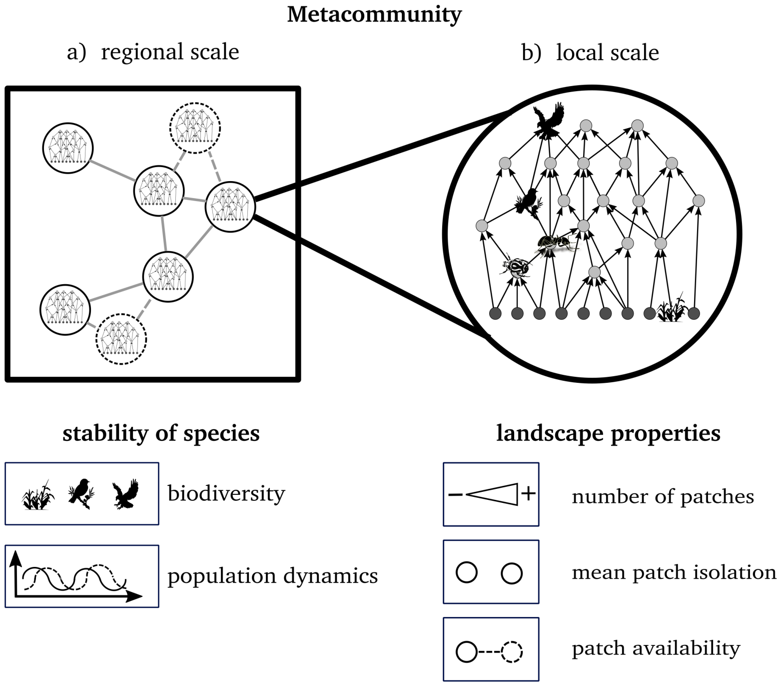

FIGURE 1.1: a) A schematic example of a spatial network of habitat patches where each habitat comprise a network of species interactions forming a meta-food web. b) Simplified schematic example of a local food web comprising the local species interactions. The impact of landscape properties, such as mean patch isolation, the number of patches, and patch availability, on metacommunities is evaluated by two measures of stability. First, a measure for biodiversity that evaluates the persistence of species at local and regional scale and, second, a measure quantifying population dynamics also at local and regional scale. - Solid lines: dispersal links among patches constantly available for species; Dashed lines: dispersal links among patches temporally available for species; Solid circle: constantly available patch for species; Dashed circle: temporally available patch for species;

1.2 Regional complexity

Spatial processes in a metacommunity can influence the coexistence of predator and prey species. For example, early classic experiments show that integrating dispersal for a predator and prey species compared to a non-spatial approach allows both species to coexist, which is even further stabilized by larger dispersal rates for the prey species (Hastings, 1977; Huffaker, 1958). However, whether spatial complexity has a stabilizing or destabilizing effect usually depends on more than a single process (Amarasekare, 2008; Leibold and Chase, 2017). For instance, the dispersal rates of both predator and prey species, the patch arrangements of a landscape, the strategy of dispersal, and fluctuations of the environment can all affect coexistence in a species community (Altermatt and Holyoak, 2012; Cooper et al.; Fahrig, 2003; Gouhier et al., 2010; Gramlich et al., 2016; Haegeman and Loreau, 2014).

Structure of landscapes

A key component influencing biodiversity and population dynamics is the structure and configuration of landscapes. Initial theoretical approaches on metacommunities considered few habitats with regular spatial structures such as rectangular grids or symmetrical habitat structures (e.g. Briggs and Hoopes (2004)). Over time it has been recognized that the geometric position of a habitat and its local environment both have an impact on a metacommunity: For example, that local clustering of habitats can increase regional diversity (Altermatt and Holyoak, 2012). Thus a more realistic approach to studying the impact of complex landscapes is to include the explicit positions of habitats, such as in a random geometric graph (RGG) (Penrose, 2003), that is used in Chapters 2 & 3 & 4 to generate the spatial structure. A use of RGGs allows to consider additional ecologically relevant aspects like the effects of the number of patches, mean patch isolation or other landscape attributes commonly evaluated in conservation studies (Fahrig, 2003; Lindborg and Eriksson, 2004; Urban and Keitt, 2001). Analyzing these attributes is more urgent than ever, especially due to the ever increasing impact human activities have on the landscape resulting in eutrophication, habitat loss, and habitat fragmentation (Foley et al., 2005).

Fragmentation of landscapes

While there is an overwhelming amount of evidence for the negative impact of habitat loss on biodiversity, the effects of habitat fragmentation on biodiversity are still subject of intense debate (Fahrig et al., 2019; Fletcher et al., 2018). According to Fahrig (2003), fragmentation per se includes three main components: the number of patches, patch size and patch isolation (while the total area of habitats remains constant). It is difficult to empirically analyze the effects of the individual components of fragmentation per se, because the individual components alone typically have a weaker effect on biodiversity and also because habitat fragmentation often appears in conjunction with habitat loss (Didham et al., 2012). Furthermore, patch isolation, for example, has been shown to have positive as well as negative effects on biodiversity (Fahrig, 2003, 2017) which makes it even more difficult to get a clear picture of the effect of a single component. A theoretical and simulation based model can help to overcome these difficulties (but see also Hadley and Betts (2016) for empirical approaches), because it allows for independent manipulation of patch isolation, number of patches and other landscape attributes and contribute to a comprehensive overview of their impact (see Figure 1.1).

Environmental fluctuations

Environmental fluctuations can have a direct effect on the population dynamics of a species, and can also implicitly impact landscape structures. For example, correlated periodic fluctuations that occur as changes in the ambient temperature or resource availability can alter demographic rates of species and can ultimately synchronize patch dynamics (Kahilainen et al., 2018; Koenig, 1999; Ranta et al., 1995). While a synchronization of population dynamics does not imply a direct limitation for a species, the same environmental fluctuations can also modify the availability of patches as habitable areas, thus temporally decreasing the number of patches (changing mean patch isolation) and limiting the availability of resources (Wellborn et al., 1996). An empirical example of such changes in a landscape, where both a temporally fluctuating environment and distinct spatial structure strongly influence ecological communities, are kettle holes in formerly glaciated regions (Kalettka and Rudat, 2006). These small pools filled with water are typically found in larger clusters, and seasonal changes in temperature and precipitation cause some of them to be temporally water-filled. If the pools run dry, the aquatic community becomes temporally extinct. Later recolonization is possible through a reimmigration of species from other permanent pools (De Meester et al., 2005). Since the process of recolonization is often temporally correlated to the onset of a rainy season, a synchronizing effect of reimmigration on population dynamics is expected. However, this is only feasible if a sufficient large number of permanent patches is available and patch isolation allows for high enough dispersal rates for a recolonization.

1.3 Local complexity

Population dynamics are an ubiquitous phenomenon and their regularity and empirical observation has fascinated ecologists for generations. Population dynamics can be further divided into subcategories: chaotic, cyclic and stationary dynamics. The different types of population dynamics have strong implications on the stability of a local species. While it is difficult to predict and analyze chaotic dynamics, analysis of a population exhibiting cyclic dynamics shows an increased risk of stochastic extinction at their local biomass minima (Pimm et al., 1988). In comparison, the risk of extinction is on average lower for a species with a stationary biomass density.

One of the first descriptions of cyclic dynamics was a lynx-hare cycle in which regular variations in capture rates were observed over a period of several years (Elton and Nicholson, 1942). Since then, such population dynamics have been observed in a range of aquatic and terrestrial habitats, and studied using simple models such as the Lotka-Volterra model (Lotka, 1925; Volterra, 1926) or the Rosenzweig-MacArthur model (Rosenzweig and MacArthur, 1963). Despite different model approaches, the consistent results on population dynamics demonstrate the interdependency of two key factors: External factors such as resource availability within a habitat, and biotic interactions between species such as predation (Berryman, 2002).

A rather recent approach tries to delineate population dynamics of metacommunities at the local and regional scale analogously to the distinction between α-, β and γ-diversity (Whittaker, 1972): local dynamics are determined using a modified measure of the coefficient of variation (α-variability), regional differences describe the synchrony of dynamics (β-variability), and regional dynamics are described by the overall variability (γ-variability) of the dynamics of a species (Wang and Loreau, 2014). This approach provides a comprehensive analysis of population dynamics with a comparison of local and spatial scale effects for a single and multiple species. Further, it provides a different perspective on the stability of a species community from the local level of population dynamics rather than species persistence (see Chapter 3). Thus, the stability of metacommunities can be examined from multiple perspectives, which is necessary to understand the complexity of an ecosystem's response to disturbances (Radchuk et al., 2019).

Synchronization of population dynamics

A common way to analyze and compare population dynamics is to evaluate the synchronization of metapopulation dynamics. Highly synchronized metapopulation dynamics are destabilizing, as there are larger variations in the amount of total biomass densities increasing the risk of a joint extinction event. In contrast, asynchronous dynamics between patches are beneficial and increase stability, for example, the possibility of a rescue effect or the portfolio effect (Blasius et al., 1999; Schindler et al., 2015; Thorson et al., 2018). The spatial portfolio effect assesses the total biomass fluctuations of a species for an increasing number of habitat patches. Empirical observations often demonstrate a decrease in total biomass fluctuations for a larger number of patches due to asynchronous biomass dynamics among them. While an increased number of patches can support stability, the structure of the landscape can also destabilize dynamics. A lower mean patch isolation (higher dispersal rates) can cause the opposite trend leading to habitat synchronization (Jansen, 2001; Sherratt et al., 2000). These contrasting trend directions make applications particularly relevant where both patch number and patch isolation are involved e.g. in the context of fragmentation per se.

In addition to the structure of the landscape, dispersal strategies of a given species can alter the synchronization between patches. For example, a density-dependent dispersal strategy of species can have a stabilizing effect, by generating a larger proportion of asynchronous dynamics (Abrams and Ruokolainen, 2011). Other theoretical approaches indicate also an impact of energetic loss during dispersal or intra- and interspecific density-dependent dispersal (Hauzy et al., 2010).

Trophic interactions & trophic cascading

The absence of a predator species and the accompanying top-down processes can strongly affect the distribution of species in a metacommunity. The local presence of a predator species and its selectivity on prey species can directly alter prey diversity by decreasing competition between prey species (Terborgh, 2015). Particular empirical relevance of predator distribution is derived from small islands or lakes with naturally fewer predator species. With fewer species interactions on average, top down control can be of great relevance there and explain the community structure (Leibold and Chase, 2017; Wellborn et al., 1996). Apart from a strong community dependence on the extent of top down control, the food chain length and the interaction pathways are of importance (Thakur and Eisenhauer, 2015; Wollrab et al., 2012).

In the case of an extinction event, top down control of a predator species can have dramatic negative effects on local diversity depending on the robustness of the species community and its respective food web. The loss of a species can cause secondary extinction events, induced by trophic cascading which propagates through the food web, decreasing the corresponding local diversity (Dunne et al., 2002; Srinivasan et al., 2007). With increasing climate and habitat change, such local extinctions of a species become more likely, and can increase the probability of further secondary extinction events. For instance, such negative effects are observed in studies demonstrating that a greater mean patch isolation results in a lower mean food chain length, suggesting a less complex metacommunity (LeCraw et al., 2014).

Bistability in ecosystems

Another phenomenon responsible for differences in local dynamics is the occurrence of multiple attractors. From theoretical approaches is known that interactions of three species are already sufficient to allow the emergence of two different stable states with different properties (Jansen, 1995), such as a low and high productive attractor (Ceulemans et al., 2019). Such multi-stabilities are regularly reported in theoretical models and empirically observed in ecosystems, and their relevance can be exemplified by the hysteresis effect (Scheffer et al., 1993). It describes how a small perturbation of a system can lead to a switch towards the second stable state, but a much larger effort is needed to return the system back to its original state. We observe such hysterises for example in aquatic ecosystems, where eutrophication turns a lake from a macrophyte dominated system to an algae dominated system (Ibelings et al., 2007). In order to get back to a state of macrophyte dominance, through reoligotrophication of the lake, the amount of nutrients must be reduced to a much lower level than before.

1.4 Modelling species interactions

A species rich and diverse community consists of a multitude of species, and can range from simple food chains to complex food webs. The first assumption about the stability of such local communities was that the more species a habitat contains and the higher the diversity, the more stable the community (MacArthur, 1955). However, it became apparent that the stability of a community could not depend on the number of interactions alone and that additional properties of a food web also have an effect on its stability (May, 1972). Given this discrepancy and knowledge gap, specific relevant properties and model classes gradually emerged, for example, describing species niches, weighting interactions, and considering energy fluxes, thereby creating complex species interactions networks (Banasek-Richter et al., 2009; Boit et al., 2012; Brose et al., 2006; Williams and Martinez, 2000). Based on these principles, the created model networks can resemble and more accurately describe properties of empirical food webs (Riede et al., 2011).

Allometric trophic network models

In the field of ecology, the allometric trophic network (ATN) approach is a widely applied class of models. The model focuses on consumer-resource interactions balancing the consumption and energy losses of consumer species and production of autotroph species through ordinary differential equations (ODE). Initially introduced as a two species food chain (Yodzis and Innes, 1992), it has been continuously developed and refined to consider higher number of species (Williams and Martinez, 2004) or plant-nutrient dynamics (Brose et al., 2005). The resulting clear hierarchical structure with multiple trophic levels is well suited to study and compare different properties of the food web, which can represent a complex network of interactions between species (Martinez, 2020; Thompson et al., 2012). Another main mechanism and strength of this approach is the incorporation of metabolic rates, based on body size of the species, which is derived from empirical measurements and can be adapted continuously. With these fundamentals, ATN models have evolved in different directions ranging from applied models for fisheries (Kuparinen et al., 2016), to models of ecosystem functions (Schneider et al., 2016) and models of plant pollinator applications (Hale et al., 2020). As the applied models mentioned above, the ATN model of Schneider et al. (2016) used in Chapters 2 - 4 was specifically spatially extended to allow dispersal of species, and enable to study effects of the spatial structure on metacommunities (see Figure 1.1).

1.5 Thesis overview

The following three Chapters examine how attributes of a landscape on local scale and in particular on regional scale explain metacommunity responses for population dynamics and diversity [see Figure 1.1]. The spatially explicit approach allows to examine landscape aspects as complex spatial networks for a very large metacommunity. Further, an integration of temporally changing landscapes enables a comparison of the extent of impact of an external environmental disturbances on a species community.

Chapter 2

I investigate in Chapter 2 how two aspects of habitat fragmentation, namely the number of habitat patches and patch isolation, affect the diversity of a food web model, forming a large metacommunity. The main results emphasize that species on higher trophic levels are more prone to extinction caused by a large mean patch isolation than species on lower trophic levels. I attribute the increased loss of species on higher trophic levels to two effects. First, a higher biomass loss for dispersal with increasing mean patch isolation. Second, due to energy limitation in highly fragmented landscapes, whereby higher trophic levels cannot survive.

Chapter 3

In Chapter 3, the focus shifts from effects on diversity towards the stability of population dynamics. I analyze a simple three species food chain, and evaluate how a landscape process, the effect of mean patch isolation, and a temporal process, the effect of periodic environmental disturbances, have an impact on the dynamics. The results show an expected relationship of higher synchronization of dynamics and lower mean patch isolation. However, a bistability of dynamics indicate also a relevance of biotic interactions and dispersal strategies on the state of synchronization. Further, the impact of periodic environmental disturbances can overrule the trends for the observed effects of mean patch isolation and aligns trends in dynamics.

Chapter 4

Based on the results of Chapter 2, I investigate in more detail which local and regional components can explain patterns for $\bar{\alpha}$-diversity and β-diversity. Using a random forest approach, I show that the trends for $\bar{\alpha}$-diversity depend mainly on the local robustness of the respective food web and, surprisingly, to a very small extent on regional mean patch isolation. In contrast, trends for β-diversity are explained to a large extent by two regional predictors, mean patch isolation and minimum distance to the nearest neighbor, but the local food web robustness also is a major driver of the observed patterns.

Bibliography

P. A. Abrams and L. Ruokolainen. How does adaptive consumer movement affect population dynamics in consumer–resource metacommunities with homogeneous patches? *J Theor Biol*, 277(1):99 – 110, 2011. ISSN 0022-5193. doi: 10.1016/j.jtbi.2011.02.019.

F. Altermatt and M. Holyoak. Spatial clustering of habitat structure effects patterns of community composition and diversity. *Ecology*, 93(5):1125–1133, 2012. doi: 10.1890/11-1190.1.

P. Amarasekare. Spatial dynamics of foodwebs. *Annu Rev Ecol Evol Syst*, 39:479–500, 2008. doi: 10.1146/annurev.ecolsys.39.110707.173434.

M. E. Assessment. Ecosystems and human well-being: Biodiversity synthesis. *World Resources Institute*, 2005.

C. Banasek-Richter, L. Bersier, M. Cattin, R. Baltensperger, J. Gabriel, Y. Merz, R. Ulanowicz, A. Tavares, D. Williams, P. de Ruiter, K. Winemiller, and R. Naisbit. Complexity in quantitative food webs. *Ecology*, 90(2):1470–7, 2009. doi: 10.1890/08-2207.1.

A. Berryman. *Population Cycles: Causes and analyses*. Oxford University Press, Oxford (United Kingdom), 2002.

B. Blasius, A. Huppert, and L. Stone. Complex dynamics and phase synchronization in spatially extended ecological systems. *Nature*, 399:354 – 359, 1999. doi: 10.1038/20676.

A. Boit, N. D. Martinez, R. J. Williams, and U. Gaedke. Mechanistic theory and modelling of complex food-web dynamics in lake constance. *Ecol Lett*, 15(6):594–602, 2012. doi: https://doi.org/10.1111/j.1461-0248.2012.01777.x.

D. E. Bowler and T. G. Benton. Causes and consequences of animal dispersal strategies: relating individual behaviour to spatial dynamics. *Biol Rev*, 80(2):205–225, 2005. doi: 10.1017/S1464793104006645.

C. J. Briggs and M. F. Hoopes. Stabilizing effects in spatial parasitoid–host and predator–prey models: a review. *Theor Popul Biol*, 65(3):299 – 315, 2004. doi: 10.1016/j.tpb.2003.11.001.

U. Brose, L. Cushing, E. L. Berlow, T. Jonsson, C. Banasek-Richter, L.-F. Bersier, J. L. Blanchard, T. Brey, S. R. Carpenter, M.-F. C. Blandenier, J. E. Cohen, H. A. Dawah, T. Dell, F. Edwards, S. Harper-Smith, U. Jacob, R. A. Knapp, M. E. Ledger, J. Memmott, K. Mintenbeck, J. K. Pinnegar, B. C. Rall, T. Rayner, L. Ruess, W. Ulrich, P. Warren, R. J. Williams, G. Woodward, P. Yodzis, and N. D. Martinez. Body sizes of consumers and their resources. *Ecology*, 86(9):2545–2545, 2005. doi: https://doi.org/10.1890/05-0379.

U. Brose, R. J. Williams, and N. D. Martinez. Allometric scaling enhances stability in complex food webs. *Ecol Lett*, 9(11):1228–1236, November 2006. doi: 10.1111/j.1461-0248.2006.00978.x.

D. M. Burke and E. Nol. Influence of food abundance, nest-site habitat, and forest fragmentation on breeding ovenbirds. *The Auk*, 115(1):96–104, 1998. doi: https://doi.org/10.2307/4089115.

M. Cadotte, A. E. M. Loreau, and E. J. B. Losos. Dispersal and species diversity: A meta-analysis. *Am Nat*, 167(6):913–924, 2006. doi: 10.1086/504850.

R. Ceulemans, U. Gaedke, T. Klauschies, and C. Guill. The effects of functional diversity on biomass production, variability, and resilience of ecosystem functions in a tritrophic system. *Sci Rep*, 9(7541), 2019. doi: 10.1038/s41598-019-43974-1.

J. H. Connell. *On the Role of Natural Enemies in Preventing Competitive Exclusion in Some Marine Animals and in Rain Forest Trees. In: Den Boer, P.J. and Gradwell, G.R., Eds., Dynamics of Populations*. Centre for Agricultural Publishing and Documentation, Wageningen, Netherlands, 1971.

J. H. Connell. Diversity in tropical rain forests and coral reefs. *Science*, 199(4335):1302–1310, 1978. doi: 10.1126/science.199.4335.1302.

J. K. Cooper, J. Li, and D. J. S. Montagnes. Intermediate fragmentation per se provides stable predator-prey metapopulation dynamics. *Ecol Lett*, 15(8):856–863. doi: https://doi.org/10.1111/j.1461-0248.2012.01808.x.

F. Cuesta, P. Muriel, L. D. Llambí, S. Halloy, N. Aguirre, S. Beck, J. Carilla, R. I. Meneses, S. Cuello, A. Grau, L. E. Gámez, J. Irazábal, J. Jácome, R. Jaramillo, L. Ramírez, N. Samaniego, D. Suárez-Duque, N. Thompson, A. Tupayachi, P. Viñas, K. Yager, M. T. Becerra, H. Pauli, and W. D. Gosling. Latitudinal and altitudinal patterns of plant community diversity on mountain summits across the tropical andes. *Ecography*, 40(12):1381–1394, 2017. doi: 10.1111/ecog.02567.

L. De Meester, S. Declerck, R. Stoks, G. Louette, F. Van De Meutter, T. De Bie, E. Michels, and L. Brendonck. Ponds and pools as model systems in conservation biology, ecology and evolutionary biology. *Aquat Conserv Mar Freshw Ecosyst*, 15(6):715–725, 2005. doi: 10.1002/aqc.748.

R. K. Didham, V. Kapos, and R. M. Ewers. Rethinking the conceptual foundations of habitat fragmentation research. *Oikos*, 121:161–170, 2012. doi: 10.1111/j.1600-0706.2011.20273.x.

J. A. Dunne, R. J. Williams, and N. D. Martinez. Food-web structure and network theory: The role of connectance and size. *PNAS*, 99(20):12917–12922, 2002.

C. Elton and M. Nicholson. The ten-year cycle in numbers of the lynx in canada. *J Anim Ecol*, 11(2):215–244, 1942. doi: 10.2307/1358.

L. Fahrig. Effects of habitat fragmentation on biodiversity. *Ann Rev Ecol Evol Syst*, 34 (1):487–515, 2003. doi: 10.1146/annurev.ecolsys.34.011802.132419.

L. Fahrig. Ecological responses to habitat fragmentation per se. *Ann Rev Ecol Evol and Syst*, 48(1):1–23, 2017. doi: 10.1146/annurev-ecolsys-110316-022612.

L. Fahrig, V. Arroyo-Rodríguez, J. R. Bennett, V. Boucher-Lalonde, E. Cazetta, D. J. Currie, F. Eigenbrod, A. T. Ford, S. P. Harrison, J. A. Jaeger, N. Koper, A. E. Martin, J.-L. Martin, J. P. Metzger, P. Morrison, J. R. Rhodes, D. A. Saunders, D. Simberloff, A. C. Smith, L. Tischendorf, M. Vellend, and J. I. Watling. Is habitat fragmentation bad for biodiversity? *Biol Conserv*, 230:179 – 186, 2019. ISSN 0006-3207. doi: 10.1016/j.biocon.2018.12.026.

R. J. Fletcher, R. K. Didham, C. Banks-Leite, J. Barlow, R. M. Ewers, J. Rosindell, R. D. Holt, A. Gonzalez, R. Pardini, E. I. Damschen, F. P. Melo, L. Ries, J. A. Prevedello, T. Tscharntke, W. F. Laurance, T. Lovejoy, and N. M. Haddad. Is habitat fragmentation good for biodiversity? *Biol Conserv*, 226:9 – 15, 2018. ISSN 0006-3207. doi: 10.1016/j.biocon.2018.07.022.

J. A. Foley, R. DeFries, G. P. Asner, C. Barford, G. Bonan, S. R. Carpenter, F. S. Chapin, M. T. Coe, G. C. Daily, H. K. Gibbs, J. H. Helkowski, T. Holloway, E. A. Howard, C. J. Kucharik, C. Monfreda, J. A. Patz, I. C. Prentice, N. Ramankutty, and P. K. Snyder. Global consequences of land use. *Science*, 309(5734):570–574, 2005. doi: 10.1126/science.1111772.

D. García, R. Zamora, and G. C. Amico. The spatial scale of plant-animal interactions: effects of resource availability and habitat structure. *Ecol Monogr*, 81(1):103–121, 2011. doi: 10.1890/10-0470.1.

N. J. Gotelli. Metapopulation models: The rescue effect, the propagule rain, and the core-satellite hypothesis. *Am Nat*, 138(3):768–776, 1991. doi: 10.2307/2462468.

T. Gouhier, F. Guichard, and A. Gonzalez. Synchrony and stability of food webs in metacommunities. *Am Nat*, 175(2):E16–E34, 2010. doi: 10.1086/649579. PMID: 20059366.

P. Gramlich, S. Plitzko, L. Rudolf, B. Drossel, and T. Gross. The influence of dispersal on a predator–prey system with two habitats. *J Theor Biol*, 398:150 – 161, 2016. ISSN 0022-5193. doi: 10.1016/j.jtbi.2016.03.015.

A. S. Hadley and M. G. Betts. Refocusing habitat fragmentation research using lessons from the last decade. *Current Landscape Ecology Reports*, 1:55–66, 2016. doi: 10.1007/s40823-016-0007-8.

B. Haegeman and M. Loreau. General relationships between consumer dispersal, resource dispersal and metacommunity diversity. *Ecol Lett*, 17(2):175–184, 2014. doi: https://doi.org/10.1111/ele.12214.

K. Hale, F. Valdovinos, and N. Martinez. Mutualism increases diversity, stability, and function of multiplex networks that integrate pollinators into food webs. *Nat Commun*, 11(2182), 2020. doi: 10.1038/s41467-020-15688-w.

A. Hastings. Spatial heterogeneity and the stability of predator-prey systems. *Theor Popul Biol*, 12(1):37–48, 1977. doi: 10.1016/0040-5809(77)90034-X.

C. Hauzy, M. Gauduchon, F. D. Hulot, and M. Loreau. Density-dependent dispersal and relative dispersal affect the stability of predator-prey metacommunities. *J Theor Biol*, 266(3):458 – 469, 2010.

C. Huffaker. Experimental studies on predation: Dispersion factors and predator-prey oscillations. *Hilgardia*, 27:343–383, 1958. doi: 10.3733/hilg.v27n14p343.

B. W. Ibelings, R. Portielje, E. H. R. R. Lammens, R. Noordhuis, M. S. van den Berg, W. Joosse, and M. L. Meijer. Resilience of alternative stable states during the recovery of shallow lakes from eutrophication: Lake veluwe as a case study. *Ecosystems*, 10:4 – 16, 2007. doi: 10.1007/s10021-006-9009-4.

V. A. Jansen. The dynamics of two diffusively coupled predator–prey populations. *Theor Popul Biol*, 59(2):119 – 131, 2001. doi: https://doi.org/10.1006/tpbi.2000.1506.

V. A. A. Jansen. Effects of dispersal in a tri-trophic metapopulation model. *J Math Biol*, 34(2):195–224, Jan 1995. doi: 10.1007/BF00178773.

A. Kahilainen, S. van Nouhuys, T. Schulz, and M. Saastamoinen. Metapopulation dynamics in a changing climate: Increasing spatial synchrony in weather conditions drives metapopulation synchrony of a butterfly inhabiting a fragmented landscape. *Glob Change Biol*, 24(9):4316–4329, SEP 2018. doi: 10.1111/gcb.14280.

T. Kalettka and C. Rudat. Hydrogeomorphic types of glacially created kettle holes in north-east germany. *Limnologica*, 36(1):54 – 64, 2006. ISSN 0075-9511. doi: 10.1016/j.limno.2005.11.001.

W. D. Koenig. Spatial autocorrelation of ecological phenomena. *Trends Ecol Evol*, 14 (1):22 – 26, 1999. doi: https://doi.org/10.1016/S0169-5347(98)01533-X.

H. Kreft, W. Jetz, J. Mutke, G. Kier, and W. Barthlott. Global diversity of island floras from a macroecological perspective. *Ecol Lett*, 11(2):116–127, 2008. doi: 10.1111/j.1461-0248.2007.01129.x.

A. Kuparinen, A. Boit, F. S. Valdovinos, H. Lassaux, and N. D. Martinez. Fishing-induced life-history changes degrade and destabilize harvested ecosystems. *Sci Rep*, 6, 2016. doi: 10.1038/srep22245.

R. M. LeCraw, P. Kratina, and D. S. Srivastava. Food web complexity and stability across habitat connectivity gradients. *Oecologia*, 176(4):903–915, 2014. doi: 10.1007/s00442-014-3083-7.

M. A. Leibold and J. M. Chase. *Metacommunity Ecology*, volume 59. Princeton University Press, Princeton, 2017.

R. Lindborg and O. Eriksson. Historical landscape connectivity affects present plant species diversity. *Ecology*, 85(7):1840–1845, 2004. doi: 10.1890/04-0367.

A. J. Lotka. *Elements of physical biology*. Williams & Wilkins Company., 1925.

R. MacArthur. Fluctuations of animal populations and a measure of community stability. *Ecology*, 36:533–536, 1955. doi: 10.2307/1929601.

N. D. Martinez. Allometric trophic networks from individuals to socio-ecosystems: Consumer–resource theory of the ecological elephant in the room. *Frontiers in Ecology and Evolution*, 8:92, 2020. doi: 10.3389/fevo.2020.00092. URL `https://www.frontiersin.org/article/10.3389/fevo.2020.00092`.

B. Matthiessen, E. Mielke, and U. Sommer. Dispersal decreases diversity in heterogeneous metacommunities by enhancing regional competition. *Ecology*, 91(7):2022–2033, 2010. doi: 10.1890/09-1395.1.

R. M. May. Will a large complex system be stable? *Nature*, 238:413 – 414, 1972. doi: https://doi.org/10.1038/238413a0.

N. Mouquet and M. Loreau. Coexistence in metacommunities: The regional similarity hypothesis. *Am Nat*, 159(4):420–426, 2002. doi: 10.1086/338996.

M. Penrose. *Random Geometric Graphs*. Oxford University Press, 2003.

S. L. Pimm, H. L. Jones, and J. Diamond. On the risk of extinction. *Am Nat*, 132(6): 757–785, 1988. doi: 10.1086/284889.

S. L. Pimm, C. N. Jenkins, R. Abell, T. M. Brooks, J. L. Gittleman, L. N. Joppa, P. H. Raven, C. M. Roberts, and J. O. Sexton. The biodiversity of species and their rates of extinction, distribution, and protection. *Science*, 344(6187), 2014. ISSN 0036-8075. doi: 10.1126/science.1246752.

V. Radchuk, F. D. Laender, J. S. Cabral, I. Boulangeat, M. Crawford, F. Bohn, J. D. Raedt, C. Scherer, J.-C. Svenning, K. Thonicke, F. M. Schurr, V. Grimm, and S. Kramer-Schadt. The dimensionality of stability depends on disturbance type. *Ecology Letters*, 22(4):674–684, 2019. doi: https://doi.org/10.1111/ele.13226.

E. Ranta, V. Kaitala, J. Lindstrom, and H. Lindén. Synchrony in population dynamics. *Proc R Soc B Biol Sci*, 262:113 –118, 1995. doi: https://doi.org/10.1098/rspb.1995.0184.

J. O. Riede, U. Brose, B. Ebenman, U. Jacob, R. Thompson, C. R. Townsend, and T. Jonsson. Stepping in elton's footprints: a general scaling model for body masses and trophic levels across ecosystems. *Ecol Lett*, 14(2):169–178, 2011. doi: doi.org/10.1111/j.1461-0248.2010.01568.x.

M. L. Rosenzweig and R. H. MacArthur. Graphical representation and stability conditions of predator-prey interactions. *Am Nat*, 97(895):209–223, 1963. doi: 10.1086/282272.

M. Scheffer, S. Hosper, M.-L. Meijer, B. Moss, and E. Jeppesen. Alternative equilibria in shallow lakes. *Trends Ecol Evol*, 8(8):275 – 279, 1993. ISSN 0169-5347. doi: 10.1016/0169-5347(93)90254-M.

D. E. Schindler, J. B. Armstrong, and T. E. Reed. The portfolio concept in ecology and evolution. *Front Ecol Environ*, 13(5):257–263, 2015. doi: 10.1890/140275.

U. E. Schlägel, V. Grimm, N. Blaum, P. Colangeli, M. Dammhahn, J. A. Eccard, S. L. Hausmann, A. Herde, H. Hofer, J. Joshi, S. Kramer-Schadt, M. Litwin, S. D. Lozada-Gobilard, M. E. H. Müller, T. M"uller, R. Nathan, J. S. Petermann, K. Pirhofer-Walzl, V. Radchuk, M. C. Rillig, M. Roeleke, M. Schäfer, C. Scherer, G. Schiro, C. Scholz, L. Teckentrup, R. Tiedemann, W. Ullmann, C. C. Voigt, G. Weithoff, and F. Jeltsch. Movement-mediated community assembly and coexistence. *Biol Rev*, 95(4):1073–1096, 2020. doi: https://doi.org/10.1111/brv.12600.

F. D. Schneider, U. Brose, B. C. Rall, and C. Guill. Animal diversity and ecosystem functioning in dynamic food webs. *Nat Commun*, 7(12718), 2016. doi: 10.1038/ncomms12718.

T. N. Sherratt, X. Lambin, S. J. Petty, J. L. Mackinnon, C. F. Coles, and C. J. Thomas. Use of coupled oscillator models to understand synchrony and travelling waves in populations of the field vole *Microtus agrestis* in northern england. *J Appl Ecol*, 37 (Suppl. 1):148 – 158, 2000. doi: https://doi.org/10.1046/j.1365-2664.2000.00472.x.

U. T. Srinivasan, J. A. Dunne, J. Harte, and N. D. Martinez. Response of complex food webs to realistic extinction sequences. *Ecology*, 88(3):671–682, 2007. doi: 10.1890/06-0971.

J. W. Terborgh. Toward a trophic theory of species diversity. *PNAS*, 112(37):11415–11422, 2015. doi: 10.1073/pnas.1501070112.

M. Thakur and N. Eisenhauer. Plant community composition determines the strength of top-down control in a soil food web motif. *Sci Rep*, 5(9134), 2015. doi: doi.org/10.1038/srep09134.

R. M. Thompson, U. Brose, J. A. Dunne, R. O. Hall, S. Hladyz, R. L. Kitching, N. D. Martinez, H. Rantala, T. N. Romanuk, D. B. Stouffer, and J. M. Tylianakis. Food webs: reconciling the structure and function of biodiversity. *Trends Ecol Evol*, 27(12): 689 – 697, 2012. doi: 10.1016/j.tree.2012.08.005.

J. T. Thorson, M. D. Scheuerell, J. D. Olden, and D. E. Schindler. Spatial heterogeneity contributes more to portfolio effects than species variability in bottom-associated marine fishes. *Proc R Soc Lond, B*, 285:20180915, 2018. doi: https://doi.org/10.1098/rspb.2018.0915.

D. Tilman. *Resource competition and community structure*. Princeton University Press, Princeton, 1982.

D. Tilman. Community invasibility, recruitment limitation, and grassland biodiversity. *Ecology*, 78(1):81–92, 1997. doi: 10.1890/0012-9658(1997)078[0081:CIRLAG]2.0.CO;2.

D. Urban and T. Keitt. Landscape connectivity: A graph-theoretical perspective. *Ecology*, 82(5):1205–1218, 2001. doi: 10.1890/0012-9658(2001)082[1205:LCAGTP]2.0.CO;2.

V. Volterra. Variazioni e fluttuazioni del numero d'individui in specie animali conviventi. *Mem Acad Lincei Roma*, 2:31–113, 1926.

S. Wang and M. Loreau. Ecosystem stability in space: α-, β- and γ-variability. *Ecol Lett*, 17(8):891–901, 2014. doi: 10.1111/ele.12292.

G. A. Wellborn, D. K. Skelly, and E. E. Werner. Mechanisms creating community structure across a freshwater habitat gradient. *Ann Rev Ecol Syst*, 27(1):337–363, 1996. doi: 10.1146/annurev.ecolsys.27.1.337.

R. H. Whittaker. Evolution and measurement of species diversity. *Taxon*, 21(2/3): 213–251, 1972. doi: 10.2307/1218190.

R. J. Williams and N. D. Martinez. Simple rules yield complex food webs. *Nature*, 404 (6774):180 – 183, 3 2000. doi: 10.1038/35004572.

R. J. Williams and N. D. Martinez. Limits to trophic levels and omnivory in complex food webs: Theory and data. *Am Nat*, 163(3):458–468, 2004. doi: 10.1086/381964.

S. Wollrab, S. Diehl, and A. M. De Roos. Simple rules describe bottom-up and top-down control in food webs with alternative energy pathways. *Ecol Lett*, 15(9):935–946, 2012. doi: https://doi.org/10.1111/j.1461-0248.2012.01823.x.

P. Yodzis and S. Innes. Body size and consumer-resource dynamics. *Am Nat*, 139(6): 1151–1175, 1992. doi: 10.2307/2462335.

Declaration of contributions

Chapter 2: "The biggest losers: Habitat isolation deconstructs complex food webs from top to bottom"
authors: Remo Ryser, Johanna Häussler, Markus Stark, Ulrich Brose, Björn C. Rall, Christian Guill
published in: Proceedings of the Royal Society B: Biological Sciences 286: 20191177
RR, JH and MS declare shared first authorship. All authors conceived and designed the modeling framework; MS led the development of the simulation code. JH and RR ran the simulations on the high-performance-cluster; RR analyzed the data with support from all other authors; all authors contributed to interpreting the results; JH wrote the first draft of the manuscript with support from RR and MS and JH and RR led the editing. All authors contributed critically to the drafts and gave final approval for publication.

Chapter 3: "Patch isolation and periodic environmental disturbances have idiosyncratic effects on local and regional population variability in meta-food chains"
authors: Markus Stark, Moritz Bach, Christian Guill
accepted in: Theoretical Ecology; https://doi.org/10.1007/s12080-021-00510-0
All authors conceived the study design. MB and MS wrote the computer code. MS performed the numerical simulations and evaluated the data. MS and CG interpreted the results. The first draft of the manuscript was written by MS, editing was lead by CG. All authors read and approved the final manuscript.

Chapter 4: ""Food web robustness, mean patch isolation and minimum nearest neighbor distance of patches determine local and between-patch diversity in a complex metacommunity model"
authors: Markus Stark, Christian Guill
in preparation:
Both authors conceived the study design. MS wrote the simulation, performed the numerical simulations and evaluated the data. MS and CG interpreted the results. The first draft of the manuscript was written by MS, editing was lead by CG. Both authors read and approved the final manuscript.

Chapter 2

Effects of number of patches and patch isolation on diversity patterns

The biggest losers: Habitat isolation deconstructs complex food webs from top to bottom

Remo Ryser[1,2], Johanna Häussler[1,2], Markus Stark[3], Ulrich Brose[1,2], Björn C. Rall[1,2]& Christian Guill[3]

published in: Proceedings of the Royal Society B: Biological Sciences, Vol. 286: 20191177 (2019)

1 - EcoNetLab, German Centre for Integrative Biodiversity Research (iDiv) Halle-Jena-Leipzig, Deutscher Platz 5e, 04103 Leipzig, Germany

2 - Institute of Biodiversity, Friedrich Schiller University Jena, Dornburger-Strasse 159, 0773 Jena, Germany

3 - Institute of Biochemistry and Biology, University of Potsdam, Maulbeerallee 2, 14469 Potsdam, Germany

Abstract

Habitat fragmentation is threatening global biodiversity. To date, there is only limited understanding of how the different aspects of habitat fragmentation (habitat loss, number of fragments and isolation) affect species diversity within complex ecological networks such as food webs. Here, we present a dynamic and spatially-explicit food web model which integrates complex food web dynamics at the local scale and species-specific dispersal dynamics at the landscape scale, allowing us to study the interplay of local and spatial processes in metacommunities. We here explore how the number of habitat patches, i.e. the number of fragments, and an increase of habitat isolation, affect the species diversity patterns of complex food webs (α-, β-, γ-diversity). We specifically test whether there is a trophic dependency in the effect of these to factors on species diversity. In our model, habitat isolation is the main driver causing species loss and diversity decline. Our results emphasize that large-bodied consumer species at high trophic positions go extinct faster than smaller species at lower trophic levels, despite being superior dispersers that connect fragmented landscapes better. We attribute the loss of top species to a combined effect of higher biomass loss during dispersal with increasing habitat isolation in general, and the associated energy limitation in highly fragmented landscapes, preventing higher trophic levels to persist. To maintain trophic-complex and species-rich communities calls for effective conservation planning which considers the interdependence of trophic and spatial dynamics as well as the spatial context of a landscape and its energy availability.

Introduction

Understanding the impact of habitat fragmentation (habitat loss, number of fragments, and isolation) on biodiversity is crucial for ecology and conservation biology (Fahrig, 2003; Haddad et al., 2015; Tilman et al., 1994). A general observation and prediction is that large-bodied predators at high trophic levels which depend on sufficient food supplied by lower trophic levels are most sensitive to fragmentation, and thus, might respond more strongly than species at lower trophic levels (Henle et al., 2004; Holt, 2002). However, most conclusions regarding the effect of fragmentation are based on single species or competitively interacting species (see references within Melián and Bascompte (2002); Rybicki and Hanski (2013); Valiente-Banuet et al. (2015), but see for example (Liao et al., 2017a,b,c) for food chains and simple food web motifs). There is thus limited understanding how species embedded in complex food webs with multiple trophic levels respond to habitat fragmentation (Amarasekare, 2008; Hagen et al., 2012; Holt and Hoopes, 2005; Holt, 2002; Martinson and Fagan, 2014), even though these networks are a central organizing theme in nature (Dunne, 2005; Elton, 1927).

The stability of complex food webs is, amongst others, determined by the number and strength of trophic interactions (May, 1972). While it is broadly recognized that habitat fragmentation can have substantial impacts on such feeding relationships (Kondoh, 2003; Valladares et al., 2006), we lack a comprehensive and mechanistic understanding of how the disruption or loss of these interactions will affect species persistence and food web stability (Dobson et al., 2006; Kondoh, 2003; Martinson and Fagan, 2014; Rooney et al., 2006). Assuming that a loss of habitat, a decreasing number of fragments, and increasing isolation of the remaining fragments disrupt or weaken trophic interactions (Valiente-Banuet et al., 2015), thereby causing species extinctions (Martinson and Fagan, 2014; Valladares et al., 2006), population and community dynamics might change in unexpected and unpredictable ways. This change in community dynamics might lead to secondary extinctions which potentially cascade through the food web (Curtsdotter et al., 2011; Dunne and Williams, 2009).

Habitat loss, i.e. the decrease of total habitable area in the landscape or a reduction in patch size, can limit population sizes and biomass production, which might drive energy-limited species extinct (Post, 2002; Takimoto and Post, 2013) and subsequently entail cascading extinctions (Dunne and Williams, 2009). Successful dispersal among habitat patches might prevent local extinctions (spatial rescue effects), and thus, ensure species persistence at the landscape scale (Brown and Kodric-Brown, 1977; Hanski, 1998). Whether dispersal is successful or not depends, among other factors, on the distance an organism has to travel to reach the next habitat patch and on the quality of the matrix the habitat patches are embedded in (in short: the habitat matrix) (Bonte et al., 2012). With progressing habitat fragmentation, suitable habitat becomes scarce and the remaining habitat fragments increasingly isolated (Fahrig, 1997; Haddad et al., 2015), affecting the dispersal network of a species. As a consequence, organisms have to disperse over longer distances to connect habitat patches, which in turn might increase dispersal mortality and thus promote species extinctions (Fahrig, 2003). Also, habitat fragmentation often increases the hostility of the habitat matrix, e.g. due to human land use and landscape degeneration (Haddad et al., 2015; LeCraw et al., 2014; Prugh et al., 2008). The increased matrix hostility might further reduce the likelihood of successful dispersal between habitat patches as the movement through a hostile habitat matrix is energy intensive, and thus, population biomass is lost (Bonte et al., 2012; Prugh et al., 2008). This loss depends on the distance an organism has to travel and its dispersal ability, i.e. its dispersal range and the energy it can invest into movement. Finally, the detrimental effects of habitat loss and increasing isolation are likely to interact, as dispersal mortality can be expected to have a larger per capita effect when a population is already declining due to decreasing habitat.

In this context, superior dispersers might have an advantage over species with restricted dispersal abilities if the distances between habitat patches expand to a point where dispersal-limited species can no longer connect habitat patches. If this is the case, increasing habitat isolation impedes the ability of organisms to move across a fragmented landscape and prevents spatial rescue effects buffering against local extinctions. Increasing habitat isolation might result in increased extinction rates and ultimately lead to the loss of dispersal-limited species from the regional species pool. As large animal species are, at least up to a certain threshold, faster than smaller ones (Hirt et al., 2017; Peters, 1983), they should also be able to disperse over longer distances (Holt, 2002; Jenkins et al., 2007; van Noordwijk et al., 2015). In fragmented landscapes, this body mass dependent scaling of dispersal range might favor large-bodied consumers such as top predators, and thus, increase top-down pressure resulting in top-down regulated communities.

Empirical evidence and results from previous modeling approaches, however, suggest that species at higher trophic positions are most sensitive to isolation (Davies et al., 2000; Holyoak, 2008; Liao et al., 2017b; Martinson and Fagan, 2014; van Nouhuys, 2005). Modeling tri-trophic food chains in a patch-dynamic framework, Liao *et al.* Liao et al. (2017b,c) for example, show that increasing habitat fragmentation leads to faster extinctions of species at higher trophic levels, which they ascribe to reduced availability of prey Liao et al. (2017b). In the fragmentation experiment by Davies *et al.* (Davies et al., 2000) on the other hand the observed loss of top species is attributed to the unstable population dynamics of top species under environmental change.

Despite its relevance, a realistic picture and comprehensive understanding of how natural food webs might respond to different aspects of fragmentation such as habitat loss or increasing isolation, and any alteration to the spatial configuration of habitat in general, are lacking. To understand how fragmentation affects the diversity of communities organized in complex food webs requires knowledge of the interplay between their local (trophic) and spatial (dispersal) dynamics. The latter are determined by the number of fragments in the landscape and the distance between them, which can potentially affect the local trophic dynamics. We address this issue using a novel modeling approach which integrates local population dynamics of complex food webs and species-specific dispersal dynamics at the landscape scale (which we hereafter refer to as meta-food-web model, see Figure 2.1 for a conceptual illustration). Our spatially-explicit dynamic meta-food-web model allows us to explore how direct and indirect interactions between species in complex food webs together with spatial processes that connect sub-populations in different habitat patches interact to produce diversity patterns across increasingly fragmented landscapes. Specifically, we ask how the number of fragments and increasing habitat isolation impact the diversity patterns in complex food webs. We further ask which species or trophic groups shape these patterns.

Following general observations and predictions, we expect species diversity within complex food webs to decrease along a gradient of isolation. Based on the substantial variation in both dispersal abilities and energy requirements among species and across trophic levels (Davies et al., 2000; Holt, 2002; Post, 2002), we expect species at different trophic levels to strongly vary in their response to isolation. Specifically, we expect certain trophic groups such as consumer species at lower trophic ranks with limited dispersal abilities or top predators with strong resource constraints to be particularly sensitive to isolation. Additionally, with a larger number of fragments we expect more potential for rescue effects, thus fostering survival. This might especially apply to species with large dispersal ranges, which allow them to connect many habitat patches. We test our expectations using Whittaker's classical approach of α-, β-, and γ-diversity (Whittaker, 1972), where α- and γ-diversity describe species richness at the local (patch) and regional (metacommunity) scale, respectively, and β-diversity accounts for compositional differences between local communities.

Methods

In the following we outline a methods summary, for detailed information on equations and parameters see the methods section in the supplement. We consider a multitrophic metacommunity consisting of 40 species on a varying number of randomly positioned habitat patches (the meta-food-web, Figure 2.1b). All patches have the same abiotic conditions and each patch can potentially harbor the full food web, consisting of 10 basal plant and 30 animal consumer species. The potential feeding links (i.e. who eats whom) are constant over all patches (Figure 2.1a,b) and are as well as the feeding dynamics determined by the allometric food web model by Schneider *et al.* (Schneider et al., 2016). We use a dynamic bioenergetic model formulated in terms of ordinary differential equations that describe the feeding and dispersal dynamics. The rate of change in biomass density of a species depends on its biomass gain by feeding and immigration and its biomass loss by metabolism, being preyed upon and emigration. We integrate dispersal as species-specific biomass flow between habitat patches (Figure 2.1b,d). Based on empirical observations (e.g. (Jenkins et al., 2007)) and previous theoretical frameworks (e.g. (Hirt et al., 2017; Holt and Hoopes, 2005; Holt, 2002; Jetz et al., 2004)), we assume that the maximum dispersal distance of animal species increases with their body mass. As plants are passive dispersers, we model their maximum dispersal distance as random and body mass independent. We model emigration rates as a function of each species' per capita net growth rate, which is summarizing local conditions such as resource availability, predation pressure, and inter- and intraspecific competition (Fronhofer et al., 2018). During dispersal, distance-dependent mortality occurs, i.e., the further two patches are apart, the more biomass is lost to the hostile matrix separating them. We constructed 30 model food webs and simulated each food web on 72 different landscapes. For each simulation we generated landscapes on two independent gradients covering two aspects of fragmentation, namely number of patches and habitat isolation (Figure 2.1c). We achieved a full range for the gradient of habitat isolation (landscape connectance ranging from 0 to 1, Figure 2.3 c). Additionally, we performed dedicated simulation runs to reference the two extreme cases, i.e. (1) landscapes in which all patches are direct neighbors without a hostile matrix, and thus, no dispersal mortality, and (2) fully isolated landscapes, in which no species can bridge between patches, and thus, a dispersal mortality of 100%. Additionally, we tested a null model in which all species have the same maximum dispersal distance. To visualize the impact of number of patches and habitat isolation on species diversity we used GAMMs from the mgcv package in R (Team, 2016). See the supplement for detailed information on the maximum dispersal distance, the additional simulations and the statistical analysis.

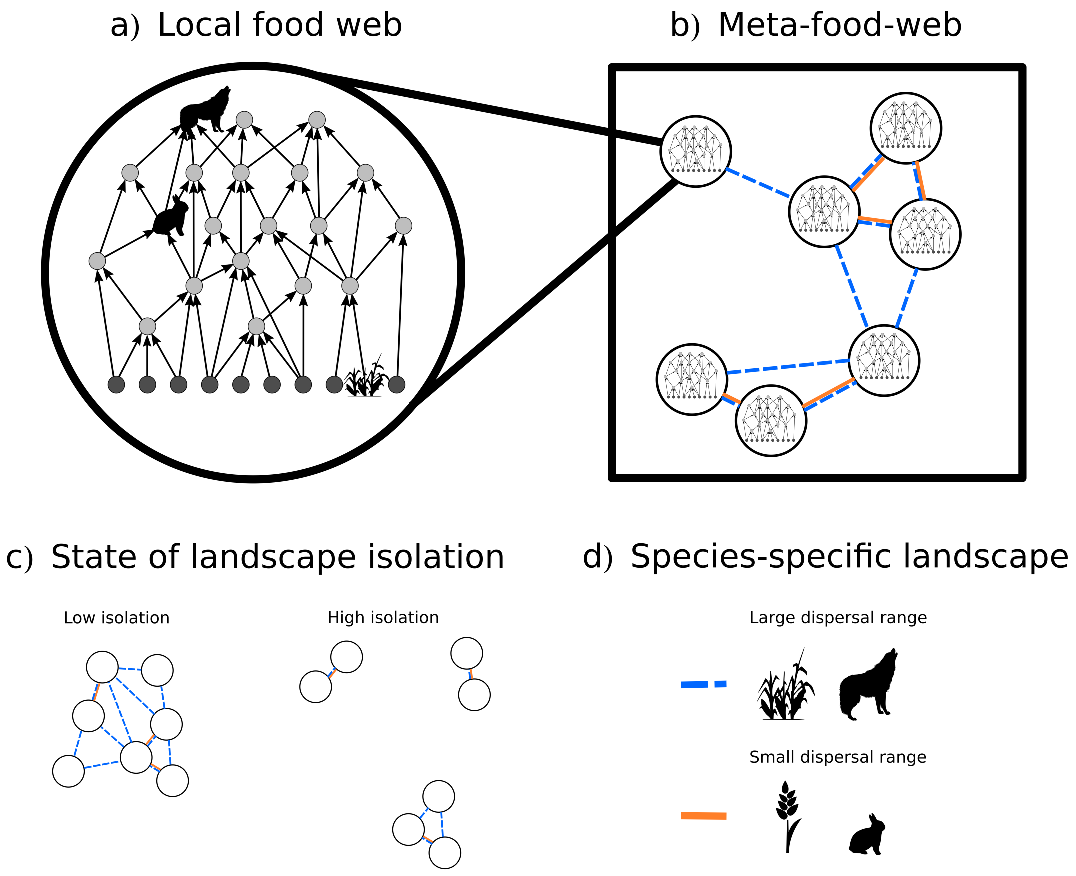

FIGURE 2.1: Conceptual illustration of our modelling framework. In our meta-food-web model (b) we link local food web dynamics at the patch level (a) through dynamic and species-specific dispersal at the landscape scale (d). We consider landscapes with identical but randomly distributed habitat patches, i.e. all patches have the same abiotic conditions, and each patch can potentially harbour the full food web. We model fragmented landscapes which differ in the number of habitat patches and the mean distance between patches (c).

Results

Species diversity patterns

Our simulation results identify habitat isolation (defined as the mean distance between habitat patches, $\overline{\tau}$, Figure 2.2, x-axis) as the key factor driving species diversity loss. As expected, we find fewer species on patches (the averaged local diversity, $\overline{\alpha}$) in landscapes in which habitats are highly isolated (Figure 2.2, left panel). In contrast to the decrease in $\overline{\alpha}$-diversity, β-diversity (Figure 2.2, middle panel), which describes differences in the community composition between patches, increases with habitat isolation. This increase happens around the infliction point of the landscape connectance at a mean patch distance $\log_{10} \overline{\tau} \approx$ of -0.5, at which 50% of all possible patch to patch connections are lost (supplement Figure A4, first panel). γ-diversity, the species diversity in the landscape, shows a more complicated pattern. First it decreases due to the loss of $\overline{\alpha}$-diversity with habitat isolation. This decrease is then reversed by the increase of β-diversity and the γ-diversity increases again with habitat isolation (Figure 2.2, right panel). The number of habitat patches in a landscape, Z (Figure 2.2, y-axis), only marginally affects the diversity patterns. The additional simulations of the two extreme cases (i.e. joint scenario with no dispersal loss and fully isolated scenario with 100% dispersal mortality) support these patterns (see the supplement, section A for the corresponding results). We further show that the isolation-induced species loss also translates into a loss of trophic complexity, i.e. isolated landscapes are characterized by reduced food webs with fewer species and fewer trophic levels (see the supplement, Figure A).

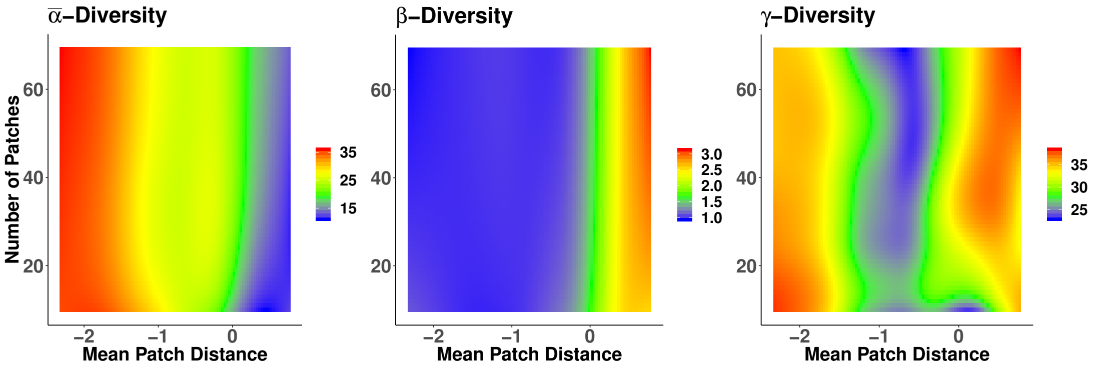

FIGURE 2.2: Heatmaps visualizing $\overline{\alpha}$-, β- and γ-diversity (color-coded; z-axis) in response to habitat isolation, i.e. the mean patch distance ($\overline{\tau}$, $\log_{10}$-transformed; x-axis) and the number of habitat patches (Z; y-axis), respectively. We generated the heatmaps based on the statistical model predictions (see the methods section).

Differences among trophic levels

As the number of patches only marginally affects species diversity patterns, we hereafter focus on the effects of habitat isolation on trophic-dependent differences among species (Figure 2.3). In Figure 2.3, biomass densities, B_i, and landscape connectances, ρ_i, represent the average of each species i over all food webs. Species are ranked according to their body mass. Thus, although species body masses differ between food webs, species 1 is always the smallest, species 2 the second smallest and so forth. The same applies to ρ_i, where the landscape connectance of consumer species is body mass dependent, but the connectance of plant species is body mass independent (see the methods section). In well-connected landscapes (i.e. landscapes with small mean patch distances, $\overline{\tau}$), large and medium-sized consumer species (except the very largest) have higher population biomass densities than smaller consumers (Figure 2.3a,c). With expanding distances between habitat patches, large-bodied consumers at high trophic positions (Figure 2.3a, red to blue lines) show a particularly strong decrease in population biomass densities. Small consumer species (Figure 2.3a, orange to yellow lines) are generally less affected by increasing habitat isolation. Plant species show a less consistent response to increased isolation, with most species slightly increasing their biomass density (Figure 2.3b, green lines). Based on our assumption that the maximum dispersal distance of animals scales with body mass, the ability to connect a landscape follows the same allometric scaling (Figure 2.3c). Despite this dispersal advantage, intermediate-sized and large animal species (Figure 2.3a, red to blue lines) lose biomass in landscapes in which they still have the potential to fully connect (almost) all habitat patches (Figure 2.3c). The differences in plant species biomass densities cannot be attributed to body mass dependent species-specific dispersal distances as for plants maximum dispersal distances were randomly assigned, and thus, there is no connection between body mass and landscape connectance (ρ_i, Figure 2.3d). Additional simulations, in which we assumed a constant maximum dispersal distance for all species of $\delta_i = \delta_{max} = 0.5$, support the negligibility of species-specific differences in dispersal ability for the emerging diversity patterns (see the supplement, Figure A3).

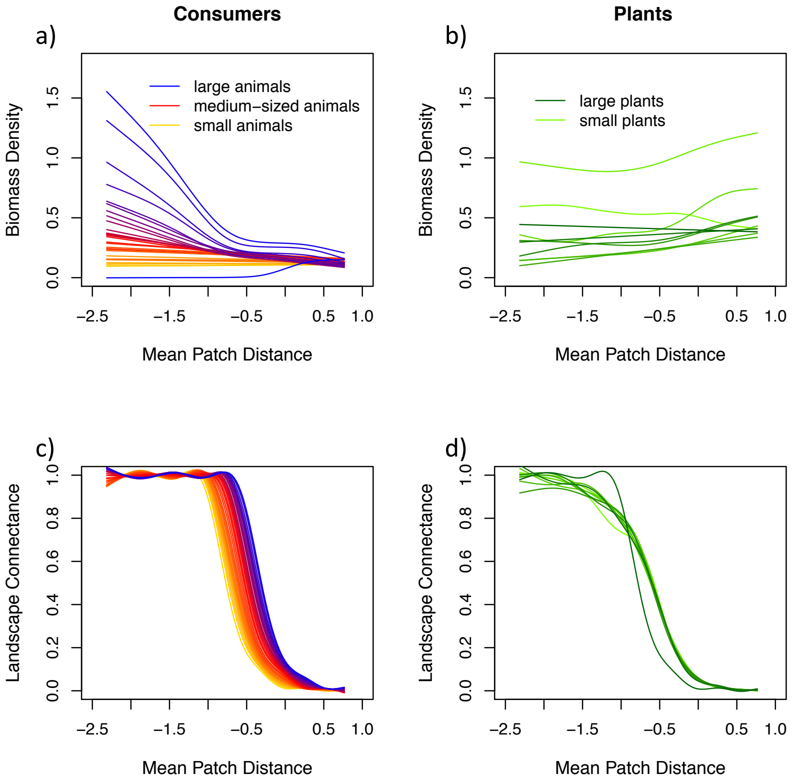

FIGURE 2.3: Top row: Mean biomass densities [log10(biomass density -1)] of animal consumer species and basal plant species (b) over all food webs (B_i, $\log_{10}$-transformed; y-axis) in response to habitat isolation, i.e. the mean patch distance ($\overline{\tau}$, $\log_{10}$-transformed; x-axis). Each color depicts the biomass density of species i averaged over all food webs: (a) color gradient where orange represents the smallest, red the intermediate and blue the largest consumer species; (b) color gradient where light green represents the smallest and dark green the largest plant species. Bottom row: Mean species-specific landscape connectance (ρ_i; y-axis) for consumer (c) and plant species (d) over all food webs as a function of the mean patch distance ($\overline{\tau}$, $\log_{10}$-transformed; x-axis). See the supplement Figure A9 for standard errors in biomass densities for four exemplary species.

Discussion

Habitat fragmentation is a major driver of global biodiversity decline. To date, a comprehensive understanding of how the different aspects of habitat fragmentation, i.e. habitat loss (Melián and Bascompte, 2002), number of fragments and isolation, affect the diversity patterns of species embedded in complex ecological networks such as food webs is lacking (see e.g. meta-analysis by Martinson and Fagan (Martinson and

Fagan, 2014), and references therein). Our simulation experiment allows us to independently explore the effects of number of fragments (i.e., number of habitat patches in the landscape), and of habitat isolation (i.e., distance between patches) on persistence and biomass densities of species in complex communities. We identified habitat isolation to be responsible for species diversity decline both at the local and regional scale. The rate at which a species loses biomass density strongly depends on its trophic position. Large-bodied consumer species at the top of the food web are most sensitive to isolation although they are dispersing most effectively (i.e. for them, increasing distances between habitat patches do not necessarily result in the loss of dispersal pathways or a substantial increase of dispersal mortality). Surprisingly, we find top species to lose biomass density and sometimes even go extinct in landscapes they can still fully connect, whereas the biomass densities of small consumer species at lower trophic levels and plant species are only marginally affected by increasing habitat isolation. We attribute the accelerated loss of top species to the energy limitation propagated through the food web: with increasing habitat isolation an increasing fraction of the biomass production of the lower trophic levels is lost due to mortality during dispersal and is thus no longer available to support the higher trophic levels. Additionally, the reduced top-down pressure on smaller consumers seems to compensate for their increased dispersal loss. Our model adds a complementary perspective to previous research pointing towards a trophic-dependent extinction risk due to constraints in resource availability with increasing habitat fragmentation (Liao et al., 2017b; van Nouhuys, 2005).

Habitat isolation drives species loss The increasing isolation of habitat fragments poses a severe threat to species persistence (but see (Fahrig, 2017; Fahrig et al., 2019)). We demonstrate in our simulation experiment that the generally observed pattern of species loss with increasing habitat isolation (e.g. (Haddad et al., 2015)) also holds for species embedded in large food webs. The loss of species occurs both at the local ($\overline{\alpha}$-diversity) and regional (γ-diversity) scale. For the latter, however, an increase in β-diversity compensates the loss in local diversity ($\overline{\alpha}$) when landscapes become very isolated and γ-diversity increases again (see below, Habitat isolation promotes β-diversity).

We modeled dispersal between habitat patches by assuming an energy loss for the dispersing organisms – a biologically realistic assumption as landscape degeneration, which often occurs concurrently with habitat fragmentation, increases the hostility of the habitat matrix (Haddad et al., 2015). Consequently, the dispersal mortality, and thus, biomass loss of populations to the habitat matrix increases substantially when dispersal distances between habitat patches expand. To account for the variation in dispersal ability among trophic groups, we incorporated species-specific maximum dispersal distances. For animal species, this maximum dispersal distance increases like a power law with body mass, therefore weakening the direct effect of habitat isolation the larger a species is. Despite this, top predators and other large consumer species respond strongly to isolation. These species exhibit a dramatic loss in biomass density or even go extinct in landscapes they still perceive as almost fully connected (landscape connectance, ρ_i, close to one), which indicates that their response to habitat isolation is mediated by indirect effects originating from the local food web dynamics.

Local food web dynamics and energy limitation drive top predator loss In local food webs energy is transported rather inefficiently from the basal to the top species, with transfer efficiency in natural systems often only around 10% (Lindeman, 1942). This energy limitation effectively controls the food chain length (Takimoto and Post, 2013) and renders large species at high trophic levels vulnerable to extinction due to resource shortage (Binzer et al., 2012). In our model, energy availability decreases if habitat isolation is high as this increases biomass loss during dispersal. This affects particularly small species at lower trophic levels since they generally have the highest metabolic costs per unit biomass and therefore the highest biomass losses per distance traveled (Peters, 1983; Schneider et al., 2016). The biomass loss during dispersal consequently reduces the net biomass production at the bottom of the food web and severely threatens species at higher trophic positions that already operate on a very limited resource supply.

Moreover, due to the feedback mechanisms regulating the community dynamics within complex food webs, a loss of top consumer species can have severe consequences for the functioning and stability of the network (Dobson et al., 2006; Rooney et al., 2006). A loss of top-down regulation can, for instance, lead to secondary extinctions resulting in simpler food webs (Brose et al., 2012; Dobson et al., 2006) – an additional mechanism that can foster the loss of biodiversity as observed in our simulations. However, we also see a much more direct effect of the changing community composition: The biomass densities of small species that suffer most from increased dispersal mortality do not, as one might expect, decline much as isolation progresses. We attribute this to a release from top-down control as their consumers lose biomass or even go extinct, which counters the negative direct effect of habitat isolation. These arguments suggest that differential dispersal capabilities are less important than energetic limitations in explaining the strong negative response of large consumers to habitat isolation. This claim is supported by the additional simulations where all species experienced the same level of dispersal mortality, which yielded similar results (see the supplement, Figure A3).

We did not find an effect of the number of patches on $\overline{\alpha}$-, β- and γ-diversity. As we model biomass densities on patches without defined area (see below, Model specifications), fewer patches do not reflect habitat loss, but rather the loss of fragments, i.e. stepping stones in the dispersal network. Thus the energy limitation in our simulated landscapes derives from direct dispersal loss and cascading effects of dispersal losses of resources. For plant and small animal species this can be understood easily, as these species are less energy limited and thus are able to persist on a single habitat patch. For larger animal species the situation is more subtle: While they can integrate over multiple patches, feeding interactions still always occur on one patch at a time. If the biomass densities of their resources (and thus also the realized feeding rate) is too low on a particular patch to cover their metabolic requirements, they gain no advantage from the addition of more patches with equally low resource abundance.

Habitat isolation promotes β-diversity Contrary to the decline in $\overline{\alpha}$-diversity with increasing habitat isolation, we find an increase in β-diversity starting from around $\log_{10}$ mean patch distance $\overline{\tau} \approx -0.5$. We assumed identical abiotic conditions on all habitat patches, i.e. there are no differences in nutrient availability or background mortality rates. Therefore, any differences in conditions experienced by the species on different patches can only originate from the initial community composition and the structure of the dispersal network. One way for such different conditions to emerge is the disintegration of the dispersal network into several smaller clusters. Up to a

$\log_{10}$ mean patch distance $\overline{\tau} \approx -0.5$, the species with the largest maximum dispersal distance (which could be both large animals that have not already gone extinct and plants with a randomly selected large dispersal distance) have a landscape connectance (ρ_i) of at least 0.5. This dispersal advantage easily allows them to connect all patches to a single network component, thereby providing homogenization for the meta-food-web. However, as the mean patch distance increases further, even these species cannot bridge all gaps in the habitat matrix any more and clusters of patches emerge that are for all species disconnected from the other patches. As these clusters vary in the number of patches and mean patch distance within the cluster, the level of dispersal mortality experienced by the species on the different clusters can also vary considerably. Any further increase in mean patch distance causes the landscape connectance to drop to nearly zero for all species and all patches within the landscape approach complete isolation. With no immigration into isolated patches, non-resident species cannot colonize them and initial community compositions drive dissimilarities among patches. However, the initial β-diversity is not sufficient in explaining the high β-diversity in strongly isolated landscapes (supplement Figure A4). This suggests that different food web positions of initial species lead to different cascading effects in local food web dynamics with more or less secondary extinctions on isolated patches further increasing differences in local community compositions. The increase in β-diversity is even stronger than the loss of local diversity resulting in an increase in γ-diversity in highly isolated landscapes. However, species contributing to this high γ-diversity tend to occur on fewer patches and thus are more prone to go extinct in the whole landscape due to stochastic extinction events.

Model specifications

The framework we propose here for modeling meta-food-webs is very general and allows for a straightforward implementation of future empirical insight where we so far had to rely on plausible assumptions. The trophic network model for the local food webs is based on a tested and realistic allometric framework (Schneider et al., 2016) with a fixed number of 40 species – a typical value in dynamic food web modeling (e.g. (Brose et al., 2006; C. Rall et al., 2008)). We based all model parameters on allometric principles (Peters, 1983; Rall et al., 2012) allowing for a simple adaptation of our modeling approach to other trophic networks such as empirically sampled food webs (Brose et al., 2006) or other food web models such as the niche model (Williams and Martinez, 2000). Moreover, empirical patch networks (e.g. the coordinates of meadows in a forest landscape) or other dispersal mechanisms (Eklöf et al., 2012; Melián and Bascompte, 2002) may be incorporated in the future. In our simulations, biomass loss during dispersal is predominantly responsible for the decline in species diversity. We linked the maximum dispersal distance of animals and thereby also their mortality during dispersal to body mass, which is plausible because larger animal species can move faster (Hirt et al., 2017), and thus, have to spend less time in the hostile habitat matrix. Interestingly, however, we did not find any empirical study relating body mass directly to mortality or biomass loss during migration. If such information becomes available in the future, it can be easily incorporated into our modeling framework. Further, we deliberately assumed all habitat patches to share the same abiotic conditions (Leibold et al., 2004) as we wanted to focus on the general effects of the interaction of complex food web and dispersal dynamics. Adding habitat heterogeneity among patches, e.g. by modifying nutrient availability or mean temperature, however, is straightforward and can be expected to yield additional insight into the mechanisms for the maintenance of species diversity in meta-food-webs. Finally, by using a dynamic model formulated in terms of biomass densities instead of absolute biomasses (or population sizes), we make the implicit assumption that patches do not have an absolute size. Thus, the number of patches in a landscape cannot be directly linked to the total amount of habitat but rather reflects the number of fragments, i.e. stepping stones in the dispersal network of a species. A decreasing number of patches thus does not necessarily imply habitat loss. In order to also address effects of habitat loss (in terms of area), the model could be adapted to include for example area specific extinction thresholds and absolute biomasses in dispersal dynamics, but this was beyond the scope of this study.

Synthesis and outlook

Our simulation experiment demonstrates that habitat isolation reduces species diversity in complex food webs in general, with differences in the effect across trophic levels. In increasingly isolated landscapes, energy becomes limited, which decreases the biomass density of large consumers or even drives them extinct. These primary extinctions may result in a cascade of secondary extinctions, given the importance of top predators for food web stability (Brose, 2008; Curtsdotter et al., 2011). The increased risk of network downsizing, i.e. simple food webs with fewer and smaller species (Duffy, 2003; Hagen et al., 2012), stresses the importance to consider both direct and indirect trophic interactions as well as dispersal when assessing the extinction risk of species embedded in complex food webs and other ecological networks.

To date, most conservation research focuses on single species and does not consider the complex networks of interactions in natural communities (Hagen et al., 2012; Valiente-Banuet et al., 2015). However, the patterns we presented here clearly support previous studies highlighting the importance of trophic interactions (e.g. (Holyoak, 2008; Liao et al., 2017b; van Nouhuys, 2005)). We show that the fragmentation-induced extinction risk of species strongly depends on their trophic position, with top species being particularly vulnerable. Given that top-down regulation can stabilize food webs (Brose, 2008; Curtsdotter et al., 2011), the loss of top predators might entail unpredictable consequences for adjacent trophic levels, destabilize food webs, reduce species diversity and trophic complexity and ultimately compromise ecosystem functioning (Curtsdotter et al., 2011; Dunne and Williams, 2009). In addition to the trophic position of a species, the trophic structure of the food web has also been shown to be an important aspect (see (Liao et al., 2017a)). Our results suggest that bottom-up energy limitation caused by dispersal mortality due to habitat isolation can be a critical factor driving species loss and the reduction of trophic complexity. The extent of this loss strongly depends on the spatial context (see also (Melián and Bascompte, 2002)). Thus, to maintain species-rich and trophic-complex natural communities under future environmental change, effective conservation planning must consider this interdependence of spatial and trophic dynamics. Notably, conservation planning should also consider habitat isolation and matrix hostility (and consequently dispersal mortality) to ensure sufficient biomass exchange between local populations, capable of inducing spatial rescue effects, and to alleviate bottom-up energy limitation of large consumers. Energy limitations can also result from habitat loss (which we did not model here), decreasing energy availability at the bottom of the food web affecting local dynamics intrinsically independent of dispersal. Thus, avoiding habitat loss remains a crucial aspect (Fahrig, 2003; Fahrig et al., 2019). We highlight the need to explore food webs and other complex ecological networks in a spatial context to achieve a more holistic understanding of biodiversity and ecosystem processes.

Acknowledgments

This study was financed by the German Research Foundation (DFG) in the framework of the research unit FOR 1748 - Network on Networks: The interplay of structure and dynamics in spatial ecological networks (RA 2339/2-2, BR 2315/16-2, GU 1645/1-1). Further, JH, RR, UB and BCR gratefully acknowledge the support of the German Centre for Integrative Biodiversity Research (iDiv) Halle-Jena-Leipzig funded by the German Research Foundation (FZT 118). The scientific results have (in part) been computed at the High-Performance Computing Cluster EVE of the Helmholtz Centre for Environmental Research - UFZ and iDiv, and we thank the staff of EVE (in particular Christian Krause from iDiv) for their support. Furthermore, we thank Thomas Boy for his technical support and assistance with programming issues.

Data accessibility

We enable full reproducibility of our study by providing the original C- and R-code on Dryad. https://datadryad.org/review?doi=doi:10.5061/dryad.c624907

Bibliography

P. Amarasekare. Spatial dynamics of foodwebs. *Annu Rev Ecol Evol Syst*, 39:479–500, 2008. doi: 10.1146/annurev.ecolsys.39.110707.173434.

A. Binzer, C. Guill, U. Brose, and B. C. Rall. The dynamics of food chains under climate change and nutrient enrichment. *Phil Trans R Soc B*, 367(1605):2935–44, 11 2012. doi: 10.1098/rstb.2012.0230.

D. Bonte, H. Van Dyck, J. M. Bullock, A. Coulon, M. Delgado, M. Gibbs, V. Lehouck, E. Matthysen, K. Mustin, M. Saastamoinen, N. Schtickzelle, V. M. Stevens, S. Vandewoestijne, M. Baguette, K. Barton, T. G. Benton, A. Chaput-Bardy, J. Clobert, C. Dytham, T. Hovestadt, C. M. Meier, S. C. F. Palmer, C. Turlure, and J. M. J. Travis. Costs of dispersal. *Biol Rev*, 87(2):290–312, 2012. doi: 10.1111/j.1469-185X.2011.00201.x.

U. Brose. Complex food webs prevent competitive exclusion among producer species. *Proc R Soc B Biol Sci*, 275(1650), 2008. doi: doi.org/10.1098/rspb.2008.0718.

U. Brose, T. Jonsson, E. L. Berlow, P. Warren, C. Banasek-Richter, L.-F. Bersier, J. L. Blanchard, T. Brey, S. R. Carpenter, M.-F. C. Blandenier, L. Cushing, H. A. Dawah, T. Dell, F. Edwards, S. Harper-Smith, U. Jacob, M. E. Ledger, N. D. Martinez, J. Memmott, K. Mintenbeck, J. K. Pinnegar, B. C. Rall, T. S. Rayner, D. C. Reuman, L. Ruess, W. Ulrich, R. J. Williams, G. Woodward, and J. E. Cohen. Consumer–resource body-size relationships in natural food webs. *Ecology*, 87(10):2411–2417, October 2006. doi: 10.1890/0012-9658(2006)87[2411:CBRINF]2.0.CO;2.

U. Brose, J. A. Dunne, J. M. Montoya, O. L. Petchey, F. D. Schneider, and U. Jacob. Climate change in size-structured ecosystems. *Phil Trans R Soc B*, 367(1605), 2012. doi: https://doi.org/10.1098/rstb.2012.0232.

J. H. Brown and A. Kodric-Brown. Turnover rates in insular biogeography: Effect of immigration on extinction. *Ecology*, 58(2):445–449, 3 1977. doi: 10.2307/1935620.

B. C. Rall, C. Guill, and U. Brose. Food-web connectance and predator interference dampen the paradox of enrichment. *Oikos*, 117(2):202–213, 2008.

A. Curtsdotter, A. Binzer, U. Brose, F. de Castro, B. Ebenman, A. Eklöf, J. O. Riede, A. Thierry, and B. C. Rall. Robustness to secondary extinctions: Comparing trait-based sequential deletions in static and dynamic food webs. *Basic Appl Ecol*, 12(7): 571–580, 11 2011. doi: 10.1016/J.BAAE.2011.09.008.

K. F. Davies, C. R. Margules, and J. F. Lawrence. Which traits of species predict population decliens in experimental forest fragments? *Ecology*, 81(5):1450–1461, 5 2000. doi: 10.1890/0012-9658(2000)081[1450:WTOSPP]2.0.CO;2.

A. Dobson, D. Lodge, J. Alder, G. S. Cumming, J. Keymer, J. McGlade, H. Mooney, J. A. Rusak, O. Sala, V. Wolters, D. Wall, R. Winfree, and M. A. Xenopoulos. Habitat loss, trophic collapse, and the decline of ecosystem services. *Ecology*, 87(8):1915–1924, 8 2006. doi: 10.1890/0012-9658(2006)87[1915:HLTCAT]2.0.CO;2.

J. E. Duffy. Biodiversity loss, trophic skew and ecosystem functioning. *Ecol Lett*, 6(8): 680–687, 8 2003. doi: 10.1046/j.1461-0248.2003.00494.x.

J. A. Dunne. The network structure of food webs. In M. Pascual and J. A. Dunne, editors, *Ecological Networks:Linking Structure to Dynamics in Food Webs*, chapter 2. Oxford University Press, 2005. ISBN 9780195188165. URL `http://books.google.ca/books?id=qe-04Y2gKscC`.

J. A. Dunne and R. J. Williams. Cascading extinctions and community collapse in model food webs. *Phil Trans R Soc B*, 364(1524):1711–23, 6 2009. doi: 10.1098/rstb.2008.0219.

A. Eklöf, L. Kaneryd, P. Münger, A. Eklof, L. Kaneryd, and P. Munger. Climate change in metacommunities: dispersal gives double-sided effects on persistence. *Phil Trans R Soc B*, 367(1605):2945–2954, 11 2012. doi: 10.1098/rstb.2012.0234.

C. S. Elton. *Animal Ecology*. University of Chicago Press, 1927. ISBN 9780226206394.

L. Fahrig. Relative effects of habitat loss and fragmentation on population extinction. *J Wildl Manage*, 61(3):603, 7 1997. doi: 10.2307/3802168.

L. Fahrig. Effects of habitat fragmentation on biodiversity. *Ann Rev Ecol Evol Syst*, 34 (1):487–515, 2003. doi: 10.1146/annurev.ecolsys.34.011802.132419.

L. Fahrig. Ecological responses to habitat fragmentation per se. *Ann Rev Ecol Evol and Syst*, 48(1):1–23, 2017. doi: 10.1146/annurev-ecolsys-110316-022612.

L. Fahrig, V. Arroyo-Rodríguez, J. R. Bennett, V. Boucher-Lalonde, E. Cazetta, D. J. Currie, F. Eigenbrod, A. T. Ford, S. P. Harrison, J. A. Jaeger, N. Koper, A. E. Martin, J.-L. Martin, J. P. Metzger, P. Morrison, J. R. Rhodes, D. A. Saunders, D. Simberloff, A. C. Smith, L. Tischendorf, M. Vellend, and J. I. Watling. Is habitat fragmentation bad for biodiversity? *Biol Conserv*, 230:179 – 186, 2019. ISSN 0006-3207. doi: 10.1016/j.biocon.2018.12.026.

E. A. Fronhofer, D. Legrand, F. Altermatt, A. Ansart, S. Blanchet, D. Bonte, A. Chaine, M. Dahirel, F. De Laender, J. De Raedt, L. Di Gesu, S. Jacob, O. Kaltz, E. Laurent, C. J. Little, L. Madec, F. Manzi, S. Masier, F. Pellerin, F. Pennekamp, N. Schtickzelle, L. Therry, A. Vong, L. Winandy, and J. Cote. Bottom-up and top-down control of dispersal across major organismal groups. *Nat Ecol Evol*, 2(12):1859–1863, 2018. doi: 10.1038/s41559-018-0686-0.

N. M. Haddad, L. A. Brudvig, J. Clobert, K. F. Davies, A. Gonzalez, R. D. Holt, T. E. Lovejoy, J. O. Sexton, M. P. Austin, C. D. Collins, W. M. Cook, E. I. Damschen, R. M. Ewers, B. L. Foster, C. N. Jenkins, A. J. King, W. F. Laurance, D. J. Levey, C. R. Margules, B. A. Melbourne, A. O. Nicholls, J. L. Orrock, D.-X. Song, and J. R. Townshend. Habitat fragmentation and its lasting impact on earth's ecosystems. *Sci Adv*, 1(2), 2015.

M. Hagen, W. D. Kissling, C. Rasmussen, M. A. D. Aguiar, L. E. Brown, D. W. Carstensen, I. Alves-Dos-Santos, Y. L. Dupont, F. K. Edwards, J. Genini, P. R. Guimarães, G. B. Jenkins, P. Jordano, C. N. Kaiser-Bunbury, M. E. Ledger, K. P. Maia, F. M. D. Marquitti, Órla Mclaughlin, L. P. C. Morellato, E. J. O'Gorman, K. Trøjelsgaard, J. M. Tylianakis, M. M. Vidal, G. Woodward, and J. M. Olesen. 2 - biodiversity, species interactions and ecological networks in a fragmented world. In U. Jacob and G. Woodward, editors, *Global Change in Multispecies Systems Part 1*, volume 46 of *Adv Ecol Res*, pages 89 – 210. Academic Press, 2012. doi: 10.1016/B978-0-12-396992-7.00002-2.

I. Hanski. Metapopulation dynamics. *Nature*, 396(6706):41–49, 11 1998. ISSN 0028-0836. doi: 10.1038/23876. URL `http://www.nature.com/articles/23876`.

K. Henle, K. F. Davies, M. Kleyer, C. Margules, and J. Settele. Predictors of species sensitivity to fragmentation. *Biodivers Conserv*, 13(1):207–251, 1 2004. doi: 10.1023/B:BIOC.0000004319.91643.9e.

M. R. Hirt, W. Jetz, B. C. Rall, and U. Brose. A general scaling law reveals why the largest animals are not the fastest. *Nat Ecol Evol*, 1:1116–1122, 2017. doi: 10.1038/s41559-017-0241-4.

R. Holt and M. Hoopes. *Food Web Dynamics in a Metacommunity Context: Modules and Beyond*. The University of Chicago Press, 2005.

R. D. Holt. Food webs in space: On the interplay of dynamic instability and spatial processes. *Ecol Res*, 17(2):261–273, 3 2002. doi: 10.1046/j.1440-1703.2002.00485.x.

M. Holyoak. Habitat subdivision causes changes in food web structure. *Ecol Lett*, 3(6): 509–515, 7 2008. doi: 10.1111/j.1461-0248.2000.00180.x.

D. G. Jenkins, C. R. Brescacin, C. V. Duxbury, J. A. Elliott, J. A. Evans, K. R. Grablow, M. Hillegass, B. N. Lyon, G. A. Metzger, M. L. Olandese, D. Pepe, G. A. Silvers, H. N. Suresch, T. N. Thompson, C. M. Trexler, G. E. Williams, N. C. Williams, and S. E. Williams. Does size matter for dispersal distance? *Glob Ecol Biogeogr*, 16(4): 415–425, 2007. doi: 10.1111/j.1466-8238.2007.00312.x.

W. Jetz, C. Carbone, J. Fulford, and J. H. Brown. The scaling of animal space use. *Science (New York, N.Y.)*, 306(5694):266–8, 10 2004. doi: 10.1126/science.1102138.

M. Kondoh. Habitat fragmentation resulting in overgrazing by herbivores. *J Theor Biol*, 225(4):453–460, 2003. doi: 10.1016/S0022-5193(03)00279-0.

R. M. LeCraw, P. Kratina, and D. S. Srivastava. Food web complexity and stability across habitat connectivity gradients. *Oecologia*, 176(4):903–915, 2014. doi: 10.1007/s00442-014-3083-7.

M. A. Leibold, M. Holyoak, N. Mouquet, P. Amarasekare, J. M. Chase, M. F. Hoopes, R. D. Holt, J. B. Shurin, R. Law, D. Tilman, M. Loreau, and A. Gonzalez. The metacommunity concept: a framework for multi-scale community ecology. *Ecol Lett*, 7 (7):601–613, 2004. doi: 10.1111/j.1461-0248.2004.00608.x.

J. Liao, D. Bearup, and B. Blasius. Food web persistence in fragmented landscapes. *Proc R Soc B*, 284(1859):20170350, 2017a. doi: 10.1098/rspb.2017.0350.

J. Liao, D. Bearup, and B. Blasius. Diverse responses of species to landscape fragmentation in a simple food chain. *J Anim Ecol*, 86:1169–1178, 2017b. doi: 10.1111/1365-2656.12702.

J. Liao, D. Bearup, Y. Wang, I. Nijs, D. Bonte, Y. Li, U. Brose, S. Wang, and B. Blasius. Robustness of metacommunities with omnivory to habitat destruction: disentangling patch fragmentation from patch loss. *Ecology*, 98(6):1631–1639, 2017c. doi: 10.1002/ecy.1830.

R. L. Lindeman. The trophic-dynamic aspect of ecology. *Ecology*, 23(4):399–417, 10 1942. doi: 10.2307/1930126.

H. M. Martinson and W. F. Fagan. Trophic disruption: a meta-analysis of how habitat fragmentation affects resource consumption in terrestrial arthropod systems. *Ecol Lett*, 17(9):1178–1189, 9 2014. doi: 10.1111/ele.12305.

R. M. May. Will a large complex system be stable? *Nature*, 238:413 – 414, 1972. doi: https://doi.org/10.1038/238413a0.

C. J. Melián and J. Bascompte. Food web structure and habitat loss. *Ecol Lett*, 5(1): 37–46, 1 2002. doi: 10.1046/j.1461-0248.2002.00280.x.

R. H. Peters. *The Ecological Implications of Body Size:*. Cambridge University Press, Cambridge, 10 1983.

D. M. Post. The long and short of food-chain length. *Trends Ecol Evol*, 17(6):269–277, 6 2002. doi: 10.1016/S0169-5347(02)02455-2.

L. R. Prugh, K. E. Hodges, A. R. E. Sinclair, and J. S. Brashares. Effect of habitat area and isolation on fragmented animal populations. *Proc Natl Acad Sci*, 105(52):20770–20775, 2008. doi: 10.1073/pnas.0806080105.

B. C. Rall, U. Brose, M. Hartvig, G. Kalinkat, F. Schwarzmüller, O. Vucic-Pestic, and O. L. Petchey. Universal temperature and body-mass scaling of feeding rates. *Philos Trans R Soc B Biol Sci*, 367(1605):2923–2934, 2012. doi: 10.1098/rstb.2012.0242.

N. Rooney, K. Mccann, G. Gellner, and J. C. Moore. Structural asymmetry and the stability of diverse food webs. *Nature*, 442(20):265–269, 2006. doi: 10.1038/nature04887.

J. Rybicki and I. Hanski. Species–area relationships and extinctions caused by habitat loss and fragmentation. *Ecol Lett*, 16(s1):27–38, 2013. doi: https://doi.org/10.1111/ele.12065.

F. D. Schneider, U. Brose, B. C. Rall, and C. Guill. Animal diversity and ecosystem functioning in dynamic food webs. *Nat Commun*, 7(12718), 2016. doi: 10.1038/ncomms12718.

G. Takimoto and D. M. Post. Environmental determinants of food-chain length: a meta-analysis. *Ecol Res*, 28(5):675–681, 9 2013. doi: 10.1007/s11284-012-0943-7.

R. C. Team. R: A language and environment for statistical computing, 2016. URL `https://www.r-project.org/`.

D. Tilman, R. M. May, C. L. Lehman, and M. A. Nowak. Habitat destruction and the extinction debt. *Nature*, 371:65–66, 1994. doi: https://doi.org/10.1038/371065a0.

A. Valiente-Banuet, M. A. Aizen, J. M. Alcántara, J. Arroyo, A. Cocucci, M. Galetti, M. B. García, D. García, J. M. Gómez, P. Jordano, R. Medel, L. Navarro, J. R. Obeso, R. Oviedo, N. Ramírez, P. J. Rey, A. Traveset, M. Verdú, and R. Zamora. Beyond species loss: the extinction of ecological interactions in a changing world. *Funct Ecol*, 29(3):299–307, 3 2015. doi: 10.1111/1365-2435.12356.

G. Valladares, A. Salvo, and L. Cagnolo. Habitat fragmentation effects on trophic processes of insect-plant food webs. *Conserv Biol*, 20(1):212–217, 2006. doi: 10.1111/j.1523-1739.2006.00337.x.

C. G. E. T. van Noordwijk, W. C. E. P. Verberk, H. Turin, T. Heijerman, K. Alders, W. Dekoninck, K. Hannig, E. Regan, S. McCormack, M. J. F. Brown, E. Remke, H. Siepel, M. P. Berg, and D. Bonte. Species–area relationships are modulated by trophic rank, habitat affinity, and dispersal ability. *Ecology*, 96(2):518–531, 2 2015. doi: 10.1890/14-0082.1.

S. van Nouhuys. Effects of habitat fragmentation at different trophic levels in insect communities. *Annales Zoologici Fennici*, 42:433–447, 2005. doi: 10.2307/23735888.

R. H. Whittaker. Evolution and measurement of species diversity. *Taxon*, 21(2/3): 213–251, 1972. doi: 10.2307/1218190.

R. J. Williams and N. D. Martinez. Simple rules yield complex food webs. *Nature*, 404 (6774):180 – 183, 3 2000. doi: 10.1038/35004572.

Chapter 3

Interplay of temporal patch availability and patch isolation on population dynamics

Patch isolation and periodic environmental disturbances have idiosyncratic effects on local and regional population variability in meta-food chains

Markus Stark[1], Moritz Bach[1], Christian Guill[1]

accepted in: Theoretical Ecology

1 - Institute of Biochemistry and Biology, University of Potsdam, Maulbeerallee 2, 14469 Potsdam, Germany

Abstract

While habitat loss is a known key driver of biodiversity decline, the impact of other landscape properties, such as patch isolation, is far less clear. When patch isolation is low, species may benefit from a broader range of foraging opportunities, but are at the same time adversely affected by higher predation pressure from mobile predators. Although previous approaches have successfully linked such effects to biodiversity, their impact on local and metapopulation dynamics has largely been ignored. Since population dynamics may also be affected by environmental disturbances that temporally change the degree of patch isolation, such as periodic changes in habitat availability, accurate assessment of its link with isolation is highly challenging. To analyze the effect of patch isolation on the population dynamics on different spatial scales, we simulate a three-species meta-food chain on complex networks of habitat patches, and assess the average variability of local populations and metapopulations, as well as the level of synchronization among patches. To evaluate the impact of periodic environmental disturbances, we contrast simulations of static landscapes with simulations of dynamic landscapes in which 30 percent of the patches periodically become unavailable as habitat. We find that increasing mean patch isolation often leads to more asynchronous population dynamics, depending on the parametrization of the food chain. However, local population variability also increases due to indirect effects of increased dispersal mortality at high mean patch isolation, consequently destabilizing metapopulation dynamics and increasing extinction risk. In dynamic landscapes, periodic changes of patch availability on a timescale much slower than ecological interactions often fully synchronize the dynamics. Further, these changes not only increase the variability of local populations and metapopulations, but also mostly overrule the effects of mean patch isolation. This may explain the often small and inconclusive impact of mean patch isolation in natural ecosystems.

Introduction

Anthropogenic habitat degradation and loss are strong negative drivers of biodiversity on local and global scales (Butchart et al., 2010; Pereira et al., 2010; Pimm et al., 2014). While habitat loss has a clear cause-effect relationship with declining diversity induced by e.g. lack of resources, habitat size restrictions, or increased mortality (Brooks et al., 2002; Duraiappah et al., 2005), the effect of other modifications of the landscape such as fragmentation are still intensely debated (Fahrig, 2017; Fahrig et al., 2019; Fletcher et al., 2018; Hanski, 2015). Following Fahrig (2003), habitat fragmentation comprises three main components, the number of patches, patch isolation and patch size, but excludes habitat loss. Their respective effects are more difficult to assess because they are usually weaker than the effects of habitat loss (Fahrig, 2003) and often confounded with the latter (Didham et al., 2012).

In metacommunities, patch isolation determines to which extent individuals can disperse through the landscape and thereby contribute to the regional distribution and persistence of species. Empirical and experimental studies report however conflicting results of patch isolation at different spatial scales: Negative effects on regional diversity have been attributed to the prevention of rescue effects (Gotelli, 1991; Levins, 1969), but also positive effects on local diversity have been recorded (Fahrig, 2017). On the local scale dispersal can also alter biotic interactions among species directly, emphasizing the interplay between local and regional dynamics in metacommunities (Walting and Donnelly, 2006). Recent modeling approaches on metacommunities try to integrate more details of local and regional aspects regarding landscape attributes and species interactions, but mainly focus on species persistence and diversity (Pillai et al., 2011; Ryser et al., 2019) and ignore effects of dispersal on local population dynamics and its relevance for stability (LeCraw et al., 2014).

A major concern of models that include explicit population dynamics are mechanisms that synchronize population cycles between habitat patches. Such synchronous oscillations destabilize metapopulations by amplifying the amplitude of oscillations in their regional abundances and increasing the extinction risk of species in entire regions due to correlated local extinction events. Conversely, asynchronous oscillations can promote regional persistence and stability through rescue effects (Blasius et al., 1999; Levins, 1969) or the portfolio effect (Schindler et al., 2015; Thorson et al., 2018). These models, which are often limited to either a small number of patches or to regular, rectangular lattices (Briggs and Hoopes, 2004), have established that the synchronicity of population oscillations between patches generally increases with dispersal rate (Jansen, 2001; Sherratt et al., 2000). Other factors affecting synchronicity are adaptive dispersal (Abrams, 2007; Abrams and Ruokolainen, 2011), inter- and intraspecific density dependence of dispersal rates (Hauzy et al., 2010), and costliness or distance dependence of dispersal (Koelle and Vandermeer, 2005). In larger networks of habitat patches, an irregular network structure favors asynchronous dynamics (Holland and Hastings, 2008), but high dispersal rates again lead to synchronous oscillations that are detrimental for species persistence (Plitzko and Drossel, 2015). At larger effective distance between patches, dispersal between them is limited (Fletcher et al., 2016; Koelle and Vandermeer, 2005), linking the results regarding synchronization of population oscillations to research on the effect of patch isolation. Indeed, it has been shown that synchronization among natural populations declines with increasing distance between them (Ranta et al., 1995).

While synchronization is often linked to dispersal rate, and thereby implicitly to landscape properties like patch isolation, it can also be directly affected by correlated environmental fluctuations (Kahilainen et al., 2018; Koenig, 1999; Moran, 1953; Ranta et al., 1995). These fluctuations can affect demographic rates of the species via changing environmental conditions (like ambient temperature or resource availability), but they can also directly influence the availability of patches as habitable areas. As an example for the latter, a landscape in which both a temporally variable environment and a pronounced spatial structure strongly affect ecological communities are kettle holes in formerly glaciated regions (Kalettka and Rudat, 2006). These small ponds are typically formed in large clusters, and seasonal changes of temperature and precipitation cause some of them to be only temporally filled with water. The local aquatic communities of these temporary ponds thus periodically become completely extinct and recolonization through dispersing species from permanent ponds is a key element to reestablish the communities (De Meester et al., 2005). As the recolonization happens in a temporally correlated manner at the beginning of the wet season, a synchronizing effect on the population dynamics can be expected. However, this is again contingent on the spatial structure of the landscape, as lower dispersal rates due to higher mean patch isolation can impede the recolonization process.

So far, the interaction between these drivers of synchronization and population variability in general remains largely unexplored (but see (Gouhier et al., 2010)), despite the fact that anthropogenic activity continues to increase both habitat degradation and environmental variability. In order to fill this gap, we examine the dynamics of a meta-food chain in large, spatially explicit networks of habitat patches and analyze its stability with respect to the mean patch isolation of the landscape and environmental disturbances that periodically render a subset of the patches uninhabitable. We chose a food chain as model system because it has on the hand a simple and tractable structure that, on the other hand, already allows for indirect effects mediated by feeding interactions on different trophic levels. In order to obtain a complete picture of the effects of patch isolation and periodic environmental disturbances on the extent and synchronicity of population oscillations in food chains, we analyze two parameterizations of the food chain that correspond to contrasting oscillation patterns. These patterns are characterized either by a relatively even distribution of biomass along the food chain (weak trophic cascade) or by marked differences among the species (strong trophic cascade), both of which are common in natural ecosystems (Carter and Rypstra, 1995; Estes and Duggins, 1995).

Our model setup explicitly addresses one aspect of fragmentation, namely patch isolation, while keeping other potentially confounding drivers such as the total amount of habitat or the number of patches constant. We consider both static landscapes, where all patches are constantly available as habitats, and dynamic landscapes, where periodic environmental disturbances regularly render some of the patches uninhabitable. The stability of the dynamics of the metacommunity is evaluated within the framework of Wang and Loreau (2014) that divides population variability into an α-, β-, and γ-component (similar to the classical diversity indices by Whittaker (1972)): α-variability is the average coefficient of variation of a species' local abundances, γ-variability is the coefficient of variation of the regional (metapopulation) abundance, and β-variability quantifies differences in oscillations between patches, i.e., how synchronously the local populations oscillate. Generally, it is assumed that higher dispersal rates synchronize population dynamics (e.g. Gouhier et al. (2010)). When mean patch isolation increases, mortality during dispersal increases, too. We expect that this decreases net dispersal flows and thus also decreases synchrony of population dynamics among patches (i.e., increases β-variability).

This may however be counteracted by (synchronous) periodic disturbances of patch availability. Furthermore, we expect local (α-) variability to decrease, as increasing mortality allows less biomass to flow up the food chain, thus weakening (and thereby stabilizing) the trophic interactions (Rip and McCann, 2011). If the local population oscillations indeed become less synchronous, this will also decrease regional (γ-) variability as habitats become more isolated.

Methods

The model comprises a tri-trophic food chain including an autotroph (A), a consumer (C) and a predator (P) species. As basis for the growth of the autotroph, a dynamic resource (R) serves as essential energy source and can be seen as a universal nutrient. This food chain is extended to a metacommunity by placing copies of it on habitat patches that are randomly distributed in space and connected via species-specific dispersal links (Figure 3.1). Where applicable, the individual parameters are derived from empirical data, largely from invertebrate communities.

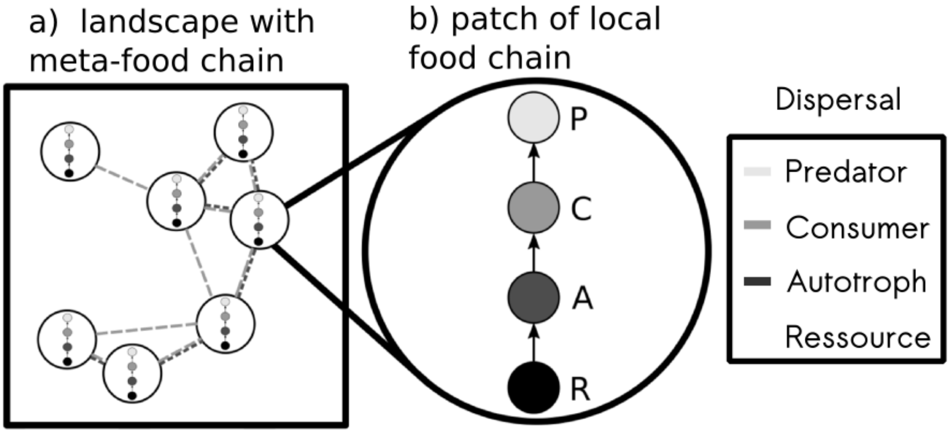

FIGURE 3.1: a) simplified example of a spatial network of habitat patches. Dashed lines of different grey tones indicate dispersal links of the respective species. The resource does not disperse between patches. b) local food chain on each patch comprising three trophic levels (autotrophs, A, consumers, C, and predators, P) plus a dynamic resource, R.

Trophic interactions

We first describe only the trophic interactions between the populations on a single patch and disregard dispersal. The local dynamics of the food chain follow a generalization of the bioenergetics approach (Brose et al., 2006b; Yodzis and Innes, 1992), supplemented with an equation for the resources. Adapted from chemostat dynamics, the rate of change of the resource density R is expressed as

$$\frac{dR}{dt} = D \cdot (R_0 - R) - G_{AR}A \tag{3.1}$$

with the resource turnover rate D and the supply concentration R_0. Uptake of resources by the autotroph A is described by a Monod function $G_{AR} = r\frac{R}{K+R}$ with maximum uptake rate r and half saturation constant K. The rates of change in biomass density for each species (A, C and P) are expressed by

$$\begin{aligned} \frac{dA}{dt} &= G_{AR}A - F_{CA}C - x_A A = g_A A \\ \frac{dC}{dt} &= e_C F_{CA}C - F_{PC}P - x_C C = g_C C \\ \frac{dP}{dt} &= e_P F_{PC}P - x_P P = g_P P\,, \end{aligned} \tag{3.2}$$

where the first terms in all three equations represent growth due to consumption, the last terms denote metabolic losses, and the middle terms in the equations for the autotroph and the consumer describe mortality through predation. The terms are summarized by the net per capita growth rates g_i ($i = A, C, P$). The parameters e_i and x_i are assimilation efficiencies and per capita respiration rates, respectively. The per capita feeding rate of species i on species j is described by a Beddington-DeAngelis functional response (Beddington, 1975; DeAngelis et al., 1975):

$$F_{ij} = \frac{1}{m_i}\frac{a_{ij}B_j}{1 + a_{ij}h_{ij}B_j + c_i B_i} \tag{3.3}$$

with the attack rate a_{ij}, the handling time h_{ij}, the interference coefficient c_i, and B_i and B_j as placeholders for the respective consumer's or resource's biomass density. Since the model is formulated in terms of biomass densities (as opposed to population densities), the functional response is scaled with $\frac{1}{m_i}$, the inverse of the respective consumer's body mass (Heckmann et al., 2012).

The parameters of the trophic dynamics scale allometrically with the body mass of the species. Mass-specific maximimum growth rate and respiration rates are assumed to decrease with a negative quarter-power law with body mass, i.e. $r = r_0 m_i^{-0.25}$ and $x_i = x_{0,i} m_i^{-0.25}$ (Brose et al., 2006b; Yodzis and Innes, 1992). Following Rall et al. (2012), handling times depend on the body masses of both consumer and resource with $h_{ij} = h_0 m_i^{-0.48} m_j^{-0.66}$. The same is true for the attack rates, but since these parameters were used to differentiate the contrasting states of top-down control, fixed values were used here (c.f. Tab. 3.1) that nevertheless obey the general trends found in Rall et al. (2012). Body masses increase by a factor of 100 per trophic level, a value commonly found in invertebrate communities and known to have a stabilising effect on population dynamics (Brose et al., 2006a,b). Freedom of choosing an appropriate set of units allows us to set the body mass of the autotroph to $m_A = 1$. In general, the model is parameterised such that the population dynamics of all species are oscillatory when dispersal is not accounted for (Tab. 3.1, Figure 3.2).

Habitat network and dispersal

We use the same rules for modeling spatial interactions as in Ryser et al. (2019). Dispersal is considered for the autotroph, consumer, and predator species in the model. The spatial setting is implemented as a random geometric graph (RGG) (Penrose, 2003), where each node of the spatial network represents a habitat patch for a local community (Urban and Keitt, 2001). The (x, y)-coordinates of each patch were drawn at random from a bivariate uniform distribution over the intervall $[0:1] \times [0:1]$. Dispersal links between the patches connect the local populations, enabling exchange of biomass between patches and thereby forming a meta-food chain (Figure 3.1).

Each species perceives its individual dispersal network depending on its body mass m_i. A dispersal link for species i exists between two patches k and l only if the distance between them is less than the species-specific maximum dispersal distance

$$D_{max,i} = D_0 m_i^{\epsilon} \ . \tag{3.4}$$

The exponent ϵ is set to a positive value to account for increased mobility and thus improved dispersal abilities of species with a larger body mass (Hein et al., 2012; Peters, 1983).

Dispersal itself is at least for animal species often an active process resulting in metabolic costs and potentially involving a higher risk of predation. To account for these costs (dispersal mortality), we assume that dispersal success $S_{i,lk}$ (i.e., the fraction of individuals *not* dying during dispersal) of species i, when moving between patches l and k, decreases linearly with the distance between the patches:

$$S_{i,lk} = \max\left(1 - d_{i,lk}, 0\right) , \tag{3.5}$$

where $d_{i,lk} = \frac{d_{lk}}{D_{max,i}}$ is the distance between the patches relative to the maximum dispersal distance of species i. For passively dispersing plants distance-depending costs can be caused by a decreasing probability of propagules finding by chance a suitable patch that is further away.

The fraction of individuals emigrating from a source patch k that move towards a target patch l is calculated using the weight function

$$W_{i,lk} = \frac{1 - d_{i,lk}}{\sum_p (1 - d_{i,pk})} , \tag{3.6}$$

where the sum in the denominator is taken over all potential target patches p that are within the maximum dispersal range of species i on patch k (i.e., those with $d_{pk} < D_{max,i}$). This weight function makes dispersal links between nearby patches stronger, implying that a larger proportion of emigrating biomass arrives there, than those between patches that are further apart. Note that while specific distances $d_{i,lk}$ and success terms $S_{i,lk}$ are symmetric for all pairs of patches, the weight function is not (i.e. $W_{i,lk} \neq W_{i,kl}$).

In general, the process of dispersal can be described as an exchange of biomass between habitat patches that is affecting the population dynamics of species i on patch l via emigration ($E_{i,l}$) from this patch and immigration ($I_{i,l}$) into the patch. The full population dynamics of species i on patch l, comprising both local, trophic dynamics, Eqs. (3.2), and dispersal dynamics, can thus be written as

$$\frac{dB_{i,l}}{dt} = g_{i,l} B_{i,l} - E_{i,l} + I_{i,l} . \tag{3.7}$$

Emigration is a complex process in nature possibly involving different environmental cues and species properties. Here we assume an adaptive emigration rate that depends on the net per capita growth rate $g_{i,l}$ of species i on patch l, reflecting its current situation in this habitat. If a species' net growth is positive, there is little need for dispersal and emigration will be low. However, if the local environmental conditions deteriorate, e.g. due to low resource availability or high predation pressure, the emigration rate increases. This is captured by the following function:

$$E_{i,l} = \frac{\mu_i B_{i,l}}{1 + e^{b\left(g_{i,l} + x_i\right)}} \, . \tag{3.8}$$

The parameter $\mu_i = \mu_0 x_i$ determines the maximum per capita emigration rate and b determines how sensitively the emigration rate depends on the net growth rate (i.e., how quickly it drops when $g_{i,l}$ increases). Finally, immigration of species i into patch l depends on the amount of emigration from all neighboring patches k as well as on the specific dispersal network, encoded in the success and weight functions $S_{i,lk}$ and $W_{i,lk}$, according to

$$I_{i,l} = \sum_k S_{i,lk} W_{i,lk} E_{i,k} \, . \tag{3.9}$$

The parameters defining the dispersal dynamics are also summarized in Tab. 3.1.

TABLE 3.1: Standard parameter set used in the model.

Parameter	**Description**	**Value**
D	resource turnover rate	0.5
R_0	resource supply concentration	5
r_0	intercept mass specific max. resource uptake rate	1
K	half saturation density for resource uptake	0.2
c_C, c_P	interference competition	0.6
e_C	assimilation efficiency consumer (C)	0.45
e_P	assimilation efficiency predator (P)	0.85
$x_{0,A}$	intercept respiration rate plant (A)	0.138
$x_{0,C}, x_{0,P}$	intercept respiration consumer (C) and predator (P)	0.314
a_{AC}	attack rate consumer	105 or 170
a_{PC}	attack rate predator	450 or 10000
h_0	intercept handling time	0.1
D_0	intercept maximum dispersal distance	[0.06: 0.5]
ϵ	scaling exponent for maximum dispersal distance	0.05
μ_0	scaling factor maximal emigration rate	2
b	curvature of emigration function	25
Z	number of habitat patches	30
σ	fraction of habitat patches blinking	0.3
λ	period length of blinking cycle	6000

Simulation setup

Static and dynamic landscapes

The baseline simulations are carried out using static landscapes, i.e., with RGG networks of $Z = 30$ habitat patches as described above, where all patches and dispersal links are permanently available. However, since the environmental conditions in nature are rarely completely constant, we also study dynamic landscapes in which a fraction σ of the patches becomes periodically unavailable as a habitat. This process is called 'blinking' and has a period length $\lambda = 6000$. This period length encompasses several hundred generation times of the autotroph, thereby providing sufficient time for the food chain to recover between blinking events. Blinking patches are turned on and off synchronously and change their state every $\frac{\lambda}{2}$ time units. When the blinking patches are turned off, the local food chains go extinct immediately. Furthermore, the dispersal network can be disrupted because these patches cannot be used as stepping stones for dispersal between patches that are too far apart for a direct dispersal link.

Patch isolation

To capture the effects of varying mean patch isolation, the intercept of the maximum dispersal distance, D_0, (Eq. (3.4)) is varied systematically between 0.06 and 0.5. This creates habitat networks that range from mostly isolated patches to systems where the predator can move in a single step between any two patches. The spatial network is quantified by the mean patch isolation of the predator's dispersal network,

$$I_{RGG,P} = 1 - \frac{L_P}{\frac{1}{2}Z \cdot (Z-1)}, \tag{3.10}$$

with L_P the number of undirected dispersal links of the predator and Z the number of habitat patches. Note that using the isolation of the dispersal network of any of the other species to define the mean patch isolation of the landscape would only rescale the x-axis of the results (Figure 3.3), but not change them qualitatively.

Ecosystem stability

We evaluated ecosystem stability according to Wang and Loreau (2014) as α-, β-, and γ-variability of autotroph, consumer, and predator. For the mean local or α-variability of a species, the coefficients of variation (CV, $\frac{\text{standard deviation}}{\text{mean}}$) of its local biomass densities on all patches are calculated and then averaged across patches (weighted with the respective local mean biomass density), while for the γ-variability (variability of the metapopulation) the CV of the total biomass density (sum over all patches) is evaluated. Similar to the α-, β-, and γ-diversity indices (Whittaker, 1972), β-variability measures differences between the patches and can thus be used to determine how synchronously local biomass densities on the different patches oscillate. It is here defined as $\beta = \frac{\alpha}{\gamma}$. In contrast to the diversity indices, however, variability decreases with an increase of spatial scale, i.e. $\gamma \leq \alpha$ and thus $\beta \geq 1$. Spatially synchronous oscillations result in a low β-variability and a γ-variability that approaches the value of the α-variability. Perfect synchronicity is obtained at $\beta = 1$. The variability measures of a species do not change if it is permanently extinct on one or several patches. An intuitive example of two species, one with synchronous and one with asynchronous oscillations, is provided in the Appendix (Figure B1).

Numerical simulations

We simulated food chains that were parameterized to exhibit either a strong or a weak trophic cascade, corresponding to a very uneven or a relatively even distribution of biomass along the food chain, respectively. The weak trophic cascade was generated by relatively low attack rates of the consumer and predator species ($a_{CA} = 105$, $a_{PC} = 450$, Figure 3.2A), while for the strong trophic cascade much higher attack rates were chosen ($a_{CA} = 170$, $a_{PC} = 10000$, Figure 3.2B). The spatial networks were either static (all patches permanently available as habitats) or dynamic (30% of the patches periodically becoming unavailable as habitats). The mean patch isolation was constant for each individual simulation run, but was gradually varied between simulations by decreasing D_0 from 0.5 to 0.06 in steps of 0.01. Simulations were carried out with a full-factorial design and 30 replicates for each combination of parameters, resulting in a total of 5400 simulation runs. Replicates differed in the randomly chosen positions of 30 patches that formed the spatial networks. Time series were simulated for 90 000 time units and split in three sections of equal length. During the first section, the systems settled on the attractor and from the second section, mean biomass densities were calculated. These mean biomass densities were then used to calculate the variability coefficients from the third section of the time series. During the simulations, a species was considered extinct on a given patch if its local biomass density fell below 10^{-20}. Global extinction of a species from the entire meta-food chain was never observed. Numerical simulations of the ODE model were performed in C (source code adopted from (Schneider et al., 2016)) using the SUNDIALS CVODE solver (Hindmarsh et al., 2005) with absolute and relative error tolerances of 10^{-10}. Output data were analysed using Python 2.7.11, 3.6 and several Python packages, in particular NumPy and Matplotlib (Hunter, 2007; Oliphant, 2015; Van der Walt et al., 2011).

Results

Food chain dynamics without dispersal

To capture how different parameterizations of trophic interactions affect the metacommunity dynamics, we analyzed two contrasting trophic cascades in the food chain that were created by assuming either low or high attack rates. The first type, called weak trophic cascade, is characterized by a weak predation pressure of the predator, a relatively even distribution of biomass along the food chain and a high oscillation frequency (note the different scales of the x-axes of the two panels in Figure 3.2). The strong trophic cascade is, in contrast, characterized by a very uneven distribution of biomass with a strong dominance of the autotroph (caused by the suppression of the consumer by the predator), a much lower oscillation frequency, and much more drastic population cycles that drive both the predator and the consumer biomass densities repeatedly to very low values. The difference between the predator attack rates in the two cases had to be this pronounced as for intermediate values, the food chain is stable and the analysis of (meta-)population variabilities is not possible (Appendix, Figure B2).

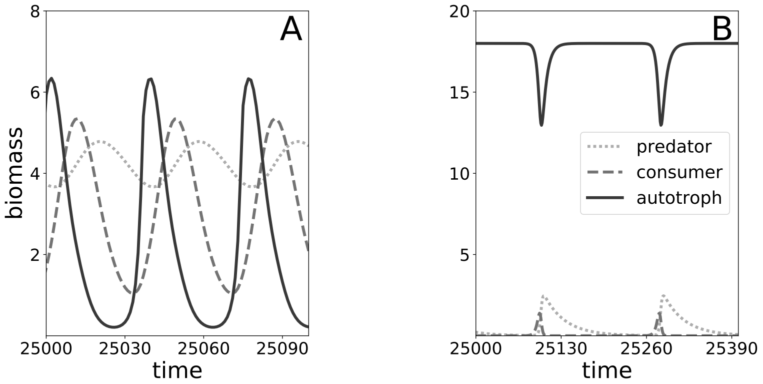

FIGURE 3.2: Timeseries of the dynamics for the weak (A) and the strong (B) trophic cascade on a single patch without dispersal dynamics. In case A, a_{CA} = 105 and a_{PC} = 450; in case B, a_{CA} = 170 and a_{PC} = 10000. All other parameters as in Tab. 3.1. Note the different scales of x- and y-axes in the two panels.

Metacommunity dynamics

We evaluated the two different landscape scenarios (static vs. dynamic) for both the weak and strong trophic cascade over a gradient of the mean patch isolation. All scenarios are evaluated with respect to local (α-variability), between patch (β-variability), and metapopulation dynamics (γ-variability). The observed trends in population variabilities on the different spatial scales were always the same for all trophic levels. We therefore only show results for the predator species. Results for the autotroph and consumer species are in the Appendix (Figures B3 and B4).

Local dynamics: α-variability

In contrast to our expectations, increasing mean patch isolation amplifies biomass oscillations in static landscapes (increasing α-variability, Figure 3.3A,B). This trend is particularly pronounced in the strong trophic cascade from intermediate mean patch isolation (where many systems even settle on a stable fixed point) to high mean patch isolation (Figure 3.3B). Because α-variability has non-zero values at low mean patch isolation, the overall pattern is u-shaped. In the weak trophic cascade, α-variability monotonously increases with mean patch isolation. In dynamic landscapes, α-variability is higher than in static landscapes, but its main trends with mean patch isolation are significantly weaker than in static landscapes (cf. also Tab. 3.2).

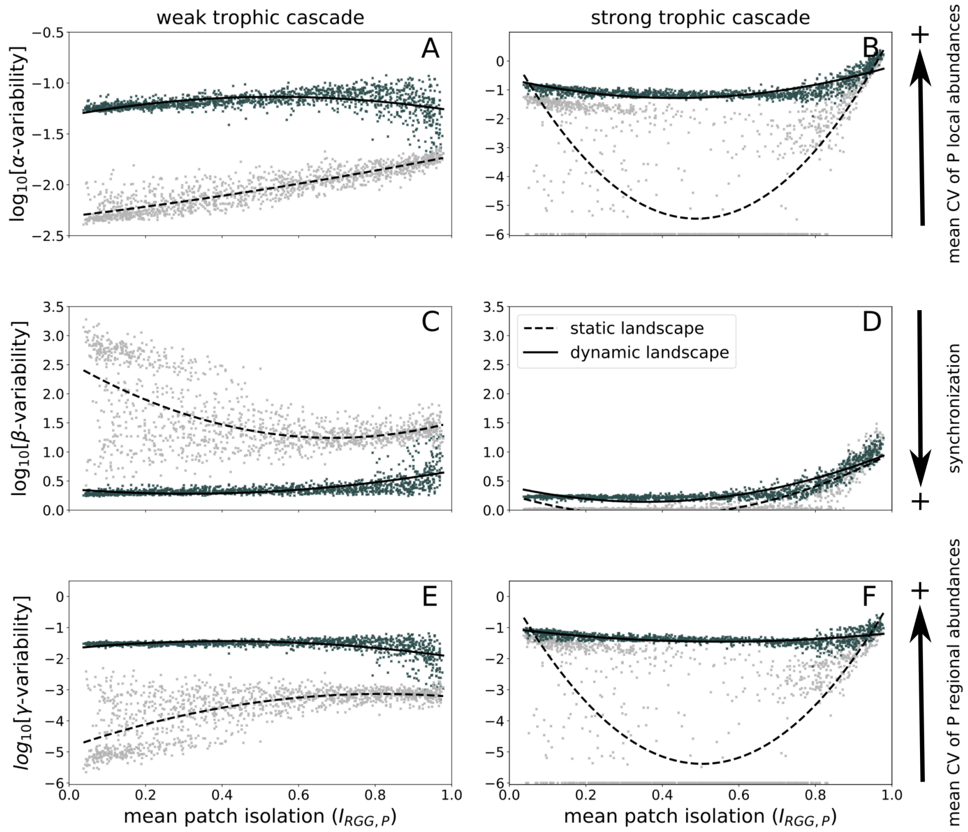

FIGURE 3.3: Local (α-variability, top row), between patch (β-variability, middle row) and metapopulation dynamics (γ-variability, bottom row) of the predator for the weak (left column) and the strong trophic cascade (right column). Light gray data points and dashed trend lines (second order fit) indicate static landscapes, dark gray data points and solid trend lines indicate dynamic landscapes. Each data point represents the result of one simulation run with a unique spatial network of habitat patches. All data points where the variability is below 10^{-6} are set to 10^{-6} as differences between them provide no meaningful information that close to the fixed point.

Synchronization of patches: β-variability

On the regional scale we evaluated to what extent the biomass dynamics between habitat patches synchronized (Figure 3.3C,D). In line with our expectations, there is in most cases a clear trend towards decreased synchronization (increased β-variability, c.f. also Table 3.2) of the dynamics as mean patch isolation increases. The apparent limitation of synchronization in dynamic landscapes (minimal β-variability $\approx$ 2 for both weak and strong trophic cascades) is only a numerical effect due to the difference between constant and blinking patches.

Only the weak trophic cascade in static landscapes deviates from the general trend: The β-variability is not only higher than in the other cases, but it also appears to decrease from low to intermediate mean patch isolation and only slightly increases at high mean patch isolation. The initial decrease is due to a separate cloud of data points with very high β-variabilities, which emerges for $I_{RGG,P} \lessapprox 0.4$. This suggests that in this part of the parameter space a second attractor with even less synchronization between the patches exists. The bistability of the system is indeed confirmed by dedicated simulations using spatial networks with fixed coordinates of the patches (cf. Appendix, Figure B5)

TABLE 3.2: Summary of the trends of α-, β- and γ-variability with increasing mean patch isolation for the weak (WTC) or strong (STC) trophic cascade in static or dynamic landscapes.

State of landscape	Type of effect	Trend for WTC	Trend for STC
static	α-variability	↑	u-shape
static	β-variability	↓ & ↗	↑
static	γ-variability	↑ & →	u-shape
dynamic	α-variability	→	↗
dynamic	β-variability	↗	↑
dynamic	γ-variability	↘	→

Metapopulation : γ-variability

For both the weak and the strong trophic cascade we find a relatively constant total biomass of the metapopulation (γ-variability $< 10^{-1}$, Figure 3.3E,F). As expected, γ-variability is higher in dynamic landscapes than in static ones. Since local biomass oscillations are often highly synchronized, the trends in the metapopulation dynamics largely follow those already observed in the local dynamics (cf. also Tab. 3.2). As with the β-variability of the weak trophic cascade in static landscapes, at low mean patch isolation ($I_{RGG} \lessapprox 0.4$) a small cloud of data points appears to be separated from the rest, which have a low γ-variability. Again, these data points can be attributed to an alternative attractor with less synchronized dynamics and correspondingly a lower γ-variability.

Discussion

The impact of habitat fragmentation on biodiversity and community dynamics is a subject of ongoing debate (Fahrig et al., 2019; Fletcher et al., 2018). Here, we evaluated the effect of mean patch isolation as one aspect of fragmentation on the population dynamics of two contrasting states of a meta-food chain in static and dynamic landscapes. Most intriguingly, we found that both local (α-) and metacommunity (γ-) variability increased with increasing mean patch isolation, despite the fact that synchronization among patches mostly decreased (β-variability increased) along the same gradient. Periodic environmental disturbances that rendered some patches regularly uninhabitable in dynamic landscapes weakened these trends, but at the prize of overall higher levels of α- and γ-variability.

Interactions between dispersal and local interactions drive the dynamics in static landscapes

Higher effective dispersal rates at low patch isolation have been shown to synchronize the dynamics of metacommunities (Gouhier et al., 2010), but our results suggest that the extent of this effect may depend on the local interactions between the populations. While our results largely confirm the negative correlation between mean patch isolation (and thus, by proxy, effective dispersal rate) and synchronization, we also observe a significant deviation from this trend in the weak trophic cascade at low mean patch isolation. There, an alternative attractor with very asynchronous population oscillations (high β-variability) emerges. However, α-variability is also relatively low on this attractor, which may explain the lack of synchronization: When the local populations do not oscillate much, their emigration rates are also almost constant over time, and there is consequently little potential for affecting the population oscillations on neighboring patches. This highlights the importance of details of the local interactions between species (in this case low attack rates in the weak trophic cascade that limit α-variability) for collective phenomena like synchronization.

Other theoretical studies also indicate a relevance of local interactions for the synchronization of population dynamics. Koelle and Vandermeer (2005) show for example opposing trends of synchronization between species in a food chain, which are due to an interaction between dispersal patterns and trophic interactions. Moreover, empirical studies provide evidence that dispersal may even alter biotic interactions between species directly (Walting and Donnelly, 2006), further underlining the importance of local species interactions for our understanding of metapopulation dynamics.

Indirect effects of local trophic interactions also explain why our initial hypothesis, regarding decreasing α-variability at increasing mean patch isolation, turned out to be incorrect in the weak trophic cascade. The hypothesis was based on the 'principle of energy flux' (Rip and McCann, 2011), according to which an increasing (dispersal) mortality at higher mean patch isolation should weaken and consequently stabilize the trophic interactions along the food chain (and thus decrease α-variability). In contrast to this prediction, high dispersal mortality does not generally result in a lower α- or γ-variability in our model. We attribute this counter-intuitive trend to an indirect effect of dispersal mortality: Despite their superior dispersal abilities, higher trophic levels often suffer most from mean patch isolation because they are energetically more limited than the species on lower trophic levels (Ryser et al., 2019). In fact, we also find that the higher the mean patch isolation, the lower the mean biomass of the predator (see Appendix, Figure B6). This decreases the per-capita predation mortality of the consumer, which more than compensates for the increase in the consumer's dispersal mortality. In line with the principle of energy flux, this destabilizes the consumer-autotroph interaction. At high mean patch isolation, the α-variability of the predator thus increases because the dynamics of the predator is driven by the increasingly unstable consumer-autotroph interaction.

This apparent mismatch between increasing β-variability (more asynchronous dynamics) and simultaneously increasing γ-variability at high mean patch isolation has also implications for the so-called 'portfolio effect' (Schindler et al., 2015), which is often considered in more applied contexts. Specifically, the spatial portfolio effect (Thorson et al., 2018) measures how much γ-variability is reduced relative to its theoretical maximum (here given by γ-variability = α-variability) due to asynchronous oscillations among different spatial locations. While we do observe such a reduction of γ-variability *relative to α-variability* when mean patch isolation increases, the indirect effect of dispersal mortality discussed above still leads to an increase of γ-variability in absolute terms. This underlines that assessing factors that affect the synchronization of population dynamics across space is not always sufficient to understand the variability of a population on the regional scale.

Bistability in the weak tropic cascade

In static landscapes, the weak trophic cascade is bistable for low to medium mean patch isolation. In this parameter range, in addition to the attractor with intermediate synchronicity, which exists for the entire range of mean patch isolation, a second attractor with very asynchronous dynamics between the patches exists.

Interestingly, the bistability concerns only the synchronicity of the dynamics (and consequently the γ-variability). Local (α-) variability is not affected by whether the populations on different patches cycle more or less in synchrony (Figure 3.3A).

Such bistability is relevant because it implies hysteresis (Scheffer et al., 1993): a small change in environmental conditions can drive the system away from one attractor, but for the system to return to it, a much larger change of the environmental conditions in the opposite direction will be necessary. This is particularly concerning here: The second attractor, which may be regarded as more desirable due to its lower metapopulation variability, loses its stability when the mean patch isolation increases beyond a certain threshold. However, the system may never return to it even when environmental conditions improve again, because the primary attractor never loses its stability.

A possible explanation for the occurrence of the alternative synchronization patterns we observe is the way the dispersal rate is modeled. Specifically, that the rate at which individuals emigrate from a given patch depends on the net growth rate they experience there. Emigration can thus be driven by a lack of resources (in which case emigration helps ending the unfavorable growth conditions and is thus self-limiting) or by an exceedingly high predation rate (in which case emigration actually intensifies the per-capita predation rate for the remaining individuals and becomes self-enforcing). Preliminary analyses suggest that dampening or amplification of net dispersal flows by synchronous and asynchronous oscillations, respectively, create different feedback loops based on these different drivers of emigration, but more detailed analyses are required to understand how these contrasting states stabilize themselves.

Effect of periodic environmental disturbances

Periodic environmental disturbances have a stronger effect on population variability on all spatial scales than local interactions or mean patch isolation. We infer this from the observation that both weak and strong trophic cascade, which behave very differently in static landscapes, exhibit almost identical variability patterns in dynamic landscapes, with elevated levels of α- and γ-variability and low β-variability. Further, all three variability measures are almost constant over a wide range from low to medium mean patch isolation. Only at high mean patch isolation, where the patch networks begin to decompose into several isolated components anyway, the effect of the periodic disruption of the patch networks by the blinking patches dwindles and the variability measures become more similar to their values in static landscapes again. Both the increase in α-variability and the synchronization of the patches, due to the periodic environmental disturbances, are of course not unexpected. The blinking of the patches increases α-variability by causing low-frequency biomass oscillations through the extinction- and recolonization process and by decreasing the mean biomass densities on these patches. Similarly, environmental fluctuations have long been known to be able to synchronize ecological dynamics in coupled habitats (Moran, 1953). More surprising is however the overruling strength of the effect of periodic environmental disturbances, considering that a blinking cycle (period length $\lambda = 6000$) is about 150 times slower than the period length of the population cycles in the weak trophic cascade.

Our approach of modeling periodic environmental disturbances as dynamic landscapes, where some patches become periodically uninhabitable, is inspired by the natural example of kettle holes that have a species-rich community during the colder and wetter seasons, but can run dry during the summer (Kalettka and Rudat, 2006). Such periodic (in the example: seasonal) environmental disturbances are a common feature of ecological systems, since in most environments seasonally fluctuating climatic drivers exist (Fretwell, 1972). Together with the above discussed surprisingly strong effect of even very rarely occurring disturbances, this may explain why empirically observed effects of patch isolation are often small and inconclusive (Fahrig, 2003). Environmental disturbances (especially seasonal ones) of course do not always lead to the abrupt extinction of entire local communities, but could for example simply modify resource availability or mortality rates. An interesting avenue for future research might therefore be to explore whether such less drastic disturbances also have the potential to overrule the effects of local interactions and landscape configuration. Furthermore, resting stages can play a critical role in the recolonization of periodically uninhabitable patches (Wade, 1990). Accounting for them in the model might decrease synchronicity, as they allow for an independent restart of the local communities.

Relevance and effects of dispersal assumptions

Details of the way species dispersal is implemented within a model can have major implications for the arising population dynamics. In nature, a multitude of causes affects an individual's decision to leave its home patch (Bowler and Benton, 2005), among them being for example intraspecific competition (Herzig, 1995), quality of food resources (Kuussaari et al., 1996), or top-down pressure through parasitism or predation (Sloggett and Weisser, 2002). In our model we use the net growth rate of a species in a given patch to determine its emigration rate. Since the net growth rate depends on both food availability and predation pressure, the model captures multiple of the above mentioned causes of dispersal. However, we assume that individuals have only knowledge about the growth conditions in the patch they are currently in and not about the conditions in potential target patches. The dispersal rate between any two patches thus only depends on the local conditions in the source patch and on the spatial arrangement of the patches. Using a consumer-resource model with two patches, Abrams and Ruokolainen (2011) showed that when the dispersal rate depends on the difference of the growth rates between source and target patch, asynchronous (antiphase) cycles frequently occur, which promotes stability. With our approach, we only find asynchronous dynamics in static landscapes, but even then synchronous metacommunity dynamics frequently occur.

Conclusions

We conclude that due to indirect effects of local ecological interactions, dispersal is not necessarily a "double-edged sword" (Hudson and Cattadori, 1999) (dubbed so because too much of it can synchronize metacommunity dynamics and increase the risk of correlated extinctions), but also that a portfolio effect due to asynchronous oscillations may not always result in reduced variability at the metacommunity level. Furthermore, in each unique landscape, comprising a multitude of abiotic factors, the impact of a periodic environmental disturbance has the potential to outweigh local interactions present in a community. The extent of the effect of mean patch isolation on the variability of population dynamics in a metacommunity thus may strongly depend on local environmental conditions which are relevant for reliable predictions. Whether this is also true for other aspects of fragmentation or habitat loss is an intriguing question for future investigations. Finally, the non-monotonous stability response curve of the strong trophic cascade shows that the effect of mean patch isolation on metacommunity dynamics may not be trivial and that there might be transitions where patch isolation might switch from having a positive to having a negative effect.

Acknowledgment

This study was financed by the German Research Foundation (DFG) in the framework of the research unit FOR 1748 - Network on Networks: The interplay of structure and dynamics in spatial ecological networks (GU 1645/1-1). We thank R. Ceulemans, S. Bolius and two anonymous reviewers for constructive remarks on the manuscript.

Funding

German Research Foundation (DFG), (GU 1645/1-1)

Conflict of interest

The authors declare no conflict of interest.

Author contributions

All authors conceived the study design. MB and MS wrote the computer code. MS performed the numerical simulations and evaluated the data. MS and CG interpreted the results. The first draft of the manuscript was written by MS, editing was led by CG. All authors read and approved the final manuscript.

Code availability

We will enable full reproducibility of our study by providing the original C- and Python-code when needed/the manuscript is accepted

Bibliography

P. Abrams. Habitat choice in predator-prey systems: Spatial instability due to interacting adaptive movements. *Am Nat*, 169(5):581–594, 2007. doi: 10.1086/512688.

P. A. Abrams and L. Ruokolainen. How does adaptive consumer movement affect population dynamics in consumer–resource metacommunities with homogeneous patches? *J Theor Biol*, 277(1):99 – 110, 2011. ISSN 0022-5193. doi: 10.1016/j.jtbi.2011.02.019.

J. R. Beddington. Mutual interference between parasites or predators and its effect on searching efficiency. *J Anim Ecol*, 44(1):331–340, 1975. doi: 10.2307/3866.

B. Blasius, A. Huppert, and L. Stone. Complex dynamics and phase synchronization in spatially extended ecological systems. *Nature*, 399:354 – 359, 1999. doi: 10.1038/20676.

D. E. Bowler and T. G. Benton. Causes and consequences of animal dispersal strategies: relating individual behaviour to spatial dynamics. *Biol Rev*, 80(2):205–225, 2005. doi: 10.1017/S1464793104006645.

C. J. Briggs and M. F. Hoopes. Stabilizing effects in spatial parasitoid–host and predator–prey models: a review. *Theor Popul Biol*, 65(3):299 – 315, 2004. doi: 10.1016/j.tpb.2003.11.001.

T. M. Brooks, R. A. Mittermeier, C. G. Mittermeier, G. A. B. Da Fonseca, A. B. Rylands, W. R. Konstant, P. Flick, J. Pilgrim, S. Oldfield, G. Magin, and C. Hilton-Taylor. Habitat loss and extinction in the hotspots of biodiversity. *Conserv Biol*, 16(4):909–923, 2002. doi: 10.1046/j.1523-1739.2002.00530.x.

U. Brose, T. Jonsson, E. L. Berlow, P. Warren, C. Banasek-Richter, L.-F. Bersier, J. L. Blanchard, T. Brey, S. R. Carpenter, M.-F. C. Blandenier, L. Cushing, H. A. Dawah, T. Dell, F. Edwards, S. Harper-Smith, U. Jacob, M. E. Ledger, N. D. Martinez, J. Memmott, K. Mintenbeck, J. K. Pinnegar, B. C. Rall, T. S. Rayner, D. C. Reuman, L. Ruess, W. Ulrich, R. J. Williams, G. Woodward, and J. E. Cohen. Consumer–resource body-size relationships in natural food webs. *Ecology*, 87(10):2411–2417, October 2006a. doi: 10.1890/0012-9658(2006)87[2411:CBRINF]2.0.CO;2.

U. Brose, R. J. Williams, and N. D. Martinez. Allometric scaling enhances stability in complex food webs. *Ecol Lett*, 9(11):1228–1236, November 2006b. doi: 10.1111/j.1461-0248.2006.00978.x.

S. H. M. Butchart, M. Walpole, B. Collen, A. van Strien, J. P. W. Scharlemann, R. E. A. Almond, J. E. M. Baillie, B. Bomhard, C. Brown, J. Bruno, K. E. Carpenter, G. M. Carr, J. Chanson, A. M. Chenery, J. Csirke, N. C. Davidson, F. Dentener, M. Foster, A. Galli, J. N. Galloway, P. Genovesi, R. D. Gregory, M. Hockings, V. Kapos, J.-F. Lamarque, F. Leverington, J. Loh, M. A. McGeoch, L. McRae, A. Minasyan, M. H. Morcillo, T. E. E. Oldfield, D. Pauly, S. Quader, C. Revenga, J. R. Sauer, B. Skolnik, D. Spear, D. Stanwell-Smith, S. N. Stuart, A. Symes, M. Tierney, T. D. Tyrrell, J.-C. Vié, and R. Watson. Global biodiversity: Indicators of recent declines. *Science*, 328 (5982):1164–1168, 2010. ISSN 0036-8075. doi: 10.1126/science.1187512.

P. E. Carter and A. L. Rypstra. Top-down effects in soybean agroecosystems: Spider density affects herbivore damage. *Oikos*, 72(3):433–439, 1995. doi: 10.2307/3546129.

L. De Meester, S. Declerck, R. Stoks, G. Louette, F. Van De Meutter, T. De Bie, E. Michels, and L. Brendonck. Ponds and pools as model systems in conservation biology, ecology and evolutionary biology. *Aquat Conserv Mar Freshw Ecosyst*, 15(6): 715–725, 2005. doi: 10.1002/aqc.748.

D. L. DeAngelis, R. A. Goldstein, and R. V. O'Neill. A model for tropic interaction. *Ecology*, 56(4):881–892, 1975. doi: 10.2307/1936298.

R. K. Didham, V. Kapos, and R. M. Ewers. Rethinking the conceptual foundations of habitat fragmentation research. *Oikos*, 121:161–170, 2012. doi: 10.1111/j.1600-0706.2011.20273.x.

A. Duraiappah, S. Naeem, T. Agardy, N. Ash, H. Cooper, S. Diaz, D. Faith, G. Mace, J. McNeely, H. Mooney, A. Oteng-Yeboah, H. Pereira, S. Polasky, C. Prip, W. Reid, C. Samper, P. Schei, R. Scholes, F. Schutyser, and A. Van Jaarsveld. *Ecosystems and human well-being: biodiversity synthesis; a report of the Millennium Ecosystem Assessment*. World Resources Institute, 2005. URL `http://hdl.handle.net/20.500.11822/8755`. Type: Report.

J. A. Estes and D. O. Duggins. Sea otters and kelp forests in alaska: Generality and variation in a community ecological paradigm. *Ecol Monogr*, 65(1):75–100, 1995. doi: 10.2307/2937159.

L. Fahrig. Effects of habitat fragmentation on biodiversity. *Ann Rev Ecol Evol Syst*, 34 (1):487–515, 2003. doi: 10.1146/annurev.ecolsys.34.011802.132419.

L. Fahrig. Ecological responses to habitat fragmentation per se. *Ann Rev Ecol Evol and Syst*, 48(1):1–23, 2017. doi: 10.1146/annurev-ecolsys-110316-022612.

L. Fahrig, V. Arroyo-Rodríguez, J. R. Bennett, V. Boucher-Lalonde, E. Cazetta, D. J. Currie, F. Eigenbrod, A. T. Ford, S. P. Harrison, J. A. Jaeger, N. Koper, A. E. Martin, J.-L. Martin, J. P. Metzger, P. Morrison, J. R. Rhodes, D. A. Saunders, D. Simberloff, A. C. Smith, L. Tischendorf, M. Vellend, and J. I. Watling. Is habitat fragmentation bad for biodiversity? *Biol Conserv*, 230:179 – 186, 2019. ISSN 0006-3207. doi: 10.1016/j.biocon.2018.12.026.

R. J. Fletcher, N. S. Burrell, B. E. Reichert, D. Vasudev, and J. D. Austin. Divergent perspectives on landscape connectivity reveal consistent effects from genes to communities. *Curr Landsc Ecol Rep*, 1(2):67–79, Jun 2016. ISSN 2364-494X. doi: 10.1007/s40823-016-0009-6.

R. J. Fletcher, R. K. Didham, C. Banks-Leite, J. Barlow, R. M. Ewers, J. Rosindell, R. D. Holt, A. Gonzalez, R. Pardini, E. I. Damschen, F. P. Melo, L. Ries, J. A. Prevedello, T. Tscharntke, W. F. Laurance, T. Lovejoy, and N. M. Haddad. Is habitat fragmentation good for biodiversity? *Biol Conserv*, 226:9 – 15, 2018. ISSN 0006-3207. doi: 10.1016/j.biocon.2018.07.022.

S. D. Fretwell. *Populations in a seasonal environment*. Monogr Popul Biol, 1972.

N. J. Gotelli. Metapopulation models: The rescue effect, the propagule rain, and the core-satellite hypothesis. *Am Nat*, 138(3):768–776, 1991. doi: 10.2307/2462468.

T. Gouhier, F. Guichard, and A. Gonzalez. Synchrony and stability of food webs in metacommunities. *Am Nat*, 175(2):E16–E34, 2010. doi: 10.1086/649579. PMID: 20059366.

I. Hanski. Habitat fragmentation and species richness. *J Biogeogr*, 42(5):989–993, 2015. doi: 10.1111/jbi.12478.

C. Hauzy, M. Gauduchon, F. D. Hulot, and M. Loreau. Density-dependent dispersal and relative dispersal affect the stability of predator-prey metacommunities. *J Theor Biol*, 266(3):458 – 469, 2010.

L. Heckmann, B. Drossel, U. Brose, and C. Guill. Interactive effects of body-size structure and adaptive foraging on food-web stability. *Ecol Lett*, 15(3):243–250, 2012. doi: 10.1111/j.1461-0248.2011.01733.x.

A. M. Hein, C. Hou, and J. F. Gillooly. Energetic and biomechanical constraints on animal migration distance. *Ecol Lett*, 15(2):104–110, 2012. doi: 10.1111/j.1461-0248.2011.01714.x.

A. L. Herzig. Effects of population density on long-distance dispersal in the goldenrod beetle trirhabda virgata. *Ecology*, 76(7):2044–2054, 1995. doi: 10.2307/1941679.

A. C. Hindmarsh, P. N. Brown, K. E. Grant, S. L. Lee, R. Serban, D. E. Shumaker, and C. S. Woodward. Sundials: Suite of nonlinear and differential/algebraic equation solvers. *ACM Trans Math Soft (TOMS)*, 31(3):363–396, 2005.

M. D. Holland and A. Hastings. Strong effect of dispersal network structure on ecological dynamics. *Nature*, 456:792–794, 2008. doi: 10.1038/nature07395.

P. J. Hudson and I. M. Cattadori. The moran effect: a cause of population synchrony. *Trends Ecol Evol*, 14:1–2, 1999. doi: https://doi.org/10.1016/S0169-5347(98)01498-0.

J. D. Hunter. Matplotlib: A 2d graphics environment. *Comput Sci Eng*, 9(3):90–95, May 2007. ISSN 1521-9615. doi: 10.1109/MCSE.2007.55.

V. A. Jansen. The dynamics of two diffusively coupled predator–prey populations. *Theor Popul Biol*, 59(2):119 – 131, 2001. doi: https://doi.org/10.1006/tpbi.2000.1506.

A. Kahilainen, S. van Nouhuys, T. Schulz, and M. Saastamoinen. Metapopulation dynamics in a changing climate: Increasing spatial synchrony in weather conditions drives metapopulation synchrony of a butterfly inhabiting a fragmented landscape. *Glob Change Biol*, 24(9):4316–4329, SEP 2018. doi: 10.1111/gcb.14280.

T. Kalettka and C. Rudat. Hydrogeomorphic types of glacially created kettle holes in north-east germany. *Limnologica*, 36(1):54 – 64, 2006. ISSN 0075-9511. doi: 10.1016/j.limno.2005.11.001.

K. Koelle and J. Vandermeer. Dispersal-induced desynchronization: from metapopulations to metacommunities. *Ecol Lett*, 8(2):167–175, 2005. doi: 10.1111/j.1461-0248.2004.00703.x.

W. D. Koenig. Spatial autocorrelation of ecological phenomena. *Trends Ecol Evol*, 14 (1):22 – 26, 1999. doi: https://doi.org/10.1016/S0169-5347(98)01533-X.

M. Kuussaari, M. Nieminen, and I. Hanski. An experimental study of migration in the glanville fritillary butterfly melitaea cinxia. *J Anim Ecol*, 65(6):791–801, 1996. doi: 10.2307/5677. URL `http://www.jstor.org/stable/5677`.

R. M. LeCraw, P. Kratina, and D. S. Srivastava. Food web complexity and stability across habitat connectivity gradients. *Oecologia*, 176(4):903–915, 2014. doi: 10.1007/s00442-014-3083-7.

R. Levins. Some demographic and genetic consequences of environmental heterogeneity for biological control1. *Bull Entomol Soc Am*, 15(3):237–240, 1969. doi: 10.1093/besa/15.3.237.

P. Moran. The statistical analysis of the canadian lynx cycle. *Aust J Zool*, 1:291 – 298, 1953. doi: 10.1071/ZO9530163.

T. E. Oliphant. *Guide to NumPy*. CreateSpace Independent Publishing Platform, USA, 2nd edition, 2015. ISBN 151730007X, 9781517300074.

M. Penrose. *Random Geometric Graphs*. Oxford University Press, 2003.

H. M. Pereira, P. W. Leadley, V. Proença, R. Alkemade, J. P. W. Scharlemann, J. F. Fernandez-Manjarrés, M. B. Araújo, P. Balvanera, R. Biggs, W. W. L. Cheung, L. Chini, H. D. Cooper, E. L. Gilman, S. Guénette, G. C. Hurtt, H. P. Huntington, G. M. Mace, T. Oberdorff, C. Revenga, P. Rodrigues, R. J. Scholes, U. R. Sumaila, and M. Walpole. Scenarios for global biodiversity in the 21st century. *Science*, 330 (6010):1496–1501, 2010. ISSN 0036-8075. doi: 10.1126/science.1196624.

R. H. Peters. *The Ecological Implications of Body Size:*. Cambridge University Press, Cambridge, 10 1983.

P. Pillai, A. Gonzalez, and M. Loreau. Metacommunity theory explains the emergence of food web complexity. *PNAS*, 108(48):19293–19298, 2011. ISSN 0027-8424. doi: 10.1073/pnas.1106235108.

S. L. Pimm, C. N. Jenkins, R. Abell, T. M. Brooks, J. L. Gittleman, L. N. Joppa, P. H. Raven, C. M. Roberts, and J. O. Sexton. The biodiversity of species and their rates of extinction, distribution, and protection. *Science*, 344(6187), 2014. ISSN 0036-8075. doi: 10.1126/science.1246752.

S. J. Plitzko and B. Drossel. The effect of dispersal between patches on the stability of large trophic food webs. *Theor Ecol*, 8(2):233–244, 2015. doi: https://doi.org/10.1007/s12080-014-0247-3.

B. C. Rall, U. Brose, M. Hartvig, G. Kalinkat, F. Schwarzmüller, O. Vucic-Pestic, and O. L. Petchey. Universal temperature and body-mass scaling of feeding rates. *Philos Trans R Soc B Biol Sci*, 367(1605):2923–2934, 2012. doi: 10.1098/rstb.2012.0242.

E. Ranta, V. Kaitala, J. Lindstrom, and H. Lindén. Synchrony in population dynamics. *Proc R Soc B Biol Sci*, 262:113 –118, 1995. doi: https://doi.org/10.1098/rspb.1995.0184.

J. M. K. Rip and K. S. McCann. Cross-ecosystem differences in stability and the principle of energy flux. *Ecol Lett*, 14(8):733–740, 2011. doi: 10.1111/j.1461-0248.2011.01636.x.

R. Ryser, J. Häussler, M. Stark, U. Brose, B. C. Rall, and C. Guill. The biggest losers: habitat isolation deconstructs complex food webs from top to bottom. *Proc R Soc B Biol Sci*, 286(1908):20191177, 2019. doi: 10.1098/rspb.2019.1177.

M. Scheffer, S. Hosper, M.-L. Meijer, B. Moss, and E. Jeppesen. Alternative equilibria in shallow lakes. *Trends Ecol Evol*, 8(8):275 – 279, 1993. ISSN 0169-5347. doi: 10.1016/0169-5347(93)90254-M.

D. E. Schindler, J. B. Armstrong, and T. E. Reed. The portfolio concept in ecology and evolution. *Front Ecol Environ*, 13(5):257–263, 2015. doi: 10.1890/140275.

F. D. Schneider, U. Brose, B. C. Rall, and C. Guill. Animal diversity and ecosystem functioning in dynamic food webs. *Nat Commun*, 7(12718), 2016. doi: 10.1038/ncomms12718.

T. N. Sherratt, X. Lambin, S. J. Petty, J. L. Mackinnon, C. F. Coles, and C. J. Thomas. Use of coupled oscillator models to understand synchrony and travelling waves in populations of the field vole *Microtus agrestis* in northern england. *J Appl Ecol*, 37 (Suppl. 1):148 – 158, 2000. doi: https://doi.org/10.1046/j.1365-2664.2000.00472.x.

J. J. Sloggett and W. W. Weisser. Parasitoids induce production of the dispersal morph of the pea aphid, acyrthosiphon pisum. *Oikos*, 98(2):323–333, 2002. doi: 10.1034/j.1600-0706.2002.980213.x.

J. T. Thorson, M. D. Scheuerell, J. D. Olden, and D. E. Schindler. Spatial heterogeneity contributes more to portfolio effects than species variability in bottom-associated marine fishes. *Proc R Soc Lond, B*, 285:20180915, 2018. doi: https://doi.org/10.1098/rspb.2018.0915.

D. Urban and T. Keitt. Landscape connectivity: A graph-theoretical perspective. *Ecology*, 82(5):1205–1218, 2001. doi: 10.1890/0012-9658(2001)082[1205:LCAGTP]2.0.CO;2.

S. Van der Walt, S. C. Colbert, and G. Varoquaux. The numpy array: A structure for efficient numerical computation. *Comp Sci Eng*, 13:22–30, 2011. doi: 10.1109/MCSE.2011.37.

P. M. Wade. The colonisation of disturbed freshwater habitats bycharaceae. *Folia Geobot Phytotaxon*, 25(3):275–278, Sep 1990. ISSN 1874-9348. doi: 10.1007/BF02913027.

J. I. Walting and M. A. Donnelly. Fragments as islands: a synthesis of faunal responses to habitat patchiness. *Conserv Biol*, 20(4):1016–1025, 2006. doi: 10.1111/j.1523-1739.2006.00482.x.

S. Wang and M. Loreau. Ecosystem stability in space: α-, β- and γ-variability. *Ecol Lett*, 17(8):891–901, 2014. doi: 10.1111/ele.12292.

R. H. Whittaker. Evolution and measurement of species diversity. *Taxon*, 21(2/3):213–251, 1972. doi: 10.2307/1218190.

P. Yodzis and S. Innes. Body size and consumer-resource dynamics. *Am Nat*, 139(6):1151–1175, 1992. doi: 10.2307/2462335.

Chapter 4

Comparison of local and regional scale processes on observed trends in $\bar{\alpha}$- and β-diversity

Food web robustness, mean patch isolation and minimum nearest neighbor distance of patches determine local and between-patch diversity in a complex meta-community model

Markus Stark[1], Christian Guill[1]

in preparation

1 - Institute of Biochemistry and Biology, University of Potsdam, Maulbeerallee 2, 14469 Potsdam, Germany

Abstract

Anthropogenic habitat change is one of the main drivers of declining biodiversity but the magnitude of the effect depends on specific properties of the landscape and the species community. To protect biodiversity, it is therefore necessary to identify relevant characteristics that explain diversity patterns and enable target oriented measures from local to regional scales. Our theoretical approach simulate dynamics of a meta-food web of 40 species on 40 habitat patches and we evaluate the emerging diversity patterns using a machine learning approach. We show that the mean local ($\bar{\alpha}$-) diversity is mainly determined by the robustness of the food web and additionally to a lesser extent by the mean patch isolation. The large standard deviation in food web robustness emphasizes that it is highly food web dependent how sensitive it reacts to a change of habitat structure. In contrast, the best predictors explaining differences in species composition between patches (β-diversity) were predictors of the landscape, namely mean patch isolation and the minimum distance to the next neighbor habitat, but the robustness of a food web still contributes to explain more than 35% of the explained variance. We conclude that, if we want to preserve species and biodiversity, we should first understand the local food web structure in which species are embedded in, and in a second step integrate landscape structure and characteristics that contribute to the preservation of a metacommunity.

Introduction

Currently we are observing a world-wide decline in biodiversity across all types of ecosystems (Assessment, 2005; Pimm et al., 2014). Despite the large number of diverse ecosystems, such as marine, grassland or tropical biota, which differ largely in their respective abioitc and biotic conditions, we can identify common relevant processes that explain how biodiversity can be maintained, e.g. Chesson (2000). These processes are often categorized into two different scales, the local and regional scale. On the local scale, ecological processes such as intra- or interspecific competition (Tilman, 1982) or trophic interactions (Connell, 1971) determine the coexistence of the local species community. Although these local processes are the basis for the coexistence of species, also regional processes have an effect on biodiversity. At the regional scale, processes such as habitat change and habitat loss e.g. due to deforestation or fragmentation, select for different species communities and limit for example the ability of species to disperse between habitats (Prugh et al., 2008). In an early experiment, Tilman already emphasized the relevance of both local and regional scale processes on species richness of plant communities through the role of dispersal limitation (Tilman, 1997). A large species richness relied on a large number of introduced seeds, but at the same time also on local soil conditions and the presence of individual species. Thus, both scales can involve processes and mechanisms that affect observed diversity patterns (Chesson, 2000; HilleRisLambers et al., 2012; Leibold and Chase, 2017). However, there is still controversy on which regional processes and resulting structural characteristics make a relevant contribution to maintaining biodiversity across ecosystems and, further, what magnitude of impact do these regional processes have on biodiversity compared to local processes (Fahrig et al., 2019; Fletcher et al., 2018).

A very well-studied regional characteristic affecting diversity patterns of communities is patch isolation, and the associated constraints for dispersal rates that has already been a central determinant in the theory of island biogeography (MacArthur and Wilson, 1967). The theory predicts a decreasing local species richness (α-diversity) with increasing patch isolation. Later theoretical approaches (e.g. Mouquet and Loreau (2002)) and an empirical review by Cadotte et al. (2006) showed a predominantly unimodal relationship between dispersal rate, with mean patch isolation used as a proxy, and α-diversity. They predict high levels of α-diversity for an intermediate mean patch isolation since at a high mean patch isolation (corresponding to a low dispersal rate), the rescue effect (Gotelli, 1991) is limiting, and species can experience increased competition due to an over-exploitation of resources. In comparison at low mean patch isolation (or high dispersal rate), biotic homogenization is often observed, where predators can forage over all patches, increasing top down control and removing prey refuges (Briggs and Hoopes, 2004; Grainger and Gilbert, 2016; LeCraw et al., 2014). Despite these advances, most of these studies either focus exclusively on the effects of the structure of the landscape on biodiversity, or largely consider local interactions on a single trophic level (Fahrig, 2003; Rybicki and Hanski, 2013), although complex food webs are a central scheme in natural habitats (Dunne, 2005). Accordingly, trophic interactions between species and their impact on diversity patterns remain largely unaddressed (but see also Amarasekare (2008); Gravel et al. (2011); Liao et al. (2017)).

Both local trophic interactions among species and regional spatial structures can affect and determine the diversity of a complex metacommunity. A central role for local trophic interactions have predator species. They can alter, for example, the dispersal behavior of prey species that affect diversity patterns on the regional scale (Cadotte et al., 2006; Macedo, 2012). Another effect of predator species is that they can reduce local competition among prey species by selectively foraging on them, which can preserve local α-diversity (Terborgh, 2015). This demonstrates that trophic interactions have considerable effects on the stability and persistence of a local species community but that trophic interactions are also linked to the regional scale and affect the species distribution among habitats (Leibold and Chase, 2017). At the same time the regional structure of the landscape and corresponding dispersal of species can contribute to diversity patterns and affect the trophic structure of a local food web. For example, an increase of mean patch isolation can have a negative effect on food web complexity, decreasing α-diversity (Gravel et al., 2011). In comparison, a positive impact on α-diversity of the landscape structure can be attributed to dispersal corridors. Their connectance of nearby habitats can buffer against species loss by increasing local food supply (Damschen et al., 2006) or can offer the possibility to temporarily escape local predation although habitats are largely isolated. Such better mechanistic understanding of these mutual dependencies between trophic and landscape structure support our knowledge on current diversity patterns, and helps to create a more holistic approach to maintain biodiversity which is a more than ever pressing task (Gross et al., 2020).

To analyze diversity patterns, we use a meta-food web approach based on an allometric trophic network (ATN) model that comprises a large community of species and is embedded in a complex network of habitat patches. We use this approach following Ryser et al. (2019) because we want to emphasize trophic interactions in metacommunities which are represented in a very complex network of interactions between species in the model, and since the model creates an allometric trophic structure that is comparable to empirical food webs (Riede et al., 2011). Further the complex network of the landscape allows for a distinction of common regional landscape attributes such as patch isolation and their impact on mean α- diversity ($\bar{\alpha}$) and differences in species composition (β-diversity). For a solid validation we use a machine learning approach (random forest) and select for relevant predictor variables. We distinguish between local, i.e. food web specific predictors and regional, i.e. landscape specific predictors. The analysis runs across a gradient of mean patch isolation that we know has an effect on both $\bar{\alpha}$- and β-diversity patterns (Ryser et al., 2019).

On the local scale we evaluate the $\bar{\alpha}$-diversity, where we expect to find food webs that are intrinsically more stable than other ones (Jacquet et al., 2016). These differences in stability and robustness of the food web suggest that they can also buffer against negative effects of landscape structure, such as a large mean patch isolation which is thought to decrease α-diversity (Gravel et al., 2011; Ryser et al., 2019). A regional structural aspect that can support $\bar{\alpha}$-diversity is the local clustering of patches, where dispersal corridors increase the likelihood of species to persist. On the regional scale, we expect an increase of β-diversity for a large patch isolation (Ryser et al., 2019) which is motivated through different routes of extinction cascades between patches. Beside regional characteristics, we also expect that the local structure of the food web has an impact on β-diversity. For example, if the intrinsic food web structure is very stable, we do not expect large differences in the species composition among patches. Yet, if the stability of a food web is low, larger differences among patches can be expected (high β-diversity), in particular in a state of high patch isolation where biotic homogenization between patches through dispersal is not possible.

Methods

General framework

We analyzed a meta-food web model in a landscape of 40 randomly distributed habitat patches (Figure 4.1), based on the model by Ryser et al. (2019). In each patch, which is a local habitat, the local food web comprises a maximum number of 40 species which interact through feedings links. On the landscape scale, dispersal links between patches describe the regional interactions that are characterized by an inflow (immigration) and an outflow (emigration) of biomass.

Feeding and dispersal dynamics are described using ordinary differential equations. The general form of the rate of change in biomass density, $B_{i,z}$, of species i on patch z is given by

$$\frac{dB_{i,z}}{dt} = T_{i,z} - E_{i,z} + I_{i,z}\,, \tag{4.1}$$

with $T_{i,z}$ the rate of change in biomass density determined by local feeding interactions (Eq. (4.2) & (4.3) & (4.4)), $E_{i,z}$ the total emigration rate of species i from patch z (Eq. 4.6), and $I_{i,z}$ the total rate of immigration of species i into patch z (Eq. 4.8).

Trophic interactions

The local trophic interactions are based on an ATN model developed by Schneider et al. (2016) taking into account allometric degree distributions of species and including empirical data for scaling relationships of body masses. Following their basic idea, we made a general distinction between animal and plant species, with a fixed number of 30 animal and 10 plant species in each food web. Gain and loss of biomass density due to trophic interactions ($T_{i,z}$, Eq. (4.1)) are described for both plant and animal species with a species specific per capita net growth rate ($v_{i,z}$). For plant species, it is given by

$$T_{i,z} = v_{i,z}B_{i,z} = r_iB_{i,z} - \sum_k B_{k,z}F_{ki,z} - x_iB_{i,z}\,, \tag{4.2}$$

with a body mass (m) dependent growth rate $r_i = m_i^{-0.25} min_l\left(\frac{N_l}{K_{i,l}+N_l}\right)$, and for animal species it is given by

$$T_{i,z} = v_{i,z}B_{i,z} = e_PB_{i,z}\sum_j F_{ij,z} + e_AB_{i,z}\sum_k F_{ik,z} - \sum_k B_{k,z}F_{ki,z} - x_iB_{i,z}\,, \tag{4.3}$$

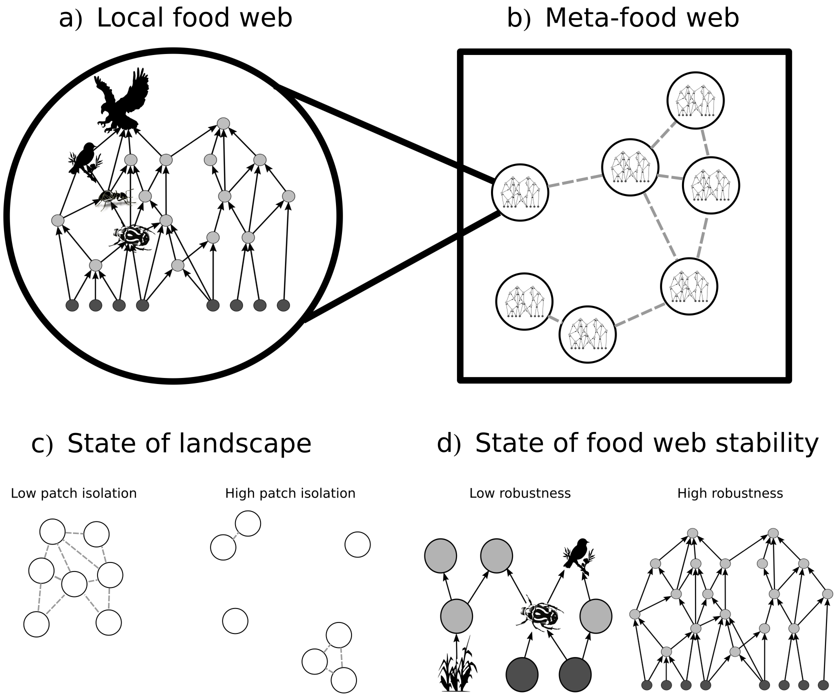

FIGURE 4.1: Overview of our meta-food web model approach: a) local food web of species connected through feeding interactions b) structure of the landscape with a set of patches where each patch comprise a local food web of species. We consider a fixed number of patches randomly distributed in the landscape. Dashed line in b) indicates dispersal links between patches and we model differently fragmented landscapes c) by varying the mean patch isolation of patches. For evaluation of the stability of the food web d) we consider a measure of robustness based on the persistence of species. A low robustness implies a low number of species that survive model simulations with and without metabolic dispersal losses from emigration, in comparison to a high robustness where a large number of species survives.

with feeding rate $F_{ij,z}$ (see below, Eq. (4.5)) and a conversion efficiency e_i. The trophic dynamics of the species on a given patch are supplemented by ODEs for the dynamics of two abiotic nutrients which serve as resources for the plants:

$$\frac{dN_{l,z}}{dt} = D(S_l - N_l) - \nu_l \sum_z r_i B_{i,z} \,. \tag{4.4}$$

For both plants and animal species (i) we assume a loss due to consumption by consumer/predator species k which is also defined as prey specific feeding rate $F_{ki,z}$. Metabolic demands are defined as $x_i = 0.138 m_i^{-0.25}$ for plant species and $x_i = 0.314 m_i^{-0.305}$ for animal species (Ehnes et al., 2011). Nutrient dynamics are based on a global turnover rate $D = 0.25$, a supply concentration S_l which defines the maximum nutrient level for each nutrient l and the plant uptake depends on a relative nutrient content ν_l of a plant species. See Table 4.1 for more information on each variable.

Feeding rates of an animal species i on a prey species j (either plant or animal species) $F_{ij,z}$ are expressed as a Beddington-DeAngelis functional response term (Beddington, 1975; DeAngelis et al., 1975):

$$F_{ij,z} = \frac{\omega_i \kappa_{ij} B_{j,z}^{1+q}}{1 + cB_{i,z} + \omega_i \sum_k \kappa_{ik} h_{ik} B_{k,z}^{1+q}} \cdot \frac{1}{m_i} \, . \tag{4.5}$$

The feeding rate of an animal species i is scaled by the respective body mass m_i of the species and considers an interference competition c, a resource specific capture coefficient κ_{ij}, a resource specific handling time h_{ij} which determines the time a species needs to kill, ingest and digest its prey, a relative consumption rate ω_i and a Hill coefficient of $1 + q$. See Table 4.1 and Supplements for more information on each variable.

Dispersal

We model dispersal between local communities as a dynamic process of emigration and immigration, assuming that dispersal occurs on the same time scale as the local population dynamics (Amarasekare, 2008).

Emigration

The rate of emigration depends on the net per capita growth rate $\upsilon_{i,z}$ of the species i on patch z, which reflects the current situation of a species in its patch. For animal species, we assumed an increased emigration when the local net growth rate decreases, which represents poor local conditions for the species. Based on empirical examples we assumed for plant species both scenarios, an increased and a decreased emigration when the local net growth rate decreases which is assigned randomly to each plant species (Macedo, 2012; Miyazaki et al., 2009).

The total rate of emigration of species i from patch z is

$$E_{i,z} = d_{i,z} B_{i,z} \, , \tag{4.6}$$

with $d_{i,z}$ as the corresponding per capita dispersal rate. We model $d_{i,z}$ as

$$d_{i,z} = \frac{a}{1 + e^{-b(-x_i - v_{i,z})}} , \tag{4.7}$$

with a, the maximum dispersal rate, b, determining the shape of the dispersal rate (Figure C1), x_i, the inflection point determined by the metabolic demands per unit biomass of species i, and $v_{i,z}$, the per capita net growth rate of species i on patch z (see Eq. (4.2) & (4.3)). The per capita dispersal rate $d_{i,z}$ thus accounts for emigration cues such as resource availability, predation pressure and inter- and intraspecific competition (Bowler and Benton, 2005; Fronhofer et al., 2018). In each simulation run a was sampled from a Gaussian distribution $(\mu_{a_A}, \sigma_{a_A})$ and b from an uniform distribution within different limits for consumer and plant species (see Table 4.1). The selected intervals reflect the different dispersal strategies of an animal and plant species.

Immigration

The immigration of species i into patch z,$I_{i,z}$, depends on the emigration rates $E_{i,n}$ of a species i from all neighbouring patches n that are within the species' dispersal range δ_{max} and on the specific dispersal network, which depends on the relative position of the patches in the landscape (see below) and is mathematically described by a success and weighting term. The immigration rate of the biomass density of the species i into the patch z follows

$$I_{i,z} = \sum_{n \in N_z} E_{i,n}(1 - \delta_{nz}) \frac{1 - \delta_{nz}}{\sum_{m \in N_n} 1 - \delta_{nm}} , \tag{4.8}$$

where N_z and N_n are the sets of all patches within dispersal range of the species i on patches z and n, respectively. The success term $(1 - \delta_{nz})$ is the fraction of successfully dispersed biomass and assumes a linear increase in biomass loss with δ_{nz}, the distance between the patches n and z relative to the maximum dispersal distance. The weighting term $\frac{1-\delta_{nz}}{\sum 1-\delta_{nm}}$ determines the proportion of biomass of specie emigrating from the source patch n to the target patch z. This proportion depends on the relative distance between the patch δ_{nz} and the relative distances to all other potential target patches m on the source patch n, δ_{nm}. For numerical reasons we do not allow dispersal flows with $I_{i,z} < 10^{-10}$. In this case we immediately set $I_{i,z}$ to 0.

Landscape properties

Landscapes with different mean patch isolation are generated by random geometric graphs, in short RGG (Penrose, 2003). The (x, y)-coordinates for each local patch are drawn randomly from a bivariate uniform distribution over the intervall $[0 : 1] \times [0 : 1]$. Between each simulation, the degree of mean patch isolation was gradually changed by the species maximum dispersal distance δ_{max}, varied systematically between 0.04 and 0.39, producing landscapes from very high to intermediate mean patch isolation (ρ_{RGG} in Table 4.2). Compared to Ryser et al. (2019)), we however kept a fixed dispersal range for all species (only minor effects of species-specific dispersal ranges in Ryser et al. (2019)) in a single simulation run.

Statistics and evaluation

We recorded the following output variables for each simulation run: the mean biomass density of each species i on each patch z over the last 20,000 time steps, $\overline{B}_{i,z}$, to determine the level of diversity on different spatial scales. By counting the species i present in the patch z (i.e. those with $\overline{B}_{i,z} > 10^{-20}$ at the end of a simulation run), we calculate α-diversity as local species richness and $\overline{\alpha}$-diversity as average α-value over all patches Z, the total regional (γ-) diversity as the number of species that have a biomass density $\overline{B}_{i,z} > 10^{-20}$ on any patch and β-diversity is the share of diversity that shows differences in species compositions between local communities. We relate $\bar{\alpha}$-, β- and γ-diversity to each other using a multiplicative approach (Whittaker, 1972), i.e. $\bar{\alpha} \cdot \beta = \gamma$. Further, we distinguish between local and regional parameters that are relevant predictors for the model input: local parameters - robustness, standard deviation of robustness and hill coefficient; regional parameters - mean patch isolation, minimum distance between two patches, maximum emigration rates of animal and plant species, shape parameter of emigration function for animal and plant species, transitivity and mean closeness centrality of patches. Table 4.2 describes the predictors used for the best model fit and the remaining predictors are described in the supplements (see Table C1).

TABLE 4.1: Model parameters and their respective description

Parameter	**Description**	**Value or formula**
	Trophic interactions between species	
e_A, e_P	conversion efficiency for animal (A) and plant species (P)	0.906, 0.545 ; (Lang et al., 2017)
x_A, x_P	scaling constant of metabolic demands for animal (A) and plant species (P)	0.314, 0.138; (Yodzis and Innes, 1992)
ω_i	relative consumption rate of predator i	$\frac{1}{\text{number of resource species of i}}$
κ_{ij}	capture coefficient of predator species i on prey species j with body masses m_i and m_j, respectively (Details in Supplement and Schneider et al. (2016)).	$\lambda_l m_i^{\beta_i} m_j^{\beta_j} \left(\frac{m_i}{m_j 100} e^{1-\frac{m_i}{m_j 100}} \right)^2$
β_i	mean and standard deviation of scaling exponent for capture coefficient	$\mu = 0.42, \sigma = 0.05$ (pred.)
β_j	for predator i and prey j. For plant species $m_j^{\beta_j} = 1$, as plants do not move.	$\mu = 0.19, \sigma = 0.04$ (prey)
h_{ij}	handling time of predator i on prey species j with a a scaling constant h_0, and a body mass scaling through the exponents η_i and η_j (Details in Supplement)	$h_0 m_i^{\eta_i} m_j^{\eta_j}$
$1 + q$	Hill coefficient	normal distribution, $\mu = 1.5, \sigma = 0.15$
	Nutrient dynamics	
$K_{i,l}$	half saturation density of nutrient uptake	uniform distribution, $\in$ (0.1, 0.2)
S_l	nutrient supply concentration	50
	Dispersal dynamics	
δ_{max}	species maximum dispersal distance	varied between [0.04,0.39]
a	maximum emigration rate for animal and plant species defined by mean and standard deviation (The cut off for the distribution is set to $3 \cdot \sigma_a$).	normal distribution, $\mu = 0.1, \sigma = 0.03$
b	shape parameter of the emigration function	uniform distribution, (0,19)-(animal); (-20,19)-(plant)

Evaluation and visualization

We used a machine learning approach called random forest (RF) that utilizes a large number of decision trees for a model prediction. For each prediction of a variable, we used 2500 individual trees calculated in parallel via bootstrapping and trained them

TABLE 4.2: Definition and ecological interpretation of local and regional predictor variables of the best model. Remaining predictors of the full model are explained in Table C1

Parameter	Description and interpretation of predictor variables	Definition
	Local predictors	
R	Robustness - mean final species richness (μ_α) of 20 simulation runs after computation of the population dynamics with and without a perturbation of a food web on a single patch. A perturbation is described as larger mortality rate for species dispersing through a fragmented landscape. The first 10 simulations assume complete dispersal loss for emigrating biomass (α_l) and the other 10 simulations no dispersal loss (α_{nl}), while replicates differed in initial nutrient biomass concentrations. The more species survive, the larger the robustness and the larger the stability of the food web.	$\frac{\mu_{\alpha_l}+\mu_{\alpha_{nl}}}{2}$
R_{SD}	Standard deviation of the robustness R. It describes the variation in species richness between a state of no dispersal loss and full dispersal loss of a food web. The larger the standard deviation between the two cases (no and complete dispersal loss), the larger can be the effect of the landscape on the species richness.	$\sqrt{\frac{\sum_{i=1}^{m}(\alpha_{l,i}-\mu_{\alpha_l})^2+(\alpha_{nl,i}-\mu_{\alpha_{nl}})^2}{m}}$
	Regional predictors	
ρ_{RGG}	Mean patch isolation of a landscape, defined as 1 - connectance of the patch network, with L, the number of undirected dispersal links. The larger the number of links the lower the mean patch isolation of the landscape.	$1-\frac{L}{\frac{1}{2}Z\cdot(Z-1)}$
d_{min}	Minimum distance between two patches n and m in each randomly constructed landscape of N patches.	$\min(D_{n,m})$
b	shape parameter of emigration function. For each species, it represents how sharp the transition of the emigration rate is between positive and negative net growth rate.	(0,19)(animal); (-20,19)(plant)

on a subset of the data set. Derived from the random forest approach, we used an importance measure (relative importance) to quantify and compare the relevance of each predictor value. The choice of predictors for the full model and best model is based on a two step selection process. All predictor variables with a linear correlation coefficient < 0.75 are selected for the full model, being not strongly correlated with each other. As a second step, the predictors for the best model are selected by the most parsimonious generalized additive model (based on p-value < 0.05 and minimal AIC) that show the same trends for diversity and similar results of explained variance (see Supplements). The maximum number of input variables for the training data set were 11 parameters as predictors (Table 4.2 and Table C1 & C3, full model) which are standardized between 0 and 1, and two different diversity measures, $\bar{\alpha}$- and β-diversity, as output. Predictors can be separated into three local predictors and eight regional predictors. Local predictors comprise a measure for robustness, its standard deviation and the Hill coefficient. We use the Hill coefficient as predictor variable because it contributes to the dynamic stability of food webs by dampening of oscillatory population dynamics (Williams and Martinez, 2004). As regional predictors we use the mean patch isolation, the minimum distance to the nearest neighbor patch for a whole landscape, the maximum emigration rates for animal and plant species as predictor for mean dispersal loss, the shape parameter of emigration function as an indicator of the intensity of a species' response to changing growth conditions, the closeness centrality averaged over the whole landscape and the transitivity, a measure closely related to the clustering coefficient.

While calculating the trees, the random forest approach used cross-validation in calculating the OOB (Out of Bag score), a measure for its accuracy which is comparable to the R^2 results of a statistical model. See Supplements for more information on the predictor variables, model selection and calculations.

Simulation details

The presented results are based on two simulation data sets. The first uses the full range of parameters, while the second is a subset selected for medium food web stability (R,[0.33,0.66]) and RGGs with a small minimum distance to the nearest neighbor ($d_{min} < 0.2$; see Table 4.1 and 4.2 for more details). We distinguish between these two data sets as we expect a larger impact of landscape structure on β-diversity for the selected subset. Based on our definition of robustness (see Table 4.2), we argue that when robustness is either very high or low, the food webs are inherently so stable or unstable, that the landscape structure can not affect $\bar{\alpha}$- and β-diversity. Consequently, we selected food webs with an intermediate robustness. A selection for RGGs with a small minimum nearest neighbor distance is motivated by the reasoning in Ryser et al. (2019), where it is argued that local cluster formation increase β-diversity, emphasizing the landscape structure. Between the simulations we varied the maximum dispersal range with a step size of 0.01 between 0.04 and 0.39 for intermediate to high mean patch isolation (see also section 4), as in this range a larger increase in β-diversity is expected (Ryser et al., 2019). For the full data set, 30 replicates of a fixed dispersal range 30 were simulated, that differ in food web structure and landscape (random position of the patches), resulting in a total number of 1085 simulation runs. Of these, 136 were terminated by reaching the maximum computation time of 5 days per simulation (resulting in 949 simulation runs that were evaluated). For the subset 720 simulations were started and 109 were terminated (total no. of simulations = 611).

For each simulation run, we initialized our model with the following conditions: Initial biomass densities $B_{i,z}$ were kept identical for each species ($B_{i,z} = 1$) to avoid stochastic extinctions due to low initial biomass densities at the start of a simulation run, as well as confounding effects on β-diversity. Also, environmental conditions on each patch are kept identical for the species (identical nutrient supply concentrations). Starting from these conditions, we numerically simulated local food web and dispersal dynamics over 100,000 time steps by integrating the system of differential equations implemented in C using procedures of the SUNDIALS CVODE solver version 2.7.0 (backward differentiation formula with absolute and relative error tolerances of 10^{-10} (Hindmarsh et al., 2005)). For numerical reasons, a local population was considered extinct once $B_{i,z} < 10^{-20}$, and $B_{i,z}$ was then immediately set to 0. We performed statistical analyses in Anaconda (Python version 3.7.6 in particular NumPy, Matplotlib, Scikit-learn and Pandas (Hunter, 2007; Oliphant, 2015; pandas development team, 2020; Pedregosa et al., 2011; Van der Walt et al., 2011) and used for parallelization of the simulations GNU parallel (Tange, 2018).

Results

With the focus on identifying key predictors that explain the trends in diversity, we selected uncorrelated predictors for the full model (11 predictors) in a first step and the most relevant predictors for a best model in a second step. We identified five relevant predictors for $\bar{\alpha}$-diversity and four predictors for β-diversity for the best model (Figure 4.2). Our full model fit explained about 90% of the variance for $\overline{\alpha}$-diversity and 48% of β-diversity (see Table 4.3). Almost equally performs the best model fit with 89% and 50% explained variance for $\overline{\alpha}$- and β-diversity, respectively. For the subset with a distinct selection of food webs and landscapes (see Methods 4), the explained variance for $\overline{\alpha}$-diversity increased to 99% and β-diversity to 84% (Table 4.3).

TABLE 4.3: Overview of model results for random forest approach.

Model	**OOB**
local $\bar{\alpha}$-diversity - full data set, all - eleven predictors	0.90
local $\bar{\alpha}$-diversity - full data set, best model - five predictors	0.89
local $\bar{\alpha}$-diversity - subset - five predictors	0.99
β-diversity - full data set, all - eleven predictors	0.48
β-diversity - full data set, best model - four predictors	0.50 [1]
β-diversity - subset - four predictors	0.84

To estimate the relevance of each predictor, relative importances were calculated with the random forest approach. The noticeably best predictor variable for $\overline{\alpha}$-diversity for all three models is one of the local predictors, the food web robustness (Figure 4.2, predictor 1), which accounts for about 60% of the total explained variance (about 90%). Furthermore, the standard deviation of robustness (Figure 4.2, predictor 2) accounted for a relative importance of about 30% of the explained variance. Compared to the two local predictors, the proportion of variance for $\overline{\alpha}$-diversity explained by landscape structure is small (around 10 - 15%) in all model approaches, highlighting the relevance of the composition of the local food web for $\overline{\alpha}$-diversity (Figure 4.2, α-diversity all & best model & subset).

For β-diversity, the relative importance of each predictor in the full model are more evenly distributed with the share of all regional predictors of around 60% and of all local predictors around 40% (Figure 4.2, β-diversity all, best model, subset). For the best model, most important is the regional predictor mean patch isolation with the largest

---

[1] The larger OOB-score for the best model compared to the full data set probably arise due to the stochastic nature of calculation, where 2500 random trees are generated for each model.

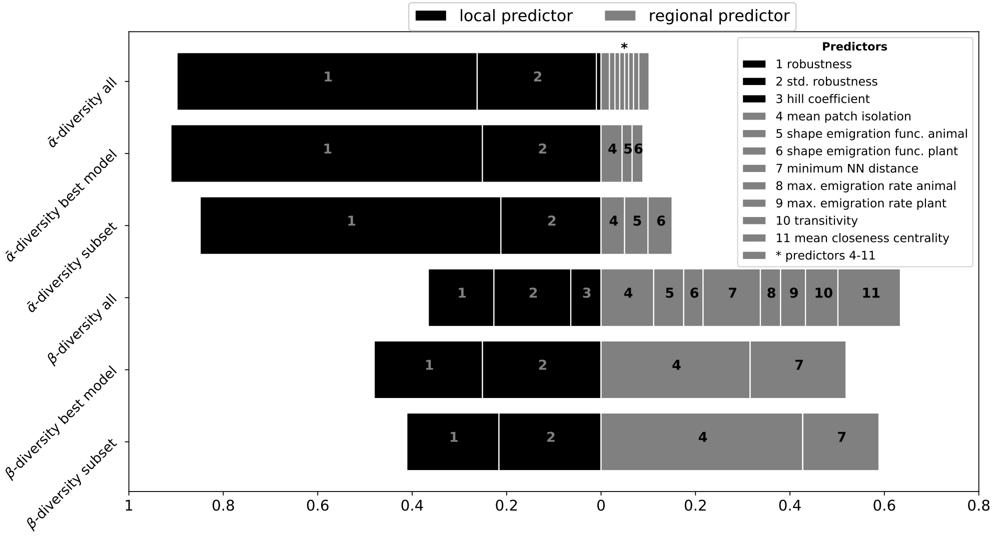

FIGURE 4.2: Proportion of relative importances for each predictor of six random forest models. The first three bars depict three model fits predicting local $\overline{\alpha}$-diversity. First row the full simulation data set with eleven uncorrelated predictors, second row the full simulation data set with five predictors (most parsimonious model for $\overline{\alpha}$-diversity) and third row a subset with five predictors. The lower three bars depict three model fits predicting regional β-diversity. Fourth row the full simulation data set with eleven predictors, fifth row the full simulation data set with four predictors (most parsimonious model for β-diversity) and sixth row a subset with four predictors.

proportion of about 30% of explained variance (Figure 4.2, predictor 4). The second largest proportion has the local predictor robustness (around 20%), closely followed by the minimum nearest neighbor distance (Figure 4.2, predictor 7) and the standard deviation in robustness (Figure 4.2, predictor 2). For the subset of the simulations (see details in Methods), the predictive power for β-diversity increases with an explained variance of almost 85% (see Table 4.3, β-diversity best model & subset). Particular noteworthy is the increased share of relative importance for the predictor mean patch isolation from around 30 to 45% (Figure 4.2, β-diversity subset). The subsequent part describes the visible trends for the random forest model.

In general, trends for local predictors are more pronounced for $\overline{\alpha}$-diversity compared to regional predictors which is consistent with their relative importances (Figure 4.2) and the trends are qualitatively the same for both, the best model of the full data set and the subset (Figure 4.3). $\overline{\alpha}$-diversity increases strongly with robustness, but decreases with the standard deviation of robustness Figure 4.3 A,B). An increase in the

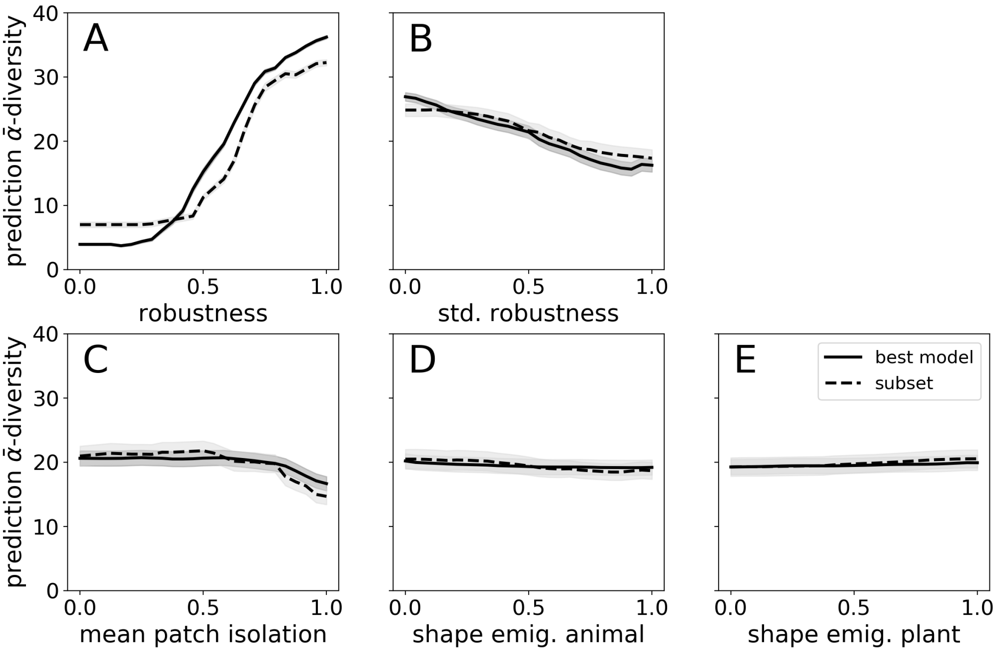

FIGURE 4.3: Partial dependence plots for $\overline{\alpha}$-diversity and five selected predictors of the best model for the full data set (solid line) and subset (dashed line). The two local predictors are the robustness and standard deviation of robustness as well as three regional predictor, the mean patch isolation, shape of emigration curve for animal and plant species. The shaded area in grey indicates the 95% confident interval of model results.

predictor of mean patch isolation results in a weak decrease in local $\overline{\alpha}$-diversity, which reflects the trends shown in the overview of replicated results of Ryser et al. (2019) (Figure C2, in Supplements). The other two regional predictors (Figure 4.3 D,E), indicate a very weak positive trend for the shape of emigration function of plant species and a very weak negative trend for animal species.

For β-diversity, the trends for the best model fit of the whole data set and subset are identical (Figure 4.4). β-diversity is increasing with the regional predictor of mean patch isolation and the local predictor of the standard deviation of robustness (Figure 4.4 B,C). In contrast, there are moderate downward trends for the minimum distance to the nearest neighbor and the robustness of the food web (Figure 4.4 A,D). Note that the actual parameter range for robustness and minimum nearest neighbor distance differ between subset and best model, as we use a selection of certain landscapes and food webs in the subset and standardize both ranges between 0 and 1.

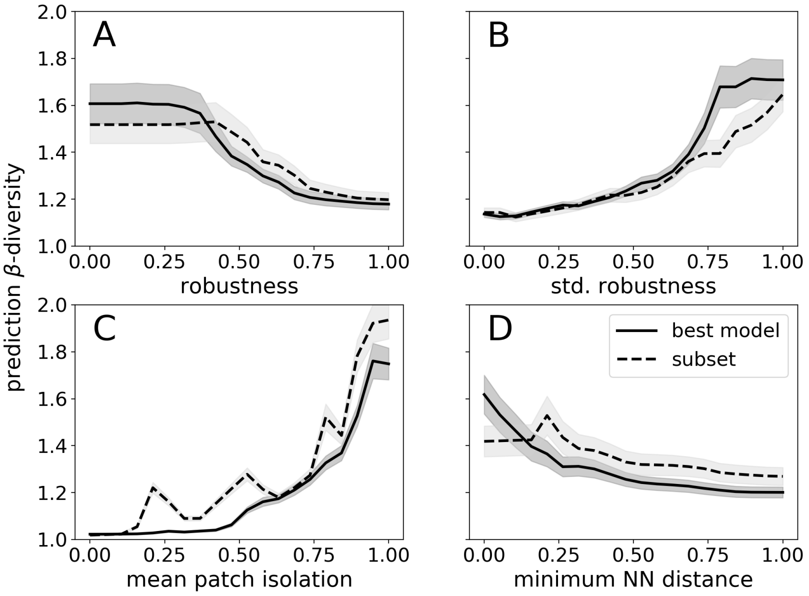

FIGURE 4.4: Partial dependence plots for β-diversity and the four predictors in the best model for the full data set (solid line) and subset (dashed line). There are two local predictors, the robustness and standard deviation of robustness as well as two regional predictors, the mean patch isolation and minimum nearest neighbor distance. The shaded area in grey indicates the 95% confident interval of model results.

Discussion

In this study, we analyzed the relevance of regional vs. local characteristics of meta-ecosystems for maintaining diversity at different spatial scales. We found that the mean local ($\bar{\alpha}$-) diversity is determined almost entirely by local characteristics such as the overall robustness of the local food web, and only to a very small extent by regional (or landscape) characteristics that capture landscape complexity and the positions of patches relative to each other. In comparison, diversity among patches (β-) depends on a combination of local and regional characteristics, with mean patch isolation being the most important predictor.

Local predictors explain $\bar{\alpha}$-diversity patterns

The two local predictors, robustness of a food web and its standard deviation, are the dominant variables predicting $\bar{\alpha}$-diversity. Our measure of robustness is defined as the mean fraction of species that survive population dynamics (Heckmann et al., 2012) with and without additional losses due to emigration of species (see methods for more details). Although the mortality caused by emigration implies the embedding of the local food web in a metacommunity, robustness is still a strictly local predictor since immigration and therefore the influence of the surrounding patch network are ignored. It is calculated in separate simulation runs and highlights, on the one hand, the relevance of the intrinsic stability of individual food webs and, on the other hand, how the food web is affected by an additional mortality term. In using this approach, we can also relate the effects of additional mortality on food webs more generally to any disturbance that leads to additional mortality, such as harvesting.

Compared to local predictors, the proportion of variance explained by regional predictors of landscape structure for $\bar{\alpha}$-diversity is small. As such, our results are in contrast to studies demonstrating that spatial characteristics and the regional scale have a larger impact on α-diversity (e.g. Jonsson et al. (2011)). This underlying discrepancy can be explained by the focus and selection of regional predictors, as well as by the analyzed species community. In particular, empirical studies that find a larger impact of the regional scale on α-diversity often refer to habitat heterogeneity as a relevant regional predictor for an increase of diversity (Jonsson et al., 2011; Stein et al., 2014). However, in our model setup, there are no differences in environmental conditions among patches. In addition, these empirical studies commonly analyze single communities, whereas we compared how different food webs, with their own inherent stability, react to changes of landscape structure.

Regional characteristics and their magnitude of effect on α-diversity may in fact depend strongly on local processes and the composition of a species community. For example, empirical studies of plant communities find small effect sizes of regional predictors on α-diversity when accounting for increased seed addition as a regional predictor reflecting a higher dispersal rate (corresponding to a low patch isolation). However, when combined with an additional community disturbance, the effect size of the regional predictor increases (Myers and Harms, 2009). This finding emphasizes that results regarding α-diversity patterns are highly context-dependent and suggest that to understand α-diversity of food webs of different origin, a comprehensive analysis of the species and their interactions should be prioritized, with the inclusion of landscape attributes as a second step.

Finally, the selected predictor of robustness stresses the importance of the local food web structure. Our measure of robustness is calculated similarly to $\bar{\alpha}$-diversity from the number of surviving species and therefore a strong correlation can be expected. However, the two metrics are not identical: $\bar{\alpha}$-diversity describes the mean species richness across all patches at the end of a simulation run, whereas robustness is derived from a separate set of simulation runs, averaging the species richness of a single patch in a state of no and full dispersal loss through emigration (see also Table 4.2). Thus, robustness does not describe a common structural property of the food web (e.g. mean generality, or degree of omnivory), but is an estimate of the contribution of food web structure and allows a comparison to the contribution of regional predictors. Other commonly evaluated food web properties such as generality or food web connectance that already demonstrated a relationship to diversity patterns (Riede et al., 2010; Thébault et al., 2007), did not show a strong correlation. A possible explanation might be the existence of an emerging property that is not reflected in a typical feature of a food web (Thompson et al., 2012). The strength of competition between species, for example, can be decisive for the impact of secondary extinctions in a food web (Thébault et al., 2007). Despite significant progress in this area of research, further efforts are needed to understand the determinants of local food web stability and diversity.

Local and regional predictors determine β-diversity

Compared to the prediction of $\bar{\alpha}$-diversity, regional parameters were an essential part of the model for predicting β-diversity. We use the spatial arrangement and dispersal distances between patches as the focus for regional processes and excluded heterogeneity as a factor within the landscape, which is also known to affect regional diversity patterns (Stein et al., 2014).

Our step-wise selection of predictors identified a high correlation between several landscape network characteristics such as the patch centrality and mean patch isolation. We decided to keep the mean patch isolation as a main regional predictor to be able to directly compare results with Ryser et al. (2019) where it was used as the main axis, and because it is a very prominent and easy-to-compute measure used in theoretical and empirical studies addressing the impact of spatial patterns on biodiversity

(Altermatt and Holyoak, 2012; Cadotte et al., 2006).

The formation of local patch clusters is the first hypothesis put forward by Ryser et al. (2019) to explain the observed increase of β-diversity with increasing mean patch isolation. It assumes that local patch cluster are beneficial for β-diversity due to less dispersal mortality and an increased amount of food supply within the cluster. Thus the patch cluster can harbor more species compared to fully isolated patches which increase differences in species composition among patches. Intuitively, the parameter most suitable to capture this is the clustering coefficient. However, it is highly correlated with mean patch isolation (see also Supplements Table C3) and was therefore not included as an independent variable in the analyses. Although the average clustering coefficient therefore does not provide evidence for this hypothesis, the minimum distance to the nearest neighbor gives an indication, that at least a small distance between two patches is beneficial for β-diversity. A possible explanation for why the minimum nearest neighbor distance can explain additional variance in β-diversity is the difference in the scale between the cluster coefficient and the minimum nearest neighbor distance. While the minimum nearest neighbor distance accounts for two patches at a time, the clustering coefficient gives an average across the entire landscape. Yet, two closely located patches can also be considered a small cluster. The advantage of two closely located habitat patches is, for example, an increased number of resources species compared to fully isolated patches and less energy limitation for higher trophic levels of consumer species (Crooks et al., 2011). If such a cluster is beneficial for α-diversity on the small scale, this also supports diversity on the regional scale. In particular, when $\bar{\alpha}$-diversity is low, a local increase in diversity in such a cluster also increase differences between habitat patches, and consequently increases β-diversity. In natural systems, such a local cluster can be established by the creation of dispersal corridors, which demonstrated to have a positive impact on α-diversity (Damschen et al., 2006). The importance of the nearest-neighbor distance is also shown by the analysis of the subset of the full data set. By selecting landscapes with at least two closely linked habitat patches, it is ensured that species have at least one local cluster with a higher food availability despite a large mean patch isolation, which increases the fraction of explained variance from 50% in the full data set to 80% in the subset.

As a second hypothesis from Ryser et al. (2019), it is assumed that different extinction cascades due to different initial species compositions and different food web positions of the species present drive the increase in β-diversity at high mean patch isolation. A prominent measure of such extinction cascades is the "structural robustness", which defines robustness as the minimum level of secondary extinction that occurs in response to a removal of a species, which is widely used in the analysis of empirical food webs (Dunne et al., 2002; Srinivasan et al., 2007). In contrast, our related measure of robustness focuses on the persistence of species under the evolution of population dynamics. As a result, our measure for robustness is limited to address the question of extinction cascades due to the fact that we do not intentionally remove a particular species from the food web, but extinctions happen over time and are driven through species interactions. Accordingly, we cannot use our predictor of robustness to directly evaluate the second hypothesis on different extinction cascades. Instead, we use the standard deviation of the robustness as an indirect indicator for the importance of extinction cascades: a high standard deviation implies that the state of the landscape can in principle have an effect on the robustness of a food web. Thus, only when the standard deviation is high, an extinction cascade can be triggered by high dispersal losses in a landscape with very isolated patches, which then causes differences in species composition. A positive trend between the standard deviation and β-diversity consequently provides evidence that extinction cascades do indeed take different routes in different clusters of patches when mean patch isolation is high. Contrary to Ryser et al. (2019), these different extinction routes are not caused by different initial species compositions, but are restricted to causes of species interactions and the inhomogeneous arrangement of patches that lead to differences in species net dispersal losses.

By linking the robustness of a food web to dispersal losses, we incorporate a spatial component into the measure. Therefore, we can infer from the predictor of robustness when landscape characteristics (i.e., greater dispersal mortality) also have a larger impact on food web stability. And indeed, we observe a larger impact of regional predictors of the landscape in a state of intermediate robustness, which we confirmed by computing additional simulation runs for a selected subset of food webs. Accordingly, landscape characteristics are of little importance when the food web has a large or small robustness. Considering this, a simple explanation is that the effects of dispersal losses are either marginal for food webs with a large robustness, causing a large number of species to survive, or so extensive that most species go extinct. However, for an intermediate robustness, the landscape can play a crucial role, since species are susceptible to dispersal losses and differences in the landscape can promote or impede the survival of species. Based on these observation, we randomly selected food webs with an intermediate robustness for a subset of simulation runs that should provide food webs where the landscape itself can at least in principle have a larger impact on species composition and diversity. In analyzing this subset, we are able to explain most of the variance for β-diversity of our meta-food web model.

Conclusion

Our results on the impact of local and regional predictors on diversity patterns emphasizes the context dependency of effects on local and regional scale. Importantly, our results do not imply that $\bar{\alpha}$-diversity in metacommunities is not at all affected by the state of the landscape. However, to understand the difference in α-diversity between two different food webs, it is more important to study their species compositions and the interactions between the species than the characteristics of the landscapes the food webs are embedded in. On the regional scale, β-diversity can be explained naturally to a larger extent through regional predictors such as the presence of patch clusters, but the relevance of local food web characteristics should not be underestimated. Thus, if we want to maintain diversity of a metacommunity, a comprehensive understanding of the local community is of great value to develop more targeted oriented natural conservation measures such as the establishment of dispersal corridors.

Bibliography

F. Altermatt and M. Holyoak. Spatial clustering of habitat structure effects patterns of community composition and diversity. *Ecology*, 93(5):1125–1133, 2012. doi: 10.1890/11-1190.1.

P. Amarasekare. Spatial dynamics of foodwebs. *Annu Rev Ecol Evol Syst*, 39:479–500, 2008. doi: 10.1146/annurev.ecolsys.39.110707.173434.

M. E. Assessment. Ecosystems and human well-being: Biodiversity synthesis. *World Resources Institute*, 2005.

J. R. Beddington. Mutual interference between parasites or predators and its effect on searching efficiency. *J Anim Ecol*, 44(1):331–340, 1975. doi: 10.2307/3866.

D. E. Bowler and T. G. Benton. Causes and consequences of animal dispersal strategies: relating individual behaviour to spatial dynamics. *Biol Rev*, 80(2):205–225, 2005. doi: 10.1017/S1464793104006645.

C. J. Briggs and M. F. Hoopes. Stabilizing effects in spatial parasitoid–host and predator–prey models: a review. *Theor Popul Biol*, 65(3):299 – 315, 2004. doi: 10.1016/j.tpb.2003.11.001.

M. Cadotte, A. E. M. Loreau, and E. J. B. Losos. Dispersal and species diversity: A meta-analysis. *Am Nat*, 167(6):913–924, 2006. doi: 10.1086/504850.

P. Chesson. Mechanisms of maintenance of species diversity. *Annu Rev Ecol Syst*, 31: 343–366, 2000. URL `https://www.jstor.org/stable/221736`.

J. H. Connell. *On the Role of Natural Enemies in Preventing Competitive Exclusion in Some Marine Animals and in Rain Forest Trees. In: Den Boer, P.J. and Gradwell, G.R., Eds., Dynamics of Populations*. Centre for Agricultural Publishing and Documentation, Wageningen, Netherlands, 1971.

K. R. Crooks, C. L. Burdett, D. M. Theobald, C. Rondinini, and L. Boitani. Global patterns of fragmentation and connectivity of mammalian carnivore habitat. *Phil Trans R Soc B Sci*, 366(1578):2642–2651, 2011. doi: 10.1098/rstb.2011.0120.

E. I. Damschen, N. M. Haddad, J. L. Orrock, J. J. Tewksbury, and D. J. Levey. Corridors increase plant species richness at large scales. *Science*, 313(5791):1284–1286, 2006. doi: 10.1126/science.1130098.

D. L. DeAngelis, R. A. Goldstein, and R. V. O'Neill. A model for tropic interaction. *Ecology*, 56(4):881–892, 1975. doi: 10.2307/1936298.

J. A. Dunne. The network structure of food webs. In M. Pascual and J. A. Dunne, editors, *Ecological Networks:Linking Structure to Dynamics in Food Webs*, chapter 2. Oxford University Press, 2005. ISBN 9780195188165. URL `http://books.google.ca/books?id=qe-04Y2gKscC`.

J. A. Dunne, R. J. Williams, and N. D. Martinez. Food-web structure and network theory: The role of connectance and size. *PNAS*, 99(20):12917–12922, 2002.

R. B. Ehnes, B. C. Rall, and U. Brose. Phylogenetic grouping, curvature and metabolic scaling in terrestrial invertebrates. *Ecol Lett*, 14(10):993–1000, 2011. doi: 10.1111/j.1461-0248.2011.01660.x.

L. Fahrig. Effects of habitat fragmentation on biodiversity. *Ann Rev Ecol Evol Syst*, 34 (1):487–515, 2003. doi: 10.1146/annurev.ecolsys.34.011802.132419.

L. Fahrig, V. Arroyo-Rodríguez, J. R. Bennett, V. Boucher-Lalonde, E. Cazetta, D. J. Currie, F. Eigenbrod, A. T. Ford, S. P. Harrison, J. A. Jaeger, N. Koper, A. E. Martin, J.-L. Martin, J. P. Metzger, P. Morrison, J. R. Rhodes, D. A. Saunders, D. Simberloff, A. C. Smith, L. Tischendorf, M. Vellend, and J. I. Watling. Is habitat fragmentation bad for biodiversity? *Biol Conserv*, 230:179 – 186, 2019. ISSN 0006-3207. doi: 10.1016/j.biocon.2018.12.026.

R. J. Fletcher, R. K. Didham, C. Banks-Leite, J. Barlow, R. M. Ewers, J. Rosindell, R. D. Holt, A. Gonzalez, R. Pardini, E. I. Damschen, F. P. Melo, L. Ries, J. A. Prevedello, T. Tscharntke, W. F. Laurance, T. Lovejoy, and N. M. Haddad. Is habitat fragmentation good for biodiversity? *Biol Conserv*, 226:9 – 15, 2018. ISSN 0006-3207. doi: 10.1016/j.biocon.2018.07.022.

E. A. Fronhofer, D. Legrand, F. Altermatt, A. Ansart, S. Blanchet, D. Bonte, A. Chaine, M. Dahirel, F. De Laender, J. De Raedt, L. Di Gesu, S. Jacob, O. Kaltz, E. Laurent, C. J. Little, L. Madec, F. Manzi, S. Masier, F. Pellerin, F. Pennekamp, N. Schtickzelle, L. Therry, A. Vong, L. Winandy, and J. Cote. Bottom-up and top-down control of dispersal across major organismal groups. *Nat Ecol Evol*, 2(12):1859–1863, 2018. doi: 10.1038/s41559-018-0686-0.

N. J. Gotelli. Metapopulation models: The rescue effect, the propagule rain, and the core-satellite hypothesis. *Am Nat*, 138(3):768–776, 1991. doi: 10.2307/2462468.

T. N. Grainger and B. Gilbert. Dispersal and diversity in experimental metacommunities: linking theory and practice. *Oikos*, 125(9):1213–1223, 2016. doi: 10.1111/oik.03018.

D. Gravel, E. Canard, F. Guichard, and N. Mouquet. Persistence increases with diversity and connectance in trophic metacommunities. *PLOS ONE*, 6(5):1–9, 05 2011. doi: 10.1371/journal.pone.0019374.

T. Gross, K. T. Allhoff, B. Blasius, U. Brose, B. Drossel, A. K. Fahimipour, C. Guill, J. D. Yeakel, and F. Zeng. Modern models of trophic meta-communities. *Philos Trans R Soc B Biol Sci*, 375(1814):20190455, 2020. doi: 10.1098/rstb.2019.0455.

L. Heckmann, B. Drossel, U. Brose, and C. Guill. Interactive effects of body-size structure and adaptive foraging on food-web stability. *Ecol Lett*, 15(3):243–250, 2012. doi: 10.1111/j.1461-0248.2011.01733.x.

J. HilleRisLambers, P. Adler, W. Harpole, J. Levine, and M. Mayfield. Rethinking community assembly through the lens of coexistence theory. *Annu Rev Ecol Evol Syst*, 43 (1):227–248, 2012. doi: 10.1146/annurev-ecolsys-110411-160411.

A. C. Hindmarsh, P. N. Brown, K. E. Grant, S. L. Lee, R. Serban, D. E. Shumaker, and C. S. Woodward. Sundials: Suite of nonlinear and differential/algebraic equation solvers. *ACM Trans Math Soft (TOMS)*, 31(3):363–396, 2005.

J. D. Hunter. Matplotlib: A 2d graphics environment. *Comput Sci Eng*, 9(3):90–95, May 2007. ISSN 1521-9615. doi: 10.1109/MCSE.2007.55.

C. Jacquet, C. Moritz, L. Morissette, P. Legagneux, F. Massol, P. Archambault, and D. Gravel. No complexity–stability relationship in empirical ecosystems. *Nature Communications*, 7:2041–1723, 2016. doi: 10.1038/ncomms12573.

M. Jonsson, G. Englund, and D. A. Wardle. Direct and indirect effects of area, energy and habitat heterogeneity on breeding bird communities. *J Biogeogr*, 38(6):1186–1196, 2011. doi: 10.1111/j.1365-2699.2010.02470.x.

B. Lang, R. B. Ehnes, U. Brose, and B. C. Rall. Temperature and consumer type dependencies of energy flows in natural communities. *Oikos*, 126(12):1717–1725, 2017. doi: 10.1111/oik.04419.

R. M. LeCraw, P. Kratina, and D. S. Srivastava. Food web complexity and stability across habitat connectivity gradients. *Oecologia*, 176(4):903–915, 2014. doi: 10.1007/s00442-014-3083-7.

M. A. Leibold and J. M. Chase. *Metacommunity Ecology*, volume 59. Princeton University Press, Princeton, 2017.

J. Liao, D. Bearup, Y. Wang, I. Nijs, D. Bonte, Y. Li, U. Brose, S. Wang, and B. Blasius. Robustness of metacommunities with omnivory to habitat destruction: disentangling patch fragmentation from patch loss. *Ecology*, 98(6):1631–1639, 2017. doi: 10.1002/ecy.1830.

R. H. MacArthur and E. O. Wilson. *The theory of island biogeography*. Princeton University Press, Princeton, 1967.

A. F. Macedo. Abiotic stress responses in plants: Metabolism to productivity. In P. Ahmad and M. Prasad, editors, *Abiotic Stress Response in Plants*, pages 41–61. Springer, New York, NY, 2012. doi: 10.1007/978-1-4614-0634-1.

Y. Miyazaki, T. Osawa, and Y. Waguchi. Resource level as a proximate factor influencing fluctuations in male flower production in cryptomeria japonica d. don. *J For Res*, 14(6):358–364, 2009. doi: 10.1007/s10310-009-0148-2.

N. Mouquet and M. Loreau. Coexistence in metacommunities: The regional similarity hypothesis. *Am Nat*, 159(4):420–426, 2002. doi: 10.1086/338996.

J. A. Myers and K. E. Harms. Seed arrival, ecological filters, and plant species richness: a meta-analysis. *Ecol Lett*, 12(11):1250–1260, 2009. doi: https://doi.org/10.1111/j.1461-0248.2009.01373.x.

T. E. Oliphant. *Guide to NumPy*. CreateSpace Independent Publishing Platform, USA, 2nd edition, 2015. ISBN 151730007X, 9781517300074.

T. pandas development team. Pandas, 2020.

F. Pedregosa, G. Varoquaux, A. Gramfort, V. Michel, B. Thirion, O. Grisel, M. Blondel, P. Prettenhofer, R. Weiss, V. Dubourg, J. Vanderplas, A. Passos, D. Cournapeau, M. Brucher, M. Perrot, and E. Duchesnay. Scikit-learn: Machine learning in python. *J Mach Learn Res*, 12(null):2825–2830, Nov. 2011. ISSN 1532-4435.

M. Penrose. *Random Geometric Graphs*. Oxford University Press, 2003.

S. L. Pimm, C. N. Jenkins, R. Abell, T. M. Brooks, J. L. Gittleman, L. N. Joppa, P. H. Raven, C. M. Roberts, and J. O. Sexton. The biodiversity of species and their rates of extinction, distribution, and protection. *Science*, 344(6187), 2014. ISSN 0036-8075. doi: 10.1126/science.1246752.

L. R. Prugh, K. E. Hodges, A. R. E. Sinclair, and J. S. Brashares. Effect of habitat area and isolation on fragmented animal populations. *Proc Natl Acad Sci*, 105(52):20770–20775, 2008. doi: 10.1073/pnas.0806080105.

J. O. Riede, B. C. Rall, C. Banasek-Richter, S. A. Navarrete, E. A. Wieters, M. C. Emmerson, U. Jacob, and U. Brose. Chapter 3 - scaling of food-web properties with diversity and complexity across ecosystems. In G. Woodward, editor, *Ecological Networks*, volume 42 of *Adv Ecol Res*, pages 139 – 170. Academic Press, 2010. doi: https://doi.org/10.1016/B978-0-12-381363-3.00003-4.

J. O. Riede, U. Brose, B. Ebenman, U. Jacob, R. Thompson, C. R. Townsend, and T. Jonsson. Stepping in elton's footprints: a general scaling model for body masses and trophic levels across ecosystems. *Ecol Lett*, 14(2):169–178, 2011. doi: doi.org/10.1111/j.1461-0248.2010.01568.x.

J. Rybicki and I. Hanski. Species–area relationships and extinctions caused by habitat loss and fragmentation. *Ecol Lett*, 16(s1):27–38, 2013. doi: https://doi.org/10.1111/ele.12065.

R. Ryser, J. Häussler, M. Stark, U. Brose, B. C. Rall, and C. Guill. The biggest losers: habitat isolation deconstructs complex food webs from top to bottom. *Proc R Soc B Biol Sci*, 286(1908):20191177, 2019. doi: 10.1098/rspb.2019.1177.

F. D. Schneider, U. Brose, B. C. Rall, and C. Guill. Animal diversity and ecosystem functioning in dynamic food webs. *Nat Commun*, 7(12718), 2016. doi: 10.1038/ncomms12718.

U. T. Srinivasan, J. A. Dunne, J. Harte, and N. D. Martinez. Response of complex food webs to realistic extinction sequences. *Ecology*, 88(3):671–682, 2007. doi: 10.1890/06-0971.

A. Stein, K. Gerstner, and H. Kreft. Environmental heterogeneity as a universal driver of species richness across taxa, biomes and spatial scales. *Ecol Lett*, 17(7):866–880, 2014. doi: 10.1111/ele.12277.

O. Tange. Gnu parallel 2018. `https://doi.org/10.5281/zenodo.1146014`, 2018.

J. W. Terborgh. Toward a trophic theory of species diversity. *PNAS*, 112(37):11415–11422, 2015. doi: 10.1073/pnas.1501070112.

R. M. Thompson, U. Brose, J. A. Dunne, R. O. Hall, S. Hladyz, R. L. Kitching, N. D. Martinez, H. Rantala, T. N. Romanuk, D. B. Stouffer, and J. M. Tylianakis. Food webs: reconciling the structure and function of biodiversity. *Trends Ecol Evol*, 27(12): 689 – 697, 2012. doi: 10.1016/j.tree.2012.08.005.

E. Thébault, V. Huber, and M. Loreau. Cascading extinctions and ecosystem functioning: contrasting effects of diversity depending on food web structure. *Oikos*, 116(1): 163–173, 2007. doi: 10.1111/j.2006.0030-1299.15007.x.

D. Tilman. *Resource competition and community structure*. Princeton University Press, Princeton, 1982.

D. Tilman. Community invasibility, recruitment limitation, and grassland biodiversity. *Ecology*, 78(1):81–92, 1997. doi: 10.1890/0012-9658(1997)078[0081:CIRLAG]2.0.CO;2.

S. Van der Walt, S. C. Colbert, and G. Varoquaux. The numpy array: A structure for efficient numerical computation. *Comp Sci Eng*, 13:22–30, 2011. doi: 10.1109/MCSE.2011.37.

R. H. Whittaker. Evolution and measurement of species diversity. *Taxon*, 21(2/3): 213–251, 1972. doi: 10.2307/1218190.

R. J. Williams and N. D. Martinez. Limits to trophic levels and omnivory in complex food webs: Theory and data. *Am Nat*, 163(3):458–468, 2004. doi: 10.1086/381964.

P. Yodzis and S. Innes. Body size and consumer-resource dynamics. *Am Nat*, 139(6): 1151–1175, 1992. doi: 10.2307/2462335.

Chapter 5

General Discussion

In the previous Chapters (Chapters 2-4), I applied the approach of a meta-food web and meta-food chain that represent a metacommunity of species on multiple trophic levels. Within this framework, it has been possible to identify relevant local and regional characteristics that explain trends and patterns for metacommunities. A key element of this analysis is to vary complexity at both local and regional scales, allowing for different perspectives and gaining a more comprehensive view of mechanisms promoting the stability of metacommunities. For example, on the local scale, the maximum number of species present in a patch varies between the approaches in Chapter 2 and 3, as do the identities of species present (Chapter 2 & 4). On the regional scale, the spatially explicit approach sets a location for each habitat, and allows for identification of regional landscape aspects that have an influence on the stability of the species community (Chapters 2 & 4). While these spatial characteristics are fixed in each simulation run, a periodic environmental disturbance also temporally altered spatial features within a simulation (Chapter 3), corresponding to an additional layer of complexity. In this chapter, I will frame the general trends within the larger context of biodiversity, provide a perspective on the synthesis of the individual sub-aspects of the Chapters, and further integrate perspectives of ongoing climate change.

5.1 From metacommunities to meta-food webs

Based on the idea of metacommunities, many models and approaches have been developed that relate spatial with local processes and emphasized different aspects important for the coexistence of multiple species (Amarasekare, 2008; Leibold et al., 2004; Mouquet and Loreau, 2003). In that respect, the meta-food web and meta-food chain approach from Chapters 2-4 particularly emphasizes the complex trophic interactions of diverse species communities and how spatial characteristics constrain or promote these communities. In the following sections I first focus on effects of local trophic interactions and then continue with the impact of the landscape structure.

5.1.1 Local trophic interactions form metacommunities

The local composition of a species community, its interactions, and the resulting biomass distribution of species forms the basis for the local coexistence of multiple species and their stability. Across Chapters 2-4, several local scale mechanisms have emerged that have an impact on diversity and population dynamics of metacommunities.

Energy limitation and extinction cascades In a broad ecological context, the productivity-diversity relationship assumes that more energy leads to faster growth, more niche differentiation, longer food chains and thus promotes diversity (Takimoto and Post, 2013). In accordance with this relationship, a limitation of available energy leads to shorter food chains on average (Chapter 2 & 4), in particularly isolated landscapes. Based on this conclusion, it can be inferred that higher trophic levels are exposed to a higher risk of extinction due to a lack of sufficient energy transported through the food web (Binzer et al., 2012). The lack of energy is caused by higher metabolic losses due to a large patch isolation, resulting in a proportionally higher species extinction rate.

While our findings support the productivity-diversity relationship and emphasize its relevance in more isolated landscapes, empirical support for the relationship so far is ambiguous (Mittelbach et al., 2001; Whittaker, 2010). There are several major causes for these seemingly contradictory results, the first being the use of different proxies for the productivity or energy (for example standing biomass, nutrients, or actual productivity), leading to difficulties in comparison. A second cause is the relevance of scale for such empirical results. For example, empirical data for productivity is often highly variable on a smaller scale (Mittelbach et al., 2001), while at larger scales a positive relationship has been found for terrestrial as well as aquatic ecosystems (Gonzalez et al., 2011; Storch et al., 2005; Tittensor et al., 2010). This noticeable difference in regional and local scale exemplifies the relevance of a metacommunity perspective (see also

Chase and Leibold (2002)) and also supports our findings of a positive relationship between productivity and diversity for a meta-food web (Leibold and Chase, 2017).

In Chapter 2, species with a larger body mass are more prone to extinction, although our approach assumes that larger animal species realize larger dispersal ranges, which benefits species persistence due to the larger colonization rates of predator species (Shulman and Chase, 2007). The large selection pressure on the higher trophic levels thus affects the composition and stability of the entire local food web (Dobson et al., 2006; Rooney et al., 2006). For example, a lack of top down regulation of large bodied predator species can trigger an extinction cascade which decreases α-diversity and simplifies the structure of a food web (Donohue et al., 2017). However, such extinction cascades can also have a positive effect (Chapter 2 & 4) on β-diversity: Differing initial positions of a species within a food web can produce different cascading pathways in local food web dynamics, resulting in contrasting local species communities when patch isolation is high. The influence of the local predictor of the standard deviation of robustness for β-diversity in Chapter 4 supports this hypothesis, and suggests that in a state of large patch isolation, a high standard deviation in the robustness of a food web can serve as an indicator for extinction cascades triggered by the landscape.

As stated in Chapter 3, consequences of weakening top down regulation are also observed for a simple food chain. A lower top-down control increases fluctuations in biomass dynamics, and thus the coefficient of variation increases (see Fig. 3.3 , Chapter 3). A population that exhibits such larger fluctuations is more susceptible to stochastic extinction events when local biomasses are at their minimum (Pimm et al., 1988). In addition to increased extinction risk, a lack of top down control had a largely positive effect on biomass densities of lower trophic levels, leading to a more uneven biomass distribution between trophic levels (Chapters 2 & 3). This particularly benefits species with a smaller body mass, although biomass loss is proportionally larger for them relative to the dispersed distance in comparison to species with larger body masses (Peters, 1983; Schneider et al., 2016).

Local food web stability To understand the local diversity of a metacommunity, one must consider both local and regional processes and their impacts on species coexistence. For example, a meta-analysis on metacommunities from Grainger and Gilbert

(2016) shows that in two-thirds of the studies the regional process of dispersal has a significant impact on local α-diversity, beside local predictors. While Chapters 2 and 4 suggest a negative impact of the mean patch isolation as a regional predictor on α-diversity, results from Chapter 4 also indicate that, remarkably, a majority of the explained variance for α-diversity are attributed to two local predictors based on the food web robustness. To a large extent this dependence also explains the broad scatter in the data from Chapter 2 and puts the impact of the regional predictor, expressed as mean patch isolation, in a perspective that is highly dependent on the local species composition.

A dominance of local predictors (Chapter 4) suggests that the effect size of regional characteristics on α-diversity can be small. For example, empirical studies from plant communities confirm that the effect of seed additions on α-diversity (with seed addition as predictor for a change in dispersal rate) is very small in the absence of an additional community disturbance which allows for an establishment of the seeds (Myers and Harms, 2009). Another study on aquatic communities emphasizes a dependence between successful colonization of a new species and the disturbance of a local community that excludes resident species. Such an exclusion increased the total amount of biomass in a local patch, while an intact local species community and their local interactions hindered successful colonization by other species (Leibold and Chase, 2017; Shurin, 2000). These findings highlight the importance of local scale effects such as robustness and composition of a species community on dispersal success. Yet, a viable extension on the regional scale representing a more diverse landscape could include habitat heterogeneity, where an increase of the impact of regional predictors on α-diversity is expected (e.g. Jonsson et al. (2011); Ryser et al. (2020); Stein et al. (2014)), and on the local scale non-trophic interactions are also suggested to contribute to diversity patterns (Kéfi et al., 2012).

Alternative stable states Another local phenomena that can affect stability are alternative stable states (ASS). ASS emerge within local species communities with identical environmental conditions when the initial state of the community determines different final population dynamics or structures of the community. Chapter 3 gives an example of an ASS promoting stability through asynchronous population dynamics between patches, thus generating a more stable amount of total biomass for a species within a metapopulation. Such an ASS can decouple correlated dynamics between communities and is relevant because it implies hysteresis (Scheffer et al., 1993): a small change in environmental conditions can put the system into a different state, but to return to the original state, a larger change of environmental conditions in the opposite direction is required.

From empirical examples it is known that there are conditions that support the occurrence of such ASS within a metacommunity. There is evidence that they are more likely to occur in environments that are more productive (Chalcraft et al., 2008), less frequently disturbed (Chase, 2003), or smaller and less interconnected (Chase, 2003; Leibold and Chase, 2017). The observed ASS of Chapter 3 also confirms the effect of disturbances on the likelihood of finding ASS since they only occur in static landscapes without periodic environmental disturbances.

For more complex food webs such as in Chapters 2 & 4, such ASS may also occur and especially promote β-diversity. In fact, the variation in species richness for a single food web that are present in the simulation runs for the predictor of the robustness in Chapter 4 (not shown in the Chapter) might point towards the presence of AAS, but further testing is needed for a confirmation.

5.1.2 Few landscape characteristics matter for metacommunities

Our environment is shaped by continuous changes of the landscape such as fragmentation or other disturbances of habitats (Foley et al., 2005; Haddad et al., 2015). In this subsection prominent regional factors are discussed that have an influence on the structure of the meta-food web and stability of species communities.

Mean patch isolation of a landscape A common assumption about the effects of patch isolation on diversity patterns is that intermediate patch isolation shows a maximum positive effect on α-diversity. This is motivated by avoidance of some negative consequences of low and high dispersal rates, which include bioitc homogenization and a lack of rescue effects (Mouquet and Loreau, 2003). In accordance with that hypothesis, Chapters 2, 3 & 4 demonstrate a destabilizing effect of a large mean patch isolation on metacommunities. In Chapters 2 and 4, this is expressed as a decrease in $\bar{\alpha}$-diversity with increasing isolation. Fewer dispersal links between patches thus increases the negative effects of energy limitation on stability and decreases $\bar{\alpha}$-diversity, as discussed in the previous section, and the absence of a rescue effect prevents recolonization (Gotelli, 1991). In contrast, even though high dispersal rates (low patch isolation) may homogenize local food webs, reflected in a low β-diversity, this homogenization does not negatively affect $\bar{\alpha}$-diversity. This disagreement with theoretical expectations likely results from the dominant role of local stability of food webs on $\bar{\alpha}$-diversity, as observed in Chapter 4. Accordingly, when the influence of the landscape is minimal for a majority of food webs, and the main reason for species loss is a limitation of energy on the lower trophic levels, the positive influence of a larger food supply outweighs that of homogenization and a low patch isolation has a net positive effect on diversity.

While we find no negative effect of biotic homogenization on diversity in Chapters 2 & 4, we do find a negative effect on population dynamics of a simple food chain (Chapter 3). A synchronization of patches in a state of low mean patch isolation increases the variation in total biomass dynamics of a species, thus increasing the risk of correlated extinction events. However, this trend is observed exclusively in food chains experiencing a strong trophic cascade, again suggesting an effect of biotic interactions. A comparable effect of contrasting biotic interactions on the synchronization of population dynamics is observed by Koelle and Vandermeer (2005). They uncover that changing trophic interactions may produce opposing trends in synchronization for intermediate to high dispersal rates of a species.

Biotic homogenization among patches at low mean patch isolation also have very relevant empirical implications for the so-called portfolio effect (Schindler et al., 2015). The spatial portfolio effect (Thorson et al., 2018) is a way to analyze the extent of synchronization among patches. In empirical systems, a common observation is that for a higher number of patches, total biomass dynamics of a species tends to be steadier over time, due to asynchronous oscillations between patches. However, our model results from Chapter 3 demonstrate that one should be cautious with this generalization. Despite a reduced biotic homogenization in a state of increased patch isolation, there is an overall increase of total biomass amplitude (γ-variability). An increase of dispersal mortality and higher metabolic losses on lower trophic levels cause an energy limitation for the upper trophic levels, decreasing their biomass and thus increases γ-variability. This illustrative example points out that the synchronization of dynamics between patches is only one of a number of possible phenomena that can strongly affect population dynamics on the regional scale, even in a rather simple three-species modeling approach.

Number of patches and patch identity In a fragmented landscape, the state of fragmentation is determined by the mean patch isolation, the number of patches, and the patch size (Fahrig, 2003). Each of these properties has a direct impact on biodiversity (Haddad et al., 2015). With a focus on the effects of mean patch isolation and the number of patches in Chapter 2, the number of patches did not affect $\overline{\alpha}$-, β- and γ-diversity in contrast to mean patch isolation. While varying the number of patches, a lower quantity does not imply a direct habitat loss for a species. Since each habitat patch has no explicit area, and the calculations are based on biomass densities, fewer patches can be interpret as there are fewer possible stepping stones for a species within a landscape and patch size effects are excluded.

In expanding on some suggestive results from Chapter 2, we demonstrate in Chapter 4 that the minimum distance between two habitats that form a small local cluster increases β-diversity. A possible explanation for why the minimum distance between two habitats has a significant impact on β-diversity in Chapter 4, and not in Chapter 2, although they are analyzed both times, is most likely the simplified modeling approach in Chapter 4. While in both approaches the generation of landscapes and food webs is the same, the main simplifications involve fixed initial conditions between simulations, for example, the same initial biomasses and the same dispersal ranges for species. In particular a fixed dispersal range for the species increase comparability of regional predictors between simulation runs and avoid confounding effects due to randomly attributed dispersal ranges for plant species. In addition, fixed initial biomass densities combined with the absence of an initial β-diversity prevent arbitrary extinctions of species in an early stage of a simulation run.

A beneficial increase of β-diversity due to a dispersal link of two nearby patches, that form a local small cluster, is especially relevant for a low mean patch isolation. For the local cluster, an increased availability of suitable resources, which prevents an energy limitation for higher trophic levels, first explains a local increase in α-diversity (Crooks et al., 2011). For comparison, empirical experiments on dispersal corridors also demonstrate that the establishment of such corridors between habitat patches has a positive effect on α-diversity (Damschen et al., 2006). On the regional scale, such a local increase in diversity can also promote differences in species composition (β-diversity) in a metacommunity if mean patch isolation is high. This effect is particularly pronounced when the $\bar{\alpha}$-diversity is very small compared to the maximum possible γ-diversity of the meta-food web. In a heterogeneous landscape, the described effect of patch position and identity in local clusters could be even stronger, due to differences in the quality of food supply. Altermatt and Holyoak (2012) demonstrated a clear positive effect of local clusters with a high food quality on β-diversity in small experimental metacommunites.

5.2 Metacommunities in temporal changing landscape structures

In addition to the question of how spatial charachteristics affect diversity patterns, I investigated the effects of temporal changes in spatial structures on population dynamics and diversity. The approach of modeling periodic environmental disturbances as a dynamic landscapes is motivated by an example of kettle holes, which have a species-rich community during a cold and wetter season, but can run dry in summer and accordingly become temporarily uninhabitable and unavailable for species (Kalettka and Rudat, 2006). Such periodic environmental disturbances are a common feature in ecological systems, for example through environmental fluctuations in coupled systems (as observed by Fretwell (1972)).

Chapter 3 demonstrates that the population dynamics of a food chain are more strongly affected by periodic environmental disturbances than by local interactions of species, or by the landscape structure. This large effect size of disturbance becomes apparent in a comparison of two food chains that are characterized as either a strong or weak trophic cascade and exhibit different population dynamics. Despite these pronounced differences, which lead to markedly different patterns in biomass variability when the food chains are undisturbed, the patterns of biomass variability are almost identical under periodic environmental disturbance. The regular occurrence of the disturbance is a probable explanation for the equalizing trends of variabilities. A periodic disturbance starting at identical time points in each habitat patch promotes a synchronization of patches, which is also known, for example, from environmental fluctuations in coupled systems (Fretwell, 1972).

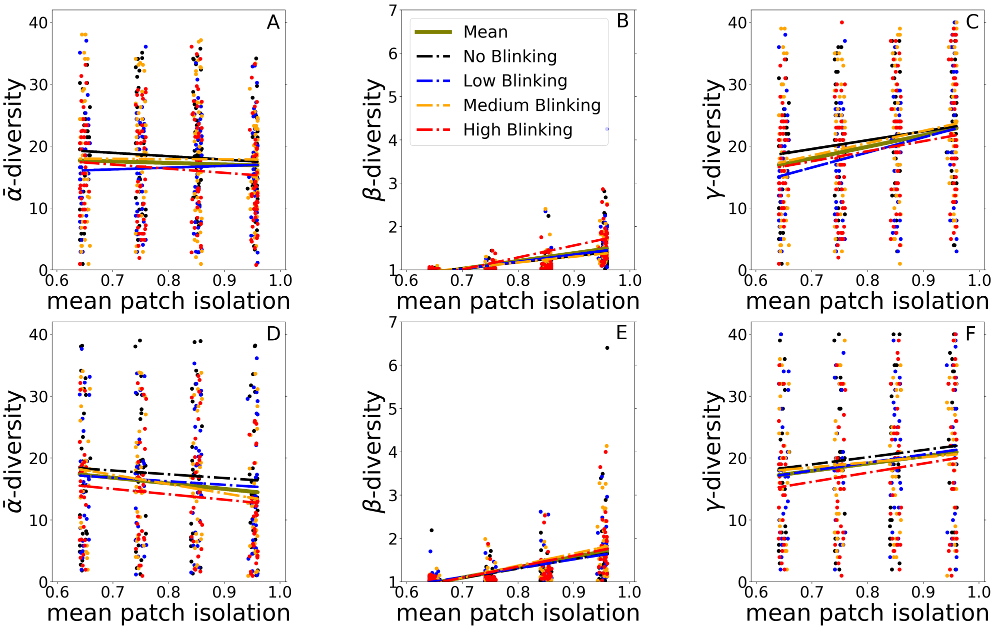

FIGURE 5.1: Level of α-,β- & γ-diversity for four distinct ranges of mean patch isolation in two scenarios. The first scenario in the first row (panels A, B, C) reflects simulation runs where in each simulation a new random food web is created. In the second scenario (panels D, E, F), food webs are selected for an intermediate robustness, and species-specific dispersal ranges are assumed. Furthermore for both scenarios, there are four different states of periodic environmental disturbances, that temporally change the degree of patch isolation. The scenarios vary in their proportion of patches that are temporally not available - High blinking: around 50 % of patches are temporally unavailable; Medium blinking: around 25 % of patches are temporally unavailable; Low blinking: around 12.5 % of patches are temporally unavailable; No blinking: 0 % of patches are temporally unavailable;

While the results from Chapter 3 suggest a large influence of periodic environmental disturbances on population dynamics, the same approach for a large meta-food web, based on the food web from Chapters 2 and 4, reveals no such pronounced influence on diversity patterns (Figure 5.1). The figure is based on separate simulation runs illustrating the impact of periodic environmental disturbance on food webs, ranging between scenarios with a large proportion of temporarily unavailable patches to no disturbance. As in Chapter 2, there is a negative trend for $\bar{\alpha}$-diversity, a positive trend for β-diversity, and a resulting increase in γ-diversity for moderate-to-high mean patch isolation. In line with empirical results (Vanschoenwinkel et al., 2013), we see a synergistic effect of patch isolation and the disturbance, with the tendency of the negative effect being most pronounced on $\bar{\alpha}$- and γ-diversity for the scenario with the largest proportion of temporally unavailable patches (Figure 5.1 A,C,D,F). A positive effect of the disturbance on β-diversity can be attributed, as already argued for Chapter 2, through the additional biomass loss and extinction cascades for species and the state of high patch isolation prevents species from recolonization, or in case of species-specific dispersal ranges (Figure 5.1 D,E,F), a recolonization by a subset of species.

Neither body mass dependent dispersal ranges for animal species, as implemented in Chapter 2, nor a selection of food webs with an intermediate robustness to increased dispersal mortality, as in Chapter 4, has a large effect on trends in diversity for a periodic environmental disturbance (compare Figure 5.1 A,B,C & D,E,F). Potential rescue effects through larger dispersal ranges of species are thus still outweighed by an increased energy limitation. And even if more variance in diversity can be explained for an intermediate robustness (Chapter 4), spatial changes do not have an appreciably larger effect on diversity patterns per se.

An explanation for why the periodic environmental disturbance has a small effect size on diversity patterns could be related to its implementation. While the disturbance itself is drastic, such that all species in a habitat go extinct, the blinking cycle has a very large period length compared to population growth rates (period length $\lambda = 300$ which can be up to 300 generations for small phytoplankton species & c.f. Chapter 3 for a comparison). This provides species sufficient time to re-establish on temporally unavailable habitats. In comparison, an empirical study on temporal ponds underlines the impact of a higher frequency of a disturbance on diversity patterns which provides less time for recolonization (Vanschoenwinkel et al., 2013). They distinguish between a high and low disturbance, based on the frequency of dry phases, and found that large effects in particular have a high frequency of disturbance (in line with our low frequency of disturbance). These results indicate that for a state of higher frequency of disturbance, also a larger effect on α-diversity can be expected for this meta-food web model approach.

In summary, the surprisingly strong effects of periodic environmental disturbances from Chapter 3 and the smaller effect sizes of the preliminary results on a meta-food web (Figure 5.1), suggest that the effect size of environmental disturbance on population dynamics is larger than on diversity per se. By causing converging trends among different communities, the presence of a periodic environmental disturbance may explain why empirically observed effects of mean patch isolation and other landscape structures are often small and inconclusive. This further aligns with the results that although local and regional scale processes are the basis to understand metacommunites, local community structure and trophic interactions can largely outweigh the impact of landscape structure (Chapter 4 and e.g. Myers and Harms (2009)).

5.3 Perspectives - metacommunities in a globally changing world

The conservation of biodiversity in our diverse ecosystems faces challenging times as climate change continues. For metacommunities, these changes can have manifold consequences. Chapter 2 & 4 illustrate that changes to the landscape structure have an impact on diversity patterns of metacommunities. By additionally including changes to the abiotic conditions of patches, isolated species communities which are limited in their dispersal may have increased difficulties to survive. For example, species may not be able to access the habitats that provide good conditions for their survival (Alexander et al., 2012; Mouquet et al., 2002). An example of the effect of changing abioitc conditions on metacommunities is shown by Baho et al. (2012), using an aquatic community of bacteria and analyzing the impact of a disturbance on the community composition by a sudden change of salinity. Their long-term chemostat experiments illustrated a long-lasting impact of such a disturbance over many generation times. The best recovery was observed for the treatment open for immigration from a regional resource pool, suggesting that reimmigration can support recovery from such a disturbance and thus may help species of a metacommunity in their ability to adapt to changing environmental conditions (Leibold and Chase, 2017).

Chapter 3 and the previous subsection already examined exemplarily one way of the impact of changing abiotic conditions, namely periodic environmental disturbances, which temporally change the structure of the landscape. With the knowledge of projected climate change in the future, the continuous increase of strong weather events and seasonal droughts further rapidly change the landscape structure. Precisely smaller ponds and kettle holes that provided inspiration as a vivid example of the model approach (c.f. Chapter 3), are in the context of climate change even more affected by such disturbances and accordingly we should be attentive with changes in biodiversity caused by climate change (Horváth et al., 2019; Vanschoenwinkel et al., 2013).

Yet our focus should not be limited to biodiversity. Important ecosystem functions may be comparatively more strongly affected by disturbances caused by climate change (Leibold and Chase, 2017). For example, by a change in abiotic conditions species could dominate a landscape that are secondarily adapted. Thus, species biodiversity could be maintained, but ecosystem functions could decline. A study on animal communities indicate that species richness is less affected by disturbances of the community, while the total abundance or the composition of a species community is stronger affected and more volatile (Supp and Ernest, 2014). A generalization of relationships between these ecological metrics, such as ecosystem function and biodiversity is still inconclusive (but see Ceulemans et al. (2021)) but is an important next step for a comprehensive overview of our ecosystems and their stability as climate change continuous.

Bibliography

H. M. Alexander, B. L. Foster, F. Ballantyne IV, C. D. Collins, J. Antonovics, and R. D. Holt. Metapopulations and metacommunities: combining spatial and temporal perspectives in plant ecology. *J Ecol*, 100(1):88–103, 2012. doi: https://doi.org/10.1111/j.1365-2745.2011.01917.x.

F. Altermatt and M. Holyoak. Spatial clustering of habitat structure effects patterns of community composition and diversity. *Ecology*, 93(5):1125–1133, 2012. doi: 10.1890/11-1190.1.

P. Amarasekare. Spatial dynamics of foodwebs. *Annu Rev Ecol Evol Syst*, 39:479–500, 2008. doi: 10.1146/annurev.ecolsys.39.110707.173434.

D. L. Baho, H. Peter, and L. J. Tranvik. Resistance and resilience of microbial communities - temporal and spatial insurance against perturbations. *Environ Microbiol*, 14 (9):2283–2292, 2012. doi: https://doi.org/10.1111/j.1462-2920.2012.02754.x.

A. Binzer, C. Guill, U. Brose, and B. C. Rall. The dynamics of food chains under climate change and nutrient enrichment. *Phil Trans R Soc B*, 367(1605):2935–44, 11 2012. doi: 10.1098/rstb.2012.0230.

R. Ceulemans, C. Guill, and U. Gaedke. Top predators govern multitrophic diversity effects in tritrophic food webs. *Ecology*, page e03379, 2021. doi: https://doi.org/10.1002/ecy.3379.

D. R. Chalcraft, S. B. Cox, C. Clark, E. E. Cleland, K. N. Suding, E. Weiher, and D. Pennington. Scale-dependent responses of plant biodiversity to nitrogen enrichment. *Ecology*, 89(8):2165–2171, 2008. doi: https://doi.org/10.1890/07-0971.1.

J. M. Chase. Community assembly: when should history matter? *Oecologia*, 136: 489–498, 2003. doi: https://doi.org/10.1007/s00442-003-1311-7.

J. M. Chase and M. A. Leibold. Spatial scale dictates the productivity-biodiversity relationship. *Nature*, 416:427–430, 2002. doi: https://doi.org/10.1038/416427a.

K. R. Crooks, C. L. Burdett, D. M. Theobald, C. Rondinini, and L. Boitani. Global patterns of fragmentation and connectivity of mammalian carnivore habitat. *Phil Trans R Soc B Sci*, 366(1578):2642–2651, 2011. doi: 10.1098/rstb.2011.0120.

E. I. Damschen, N. M. Haddad, J. L. Orrock, J. J. Tewksbury, and D. J. Levey. Corridors increase plant species richness at large scales. *Science*, 313(5791):1284–1286, 2006. doi: 10.1126/science.1130098.

A. Dobson, D. Lodge, J. Alder, G. S. Cumming, J. Keymer, J. McGlade, H. Mooney, J. A. Rusak, O. Sala, V. Wolters, D. Wall, R. Winfree, and M. A. Xenopoulos. Habitat loss, trophic collapse, and the decline of ecosystem services. *Ecology*, 87(8):1915–1924, 8 2006. doi: 10.1890/0012-9658(2006)87[1915:HLTCAT]2.0.CO;2.

I. Donohue, O. L. Petchey, S. Kéfi, A. Génin, A. L. Jackson, Q. Yang, and N. E. O'Connor. Loss of predator species, not intermediate consumers, triggers rapid and dramatic extinction cascades. *Glob Chang Biol*, 23(8):2962–2972, 2017. doi: 10.1111/gcb.13703.

L. Fahrig. Effects of habitat fragmentation on biodiversity. *Ann Rev Ecol Evol Syst*, 34 (1):487–515, 2003. doi: 10.1146/annurev.ecolsys.34.011802.132419.

J. A. Foley, R. DeFries, G. P. Asner, C. Barford, G. Bonan, S. R. Carpenter, F. S. Chapin, M. T. Coe, G. C. Daily, H. K. Gibbs, J. H. Helkowski, T. Holloway, E. A. Howard, C. J. Kucharik, C. Monfreda, J. A. Patz, I. C. Prentice, N. Ramankutty, and P. K. Snyder. Global consequences of land use. *Science*, 309(5734):570–574, 2005. doi: 10.1126/science.1111772.

S. D. Fretwell. *Populations in a seasonal environment*. Monogr Popul Biol, 1972.

A. Gonzalez, B. Rayfield, and Z. Lindo. The disentangled bank: How loss of habitat fragments and disassembles ecological networks. *J Bot*, 98(3):503–516, 2011. doi: 10.3732/ajb.1000424.

N. J. Gotelli. Metapopulation models: The rescue effect, the propagule rain, and the core-satellite hypothesis. *Am Nat*, 138(3):768–776, 1991. doi: 10.2307/2462468.

T. N. Grainger and B. Gilbert. Dispersal and diversity in experimental metacommunities: linking theory and practice. *Oikos*, 125(9):1213–1223, 2016. doi: 10.1111/oik.03018.

N. M. Haddad, L. A. Brudvig, J. Clobert, K. F. Davies, A. Gonzalez, R. D. Holt, T. E. Lovejoy, J. O. Sexton, M. P. Austin, C. D. Collins, W. M. Cook, E. I. Damschen, R. M. Ewers, B. L. Foster, C. N. Jenkins, A. J. King, W. F. Laurance, D. J. Levey, C. R. Margules, B. A. Melbourne, A. O. Nicholls, J. L. Orrock, D.-X. Song, and J. R. Townshend. Habitat fragmentation and its lasting impact on earth's ecosystems. *Sci Adv*, 1(2), 2015.

Z. Horváth, R. Ptacnik, C. F. Vad, and J. M. Chase. Habitat loss over six decades accelerates regional and local biodiversity loss via changing landscape connectance. *Ecol Lett*, 22(6):1019–1027, 2019. doi: https://doi.org/10.1111/ele.13260.

M. Jonsson, G. Englund, and D. A. Wardle. Direct and indirect effects of area, energy and habitat heterogeneity on breeding bird communities. *J Biogeogr*, 38(6):1186–1196, 2011. doi: 10.1111/j.1365-2699.2010.02470.x.

T. Kalettka and C. Rudat. Hydrogeomorphic types of glacially created kettle holes in north-east germany. *Limnologica*, 36(1):54 – 64, 2006. ISSN 0075-9511. doi: 10.1016/j.limno.2005.11.001.

K. Koelle and J. Vandermeer. Dispersal-induced desynchronization: from metapopulations to metacommunities. *Ecol Lett*, 8(2):167–175, 2005. doi: 10.1111/j.1461-0248.2004.00703.x.

S. Kéfi, E. L. Berlow, E. A. Wieters, S. A. Navarrete, O. L. Petchey, S. A. Wood, A. Boit, L. N. Joppa, K. D. Lafferty, R. J. Williams, N. D. Martinez, B. A. Menge, C. A. Blanchette, A. C. Iles, and U. Brose. More than a meal... integrating non-feeding interactions into food webs. *Ecol Lett*, 15(4):291–300, 2012. doi: https://doi.org/10.1111/j.1461-0248.2011.01732.x.

M. A. Leibold and J. M. Chase. *Metacommunity Ecology*, volume 59. Princeton University Press, Princeton, 2017.

M. A. Leibold, M. Holyoak, N. Mouquet, P. Amarasekare, J. M. Chase, M. F. Hoopes, R. D. Holt, J. B. Shurin, R. Law, D. Tilman, M. Loreau, and A. Gonzalez. The metacommunity concept: a framework for multi-scale community ecology. *Ecol Lett*, 7 (7):601–613, 2004. doi: 10.1111/j.1461-0248.2004.00608.x.

G. G. Mittelbach, C. F. Steiner, S. M. Scheiner, K. L. Gross, H. L. Reynolds, R. B. Waide, M. R. Willig, S. I. Dodson, and L. Gough. What is the observed relationship between species richness and productivity? *Ecology*, 82(9):2381–2396, 2001. doi: https://doi.org/10.1890/0012-9658(2001)082[2381:WITORB]2.0.CO;2.

N. Mouquet and M. Loreau. Community patterns in source-sink metacommunities. *Am Nat*, 162(5):544–557, 2003. doi: 10.1086/378857.

N. Mouquet, J. L. Moore, and M. Loreau. Plant species richness and community productivity: why the mechanism that promotes coexistence matters. *Ecol Lett*, 5(1): 56–65, 2002. doi: https://doi.org/10.1046/j.1461-0248.2002.00281.x.

J. A. Myers and K. E. Harms. Seed arrival, ecological filters, and plant species richness: a meta-analysis. *Ecol Lett*, 12(11):1250–1260, 2009. doi: https://doi.org/10.1111/j.1461-0248.2009.01373.x.

R. H. Peters. *The Ecological Implications of Body Size:*. Cambridge University Press, Cambridge, 10 1983.

S. L. Pimm, H. L. Jones, and J. Diamond. On the risk of extinction. *Am Nat*, 132(6): 757–785, 1988. doi: 10.1086/284889.

N. Rooney, K. Mccann, G. Gellner, and J. C. Moore. Structural asymmetry and the stability of diverse food webs. *Nature*, 442(20):265–269, 2006. doi: 10.1038/nature04887.

R. Ryser, M. R. Hirt, J. Häussler, D. Gravel, and U. Brose. Landscape heterogeneity buffers biodiversity of meta-food-webs under global change through rescue and drainage effects. *bioRxiv*, 2020. doi: 10.1101/2020.06.03.131425.

M. Scheffer, S. Hosper, M.-L. Meijer, B. Moss, and E. Jeppesen. Alternative equilibria in shallow lakes. *Trends Ecol Evol*, 8(8):275 – 279, 1993. ISSN 0169-5347. doi: 10.1016/0169-5347(93)90254-M.

D. E. Schindler, J. B. Armstrong, and T. E. Reed. The portfolio concept in ecology and evolution. *Front Ecol Environ*, 13(5):257–263, 2015. doi: 10.1890/140275.

F. D. Schneider, U. Brose, B. C. Rall, and C. Guill. Animal diversity and ecosystem functioning in dynamic food webs. *Nat Commun*, 7(12718), 2016. doi: 10.1038/ncomms12718.

R. S. Shulman and J. M. Chase. Increasing isolation reduces predator:prey species richness ratios in aquatic food webs. *Oikos*, 116(9):1581–1587, 2007. doi: https://doi.org/10.1111/j.0030-1299.2007.14690.x.

J. B. Shurin. Dispersal limitation, invasion resistance, and the structure of pond zooplankton communities. *Ecology*, 81(11):3074–3086, 2000. doi: 10.1890/0012-9658(2000)081[3074:DLIRAT]2.0.CO;2.

A. Stein, K. Gerstner, and H. Kreft. Environmental heterogeneity as a universal driver of species richness across taxa, biomes and spatial scales. *Ecol Lett*, 17(7):866–880, 2014. doi: 10.1111/ele.12277.

D. Storch, K. L. Evans, and K. J. Gaston. The species-area-energy relationship. *Ecol Lett*, 8(5):487–492, 2005. doi: https://doi.org/10.1111/j.1461-0248.2005.00740.x.

S. R. Supp and S. K. M. Ernest. Species-level and community-level responses to disturbance: a cross-community analysis. *Ecology*, 95(7):1717–1723, 2014. doi: https://doi.org/10.1890/13-2250.1.

G. Takimoto and D. M. Post. Environmental determinants of food-chain length: a meta-analysis. *Ecological Research*, 28(5):675–681, 2013. doi: 10.1007/s11284-012-0943-7.

J. T. Thorson, M. D. Scheuerell, J. D. Olden, and D. E. Schindler. Spatial heterogeneity contributes more to portfolio effects than species variability in bottom-associated marine fishes. *Proc R Soc Lond, B*, 285:20180915, 2018. doi: https://doi.org/10.1098/rspb.2018.0915.

D. P. Tittensor, C. Mora, W. Jetz, H. K. Lotze, D. Ricard, E. V. Berghe, and B. Worm. Global patterns and predictors of marine biodiversity across taxa. *Nature*, 466:1098–1101, 2010. doi: https://doi.org/10.1038/nature09329.

B. Vanschoenwinkel, F. Buschke, and L. Brendonck. Disturbance regime alters the impact of dispersal on alpha and beta diversity in a natural metacommunity. *Ecology*, 94(11):2547–2557, 2013. doi: http://www.jstor.org/stable/23597216.

R. J. Whittaker. Meta-analyses and mega-mistakes: calling time on meta-analysis of the species richness-productivity relationship. *Ecology*, 91(9):2522–2533, 2010. doi: https://doi.org/10.1890/08-0968.1.

Appendix A

Supplementary material to Chapter 2

Food web and local population dynamics

We consider a multitrophic metacommunity consisting of 40 species on a varying number of randomly positioned habitat patches, Z (the meta-food-web, Figure 2.1). All patches have the same abiotic conditions and each patch can potentially harbor the full food web, consisting of 10 basal plant and 30 animal consumer species. The feeding links (i.e. who eats whom) are constant over all patches (Figure 2.1 a,b) and are as well as the feeding dynamics determined by the allometric food web model by Schneider et al. (2016). We integrate dispersal as species-specific biomass flow between habitat patches (Figure 2.1 b,d).

Using ordinary differential Equations to describe the feeding and dispersal dynamics, the rate of change in biomass density, $B_{i,z}$, of species i on patch z is given by

$$\frac{dB_{i,z}}{dt} = T_{i,z} - E_{i,z} + I_{i,z}\,, \tag{A.1}$$

with $T_{i,z} = v_{i,z} \cdot B_{i,z}$ as the rate of change in biomass density determined by local feeding interactions (where $v_{i,z}$ is the per capita growth rate), $E_{i,z}$ as the total emigration rate of species i from patch z (Equation (A.2)), and $I_{i,z}$ as the total rate of immigration of species i into patch z (Equation (A.4)).

Local food web dynamics

We use an allometric trophic network model (ATN model) based on the work of Schneider *et al.* Schneider et al. (2016) & Kalinkat *et al.* Kalinkat et al. (2013) to simulate the trophic dynamics of local populations ($T_{i,z}$ in Equation (A.1)). Regarding this term, we distinguish between animal species (Equation T1-1) and basal plant species (Equation T1-6). In each patch, the biomass dynamics of animal species (biomass densities $A_{i,z}$) is given by the differences between growth due to consumption of animal or plant species and losses due to mortality through predation and metabolic demands. The rate of change in plant biomass densities, $P_{i,z}$, depends on the uptake of the two resources, mortality through grazing, and also accounts for metabolic losses. We used a dynamic nutrient model (Equation T1-8) with two nutrients (concentrations $N_{l,z}$) of different importance as the energetic basis of our food web (Brose, 2008; Schneider et al., 2016).

The topological network model is an extension of the niche model originally introduced by Williams & Martinez Williams and Martinez (2000) and accounts for allometric degree distributions and recent data on scaling relationships for species body mass and trophic levels (Riede et al., 2011). Each species i is fully characterized by its average adult body mass m_i. We sampled $\log_{10}$ body masses of animal species randomly with a uniform probability density from the inclusive interval $(2, 12)$ and the $\log_{10}$ body masses of plant species from the inclusive interval $(0, 6)$ (for empirical examples see Brose et al. (2019)). This step makes the model inherently stochastic, but from hereon, all other steps are completely deterministic. The model is designed such that animal consumers feed on resources, which can be both plants and other animal species that are smaller than themselves. Body masses further determine the interaction strengths of feeding links as well as the metabolic demands of species.

Data from empirical feeding interactions are used to parametrize the functions that characterize the optimal prey body mass and the location and width of the feeding niche of a predator. From each m_i a unimodal attack kernel, called feeding efficiency, L_{ij}, is constructed which determines the probability of consumer species i to attack and capture an encountered resource species j. We model L_{ij} as an asymmetrical hump-shaped Ricker's function (Equation T1-4) that is maximized for an energetically optimal resource body mass (optimal consumer-resource body mass ratio $R_{opt} = 100$)

and has a width of $\gamma = 2$. The maximum of the feeding efficiency L_{ij} equals 1. Table A1 list the full set of Equation and Table A2 is an overview of the standard parameter set for the equations. See also Schneider *et al.* (Schneider et al., 2016) for further information regarding the allometric food web model.

TABLE A1: Ordinary differential equations describing the local population dynamics driven by feeding interactions (see Schneider *et al.* Schneider et al. (2016). We use the same allometric constraints and parameter ranges.

Equation No.	Model equations	Description
Equation T1-1	Animal population dynamics $\frac{dA_{i,z}}{dt} = e_P A_{i,z} \sum_j F_{ij,z} + e_A A_{i,z} \sum_k F_{ik,z} - \sum_k A_{k,z} F_{ki,z} - x_i A_{i,z}$	Rate of change of biomass density of animal species i on patch z; with conversion efficiency $e_P = 0.545$ typical for herbivory (Lang et al., 2017); conversion efficiency $e_A = 0.906$ typical for carnivory (Lang et al., 2017); feeding rate $F_{ij,z}$ of consumer i on resource j on patch z; metabolic demands per unit biomass for animals $x_i = x_A m_i^{-0.305}$ with scaling constant $x_A = 0.314$ (Ehnes et al., 2011; Yodzis and Innes, 1992). The first sum goes over all plant resources j, the second over all animal resources k and the third over all animal predators k of animal species i.
Equation T1-2	Functional response $F_{ij,z} = \frac{\omega_i \kappa_{i,j} R_{j,z}^{1+q}}{1 + cA_{i,z} + \omega_i \sum_k \kappa_{ik} h_{ik} R_{k,z}^{1+q}} \cdot \frac{1}{m_i}$	Per unit biomass feeding rate of consumer i as function of its own biomass density, A_i, (taking interference competition c, which is the time lost due to intraspecific encounters, sampled from a normal distribution with mean $\mu_c = 0.8$ and s.d. $\sigma_c = 0.2$ for each food web), and biomass density of the resource R_j (either animal A_j or plant species P_j); with ϕ_{ij}, resource specific capture coefficient (Eq. T1-3); h_{ij}, resource-specific handling time (Eq. T1-5); $\omega_i = 1/($number of resource species of $i)$, relative consumption rate accounting for the fact that a consumer has to split its consumption if it has more than one resource species.

Continued on next page

Table A1 – continued from previous page

Equation No.	Model equations	Description
Equation T1-3	Capture coefficient $\kappa_{ij} = \lambda_l m_i^{\beta_i} m_j^{\beta_j} L_{ij}$	Resource specific capture coefficient of consumer species i on resource species j scaling the feeding kernel L_{ij} by a power function of consumer and resource body mass, assuming that the encounter rate between consumer and resource scales with their respective movement speed. We sample the exponents β_i and β_j from normal distributions (mean $\mu_{\beta_i} = 0.42$, s.d. $\sigma_{\beta_i} = 0.05$; $\mu_{\beta_j} = 0.19$, s.d. $\sigma_{\beta_j} = 0.04$, respectively (Hirt et al., 2017)). We divide here the group of consumer species into the subgroup of carnivorous and herbivorous species each comprising a constant scaling factor for their capture coefficients λ_l with $l \in 0, 1$ ($\lambda_0 = 40$ for carnivorous species and $\lambda_1 = 5000$ for herbivorous species); For plant resources, $m_j^{\beta_j}$ was replaced with the constant value of 1 (as plants do not move).
Equation T1-4	Feeding efficiency $L_{ij} = \left(\frac{m_i}{m_j R_{opt}} e^{1 - \frac{m_i}{m_j R_{opt}}} \right)^{\gamma}$	The probability of consumer i to attack and capture an encountered resource j (which can be either plant or animal), described by an asymmetrical hump-shaped curve (Ricker's function), with width $\gamma = 2$ centered around an optimal consumer-resource body mass ratio $R_{opt} = 100$.

Continued on next page

Table A1 – continued from previous page

Equation No.	Model equations	Description
Equation T1-5	Handling time $h_{ij} = h_0 m_i^{\eta_i} m_j^{\eta_j}$	The time consumer i needs to kill, ingest and digest resource species j, with scaling constant $h_0 = 0.4$ and allometric exponents η_i and η_j drawn from normal distributions with means $\mu_{\eta_i} = -0.48$ and $\mu_{\eta_j} = -0.66$, and standard deviations $\sigma_{\eta_i} = 0.03$ and $\sigma_{\eta_i} = 0.02$, respectively (Rall et al., 2012).
Equation T1-6	Plant population dynamics $\frac{dP_{i,z}}{dt} = r_i G_i P_{i,z} - \sum_k A_{k,z} F_{ki,z} - x_i P_{i,z}$	Rate of change of biomass density of plant species i on patch z; with predation loss $F_{ki,z}$ summed over all consumer species k feeding on plant species i; metabolic demands per unit biomass for plants $x_i = x_P m_i^{-0.25}$ with $x_P = 0.138$; intrinsic growth rate $r_i = m_i^{-0.25}$; species specific growth factor G_i (Eq. T1-7).
Equation T1-7	Growth factor for plants $G_i = min\left(\frac{N_1}{K_{i,1} + N_1}, \frac{N_2}{K_{i,2} + N_2}\right)$	Species-specific growth factor of plants determined dynamically by the most limiting nutrient $l \in 1,2$; with $K_{i,l}$, half-saturation densities determining the nutrient uptake efficiency assigned randomly for each plant species i and nutrient l (uniform distribution within (0.1, 0.2)). The term in the minimum operator approaches 1 for high nutrient concentrations.

Continued on next page

Table A1 – continued from previous page

Equation No.	Model equations	Description
Equation T1-8	Nutrient dynamics $\frac{dN_{l,z}}{dt} = D(S_l - N_l) - v_l \sum_{i,z} r_i G_i P_{i,z}$	Rate of change of nutrient concentration N_l of nutrient $l \in \{1, 2\}$ on patch z, with global turnover rate $D = 0.25$, determining the rate at which nutrients are refreshed; supply concentration S_l, determining the maximum nutrient level of each nutrient, l, drawn from normal distributions with mean $\mu_S = 50$ and standard deviation $\sigma_S = 2$ (provided $S_l > 0$); relative nutrient content in plant species biomass v_l ($v_1 = 1$, $v_2 = 0.5$).

Generating landscapes

We generated differently fragmented landscapes, represented by random geometric graphs (Penrose, 2003), by randomly drawing the locations of Z patches from a uniform distribution between 0 and 1 for x- and y-coordinates respectively. We created landscapes of different size by scaling the maximum dispersal distance of all organisms δ_{max} with a factor, Q, to represent landscape sizes with edge lengths between 0.01 and 10. We obtained the number of patches, Z, by using a stratified random sampling approach, i.e. we added a random number drawn from an integer uniform distribution between 0 and 9 to a series of numbers of $10, 20, \ldots, 60$. Similarly, we set the landscape size, Q, by adding a random number drawn from a uniform distribution between 0 and 1 (respectively 0 and 0.1 for landscape sizes below 1) to a series of numbers of $0.01, 0.1, 0.2, 0.3, 0.5, 0.7, 0.9, 1, 3, 5, 7, 9$.

Dispersal

We model dispersal between local communities as a dynamic process of emigration and immigration, assuming dispersal to occur at the same timescale as the local population dynamics (Amarasekare, 2008). Thus, biomass flows dynamically between local populations and the dispersal dynamics directly influence local population dynamics and vice versa (Fronhofer et al., 2018). Similar approaches have been used by e.g. Abrams & Ruokolainen Abrams and Ruokolainen (2011) and Ims & Andreassen Ims and Andreassen (2005). We model a hostile matrix between habitat patches that does not allow for feeding interactions to occur during dispersal, and thus, assume the biomass lost to the matrix to scale linearly with the distance traveled.

Emigration The total rate of emigration of species i from patch z is

$$E_{i,z} = d_{i,z} B_{i,z} \, , \tag{A.2}$$

with $d_{i,z}$ as the corresponding per capita dispersal rate. We model $d_{i,z}$ as

$$d_{i,z} = \frac{a}{1 + e^{b(x_i - v_{i,z})}} \, , \tag{A.3}$$

with a, the maximum dispersal rate, b, a parameter determining the shape of the dispersal rate (Figure A1), x_i, the inflection point determined by the metabolic demands per unit biomass of species i, and $\upsilon_{i,z}$, the per capita net growth rate of species i on patch z. We chose to model $d_{i,z}$ as a function of each species' per capita net growth rate to account for emigration triggers such as resource availability, predation pressure and inter- and intraspecific competition (Bowler and Benton, 2005; Fronhofer et al., 2018). If for example an animal species' net growth is positive, there is no need for dispersal and emigration will be low. However, if the local environmental conditions deteriorate, the growing incentives to search for a better habitat increase the fraction of individuals emigrating. For plants, we assumed an additional scenario as there are examples of different life history strategies. There are for example plant species which disperse from their local habitat when they are doing well, i.e. they have a high net growth rate, as they can allocate more resources into reproduction resulting in higher seed dispersal (Miyazaki et al., 2009). However, there are also examples where plants reallocate resources into reproduction when they are doing poorly (Macedo, 2012) (Figure A1b).

For each simulation run, a was sampled from a Gaussian distribution (μ_{aS}, σ_{aS}) and b was sampled from an integer uniform distribution within inclusive limits that differed between consumer and plant species (see Table A2). The different intervals reflect different dispersal triggers for animals and plants.

Immigration The rate of immigration of biomass density of species i into patch z follows

$$I_{i,z} = \sum_{n \in N_z} E_{i,n}(1 - \delta_{i,nz}) \frac{1 - \delta_{i,nz}}{\sum_{m \in N_n} 1 - \delta_{i,nm}}, \tag{A.4}$$

where N_z and N_n are the sets of all patches within the dispersal range of species i on patches z and n, respectively. In this equation, $E_{i,n}$ is the emigration rate of species i from patch n, $(1 - \delta_{i,nz})$ is the fraction of successfully dispersing biomass, i.e. the fraction of biomass not lost to the matrix, and $\delta_{i,nz}$ is the distance between patches n and z relative to species i's maximum dispersal distance δ_i (see below paragraph Maximum dispersal distance). The term $\frac{1-\delta_{i,nz}}{\sum 1-\delta_{i,nm}}$ determines the fraction of biomass of species i emigrating from source patch n towards target patch z. This fraction depends on the relative distance between the patches, $\delta_{i,nz}$, and the relative distances to all

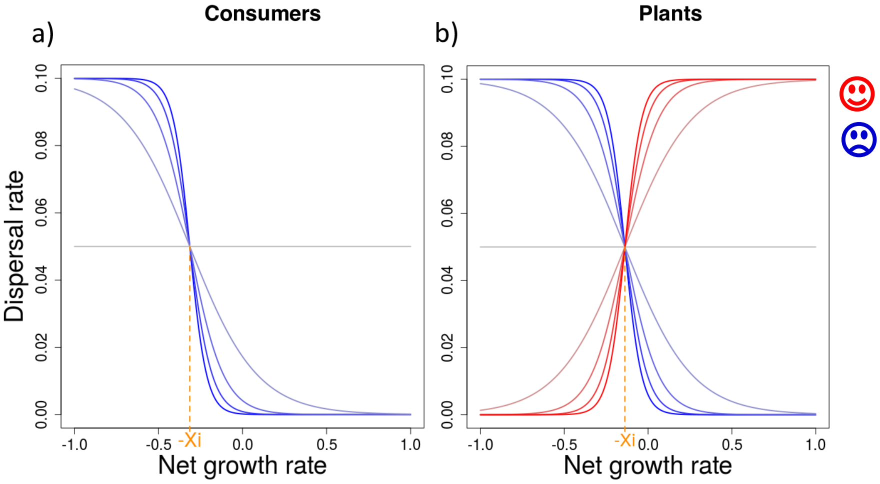

FIGURE A1: Functions illustrating the dispersal rate d_i for animal (a) and plant species (b), where x_i marks the inflection point for each species i determined by the metabolic demands (x_i) per unit biomass of species i (see Table A1). The colors blue and red represent different dispersal strategies and the respective color gradients depict the parameter range of b, which determines the slope of the dispersal rate (see Equation (A.3)). For the purpose of illustration, we set the maximum dispersal rate to $a = 0.1$ and for animals and plants $x_{i_A} = 0.314$ and $x_{i_P} = 0.1384$, respectively.

other potential target patches m of species i on the source patch n, $\delta_{i,nm}$. Thus, the flow of biomass is greatest between patches with small distances. For numerical reasons, we did not allow for dispersal flows with $I_{i,z} < 10^{-10}$. In this case, we immediately set $I_{i,z}$ to 0.

Maximum dispersal distance Based on empirical observations (e.g. (Jenkins et al., 2007)) and previous theoretical frameworks (e.g. (Hirt et al., 2017; Holt and Hoopes, 2005; Holt, 2002; Jetz et al., 2004)), we assume that the maximum dispersal distance δ_i of animal species increases with their body mass. For animal species, the body mass m_i determines how fast and how far they can travel through the matrix before needing

TABLE A2: Model parameters and output variables.

Parameter	Description	Value
	Trophic interactions between species	
e_A	conversion efficiency animal species	0.906; (Lang et al., 2017)
e_P	conversion efficiency plant species	0.545; (Lang et al., 2017)
x_A	scaling constant metabolic demands animal species	0.314; (Yodzis and Innes, 1992)
x_P	scaling constant metabolic demands plant species	0.138; (Yodzis and Innes, 1992)
μ_c, σ_c	mean and standard deviation for interference competition	0.8, 0.2
λ_0	scaling factor capture coefficient for carnivorous species	40
λ_1	scaling factor capture coefficient for herbivorous species	5000
$\mu_{\beta_i}, \sigma_{\beta_i}$	mean and standard deviation allometric exponent for attack rates consumer	0.42, 0.05; (Hirt et al., 2017)
$\mu_{\beta_j}, \sigma_{\beta_j}$	mean and standard deviation allometric exponent for encounter of prey	0.19, 0.04; (Hirt et al., 2017)
ω_i	relative consumption rate	$\frac{1}{\text{number of prey species } i}$
R_{opt}	optimal consumer-resource body mass ratio	100
γ	scaling exponent Ricker's function	2
h_0	scaling factor handling time	0.4
$\mu_{\eta_i}, \sigma_{\eta_i}$	mean and standard deviation allometric exponent handling time consumer	-0.48, 0.03; (Rall et al., 2012)
$\mu_{\eta_j}, \sigma_{\eta_j}$	mean and standard deviation allometric exponent handling time resource	-0.66, 0.02; (Rall et al., 2012)
μ_q, σ_q	mean and standard deviation hill coefficient	1.5, 0.2
	Nutrient dynamics	
K	half saturation density nutrient uptake	(0.1, 0.2)
D	nutrient turnover rate	0.25
μ_{S_l}, σ_{S_l}	mean and standard deviation of nutrient supply concentration	50, 2
ν_1, ν_2	relative nutrient content in plant species biomass	1, 0.5
	Dispersal dynamics	
δ_{max}	species-specific maximum dispersal distance	0.5
ϵ	scaling exponent for species-specific maximum dispersal distance	0.05
μ_{a_S}, σ_{a_S}	mean and standard deviation of max. emigration	0.1, 0.03
θ	cut off emigration function	$3 \cdot \sigma_{a_S}$
b	shape parameter of the emigration function	(0,19) (cons.) (-20,19) (plants)
	Output variables	
$\overline{\tau}$	mean distance between all habitat patches, with τ_{nm}, the absolute distance between patches n and m, and $(Z^2 - Z)$, the total number of potential directed links between all Z habitat patches	$\frac{\sum_{n,m=1}^{Z} \tau_{nm}}{Z^2 - Z}$
ρ_i	landscape connectance of species i, with L_i, the number of directed dispersal links of species i	$\frac{L_i}{Z^2 - Z}$

to rest and feed in a habitat patch. Thus animal species at high trophic positions can disperse further than smaller animals at lower trophic levels. Each animal species perceives its own dispersal network dependent on its species-specific maximum dispersal distance

$$\delta_i = \delta_0 m_i^{\epsilon} , \tag{A.5}$$

where the exponent $\epsilon = 0.05$ determines the slope of the body mass scaling of δ_i. We chose a positive value for ϵ to account for a higher mobility of animals with larger body masses. The intercept $\delta_0 = 0.1256$ was chosen such that the animal species with the largest possible body mass of $m_i = 10^{12}$ had a maximum dispersal distance of $\delta_i = 0.5$. Thus, the animal species with the smallest possible body mass of $m_i = 10^2$ had a maximum dispersal distance of $\delta_i = 0.158$.

As plants are passive dispersers driven by e.g. wind with no clear relationship between body mass and dispersal distance, we model their maximum dispersal distance as random and body mass independent (Jenkins et al., 2007). We sampled δ_i for each plant species from a uniform probability density within the interval $(0, 0.5)$. Thus, the best plant disperser can potentially have the same maximum dispersal distance as the largest possible animal species (Table A2). Additionally, we tested a null model in which all species have the same maximum dispersal distance of $\delta_i = \delta_{max}$. See section A for further information on the additional simulations.

Numerical simulations and data analysis

We constructed 30 model food webs, each comprising 10 plant and 30 animal species. To avoid confounding effects of different initial species diversities, we kept both the number of species S and the fraction of plants and animals constant among all food webs. For each simulation, we randomly generated a landscape of size Q (edge length of a square landscape) with Z randomly distributed habitat patches. To test each food web across a gradient of number of habitat patches and habitat isolation, we drew the number of habitat patches, Z, from the inclusive interval $(10, 69)$ and the size of the landscape, Q, from the inclusive interval $(0.01, 10)$ using a stratified random sampling approach (see also section A for further information). With this approach, we generated landscapes on two independent gradients covering two aspects of fragmentation, namely number of fragments and habitat isolation. To cover the full parameter range of Z and Q, we simulated each food web on 72 landscapes resulting in a total of 2160 simulations. We achieved a full range for the gradient of habitat isolation (landscape connectance ranging from 0 to 1, Figure A3c). The upper limit for the number of patches was chosen to conform to the maximum usage time of 10 days per simulation on the high-performance-cluster we used (Schnicke et al., 2017). Additionally, we performed dedicated simulation runs to reference the two extreme cases, i.e. (1) landscapes in which all patches are direct neighbors without a hostile matrix, and thus, no dispersal mortality, and (2) fully isolated landscapes, in which no species can bridge between patches, and thus, a dispersal mortality of 100% .

For each simulation run, we initialized our model with random conditions: Each habitat patch z holds a random selection of 21 to 40 species (with each of the 40 species of the full food web existing on at least one patch) and initial biomass densities $B_{i,z}$ and nutrient concentrations N_l ($l \in 1, 2$) were randomly sampled with uniform probability density within the intervals $(0, 10)$ for $B_{i,z}$ and $(S_l/2, S_l)$ for N_l, respectively. Here, S_l are the supply concentrations of the nutrients, which are constant on all habitat patches but differ between the two nutrients. See Table A2, Equation T1-8 and Schneider *et al.* Schneider et al. (2016) for further information on the nutrient dynamics.

Starting from these random initial conditions, we numerically simulated local food web and dispersal dynamics over 50,000 time steps by integrating the system of differential equations implemented in C++ using procedures of the SUNDIALS CVODE solver version 2.7.0 (backward differentiation formula with absolute and relative error tolerances of 10^{-10} (Hindmarsh et al., 2005)). Successful dispersal between local populations thereby enabled species to establish populations on patches where they were initially absent. For numerical reasons, a local population was considered extinct once $B_{i,z} < 10^{-20}$, and $B_{i,z}$ was then immediately set to 0.

Output variables

We recorded the following output variables for each simulation run: (1) the mean biomass density of each species i on each habitat patch z over the last 20,000 time steps, $\overline{B}_{i,z}$; (2) the number of habitat patches in a landscape, Z; (3) habitat isolation, i.e. the mean distance between all habitat patches, $\overline{\tau}$ (see Table A2); and (4) the landscape connectance of each species i, ρ_i (see Table A2). Thus, ρ_i determines the ability of a species to connect habitat patches in a fragmented landscape.

Statistical models and data visualization We tested for correlation between initialized and emerged β-diversity, which was however not the case (see section A). Further, we used generalized additive mixed models (GAMM) from the mgcv package in R (Wood, 2017) to visualize the impact of number of patches and habitat isolation on species diversity. To fit the model assumptions, we logit-transformed $\overline{\alpha}$-diversity, and log-transformed β-diversity. We analyzed each diversity index separately, with the number of patches Z (log-transformed), the mean patch distance $\overline{\tau}$ (log-transformed) and their interaction as fixed effects and the ID of the food web (1 - 30) as random factor (with normal distribution for $\overline{\alpha}$- and β-diversity, and binomial distribution for γ-diversity). Similarly, we analyzed the mean biomass densities, $\overline{B}_{i,z}$ (log-transformed), and species-specific landscape connectance, ρ_i, for each species (ID 1 - 40) using GAMM with a normal distribution.

Analysis

Out of the 2160 simulations we started, 57 were terminated by reaching the maximum usage time of 10 days per simulation on the high-performance-cluster we used (Schnicke et al., 2017). We further deleted 30 simulations as they had entirely isolated landscapes with no dispersal links. We performed all statistical analyses in R version 3.3.2. (Team, 2016) using the output of the remaining 2073 simulations. See also section A for additional information.

Species diversity We quantified Whittaker's α-, β-, and γ-diversity (Whittaker, 1972) using presence-absence data derived from the recorded mean biomass densities, $\overline{B}_{i,z}$, counting species i present on patch z when $\overline{B}_{i,z} > 10^{-20}$. In Whittaker's approach, α

accounts for the local species richness, β is the component of regional diversity that accumulates from compositional differences between local communities, and γ is the regional diversity, i.e. the species richness at the landscape scale (Whittaker, 1972). We relate α, β and γ to each other using multiplicative partitioning (Whittaker, 1972), i.e. $\alpha \cdot \beta = \gamma$. Here, we use α averaged over all habitat patches Z (which we hereafter refer to as $\overline{\alpha}$) to get a measure at the landscape level comparable to β and γ.

Maximum trophic level

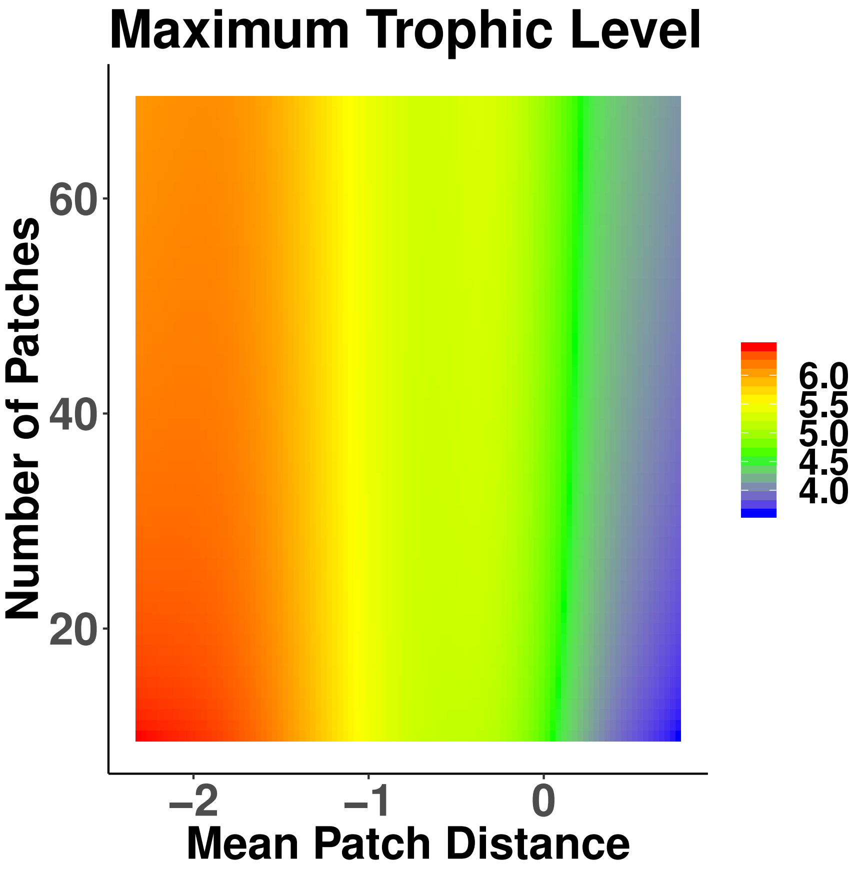

FIGURE A2: Heatmap visualizing the maximum trophic level within a food web (colour-coded; z-axis) in response to habitat isolation, i.e. the mean patch distance ($\overline{\tau}$, $\log_{10}$-transformed; x-axis) and the number of habitat patches (Z; y-axis). The heatmap was generated based on the statistical model predictions. The loss of species diversity driven by habitat isolation also translates into a loss of the maximum trophic level.

Additional simulations with a constant maximum dispersal distance

We repeated all simulations with a constant maximum dispersal range for all species of $\delta_{const.} = 0.5$, i.e. all species have the same spatial network, to understand the effect of the dispersal advantage of larger animals. The results from these simulations are very similar to the results with the species-specific scaling of dispersal ranges, showing the same biomass density drop of larger animals at low mean distances (Figure A3).

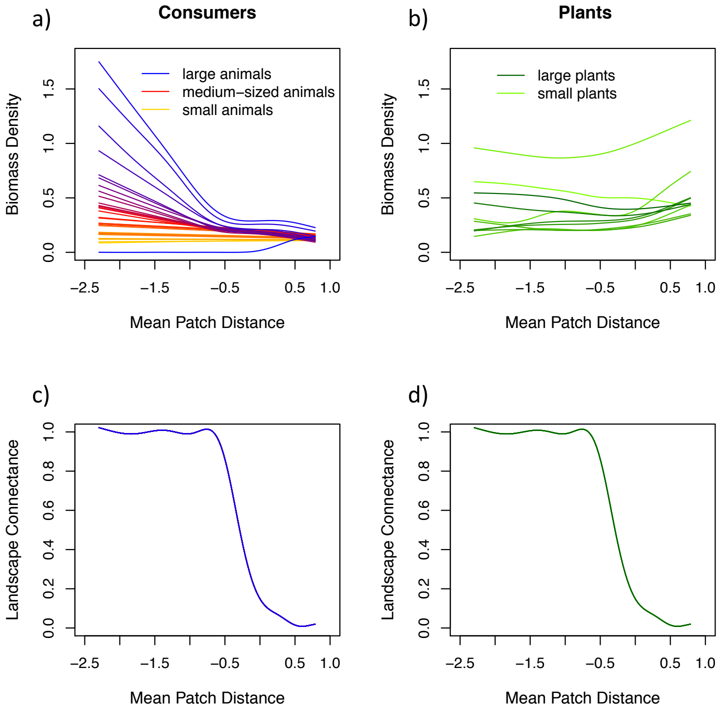

FIGURE A3: Top row: Mean biomass densities of consumer (a) and plant species (b) over all food webs (B_i, $\log_{10}$-transformed; y-axis) in response to habitat isolation, i.e. the mean patch distance ($\overline{\tau}$, $\log_{10}$-transformed; x-axis). Each color depicts the biomass density of species i averaged over all food webs: (a) color gradient where orange represents the smallest, red the intermediate and blue the largest consumer species; (b) color gradient where light green represents the smallest and dark green the largest plant species. Bottom row: Mean species-specific landscape connectance (ρ_i; y-axis) for consumer species (c) and plant species (d) over all food webs as a function of the mean patch distance ($\overline{\tau}$, $\log_{10}$-transformed; x-axis), using the same maximum dispersal distance for all species, $\delta_{const} = 0.5$.

Additional simulations of the two extreme cases

To explore the extreme cases of fragmentation in our model framework, we conducted additional simulations with emigration but no immigration on patches to represent completely isolated patches (disconnected), and landscapes with patches containing all species of the meta-food-web and neither emigration nor immigration to represent one joint landscape with no fragmentation (joint). For the disconnected scenario we simulated 12 replicates for each of the 30 food webs covering in the same stratified random gradient of patch numbers between 10 and 69 as in the main simulations and were also initialized with a subset of species (see section S4). For the joint scenario we simulated 20 replicates for each food web containing 2 independent patches initialized with all species and no dispersal.

(1) Joint scenario with no dispersal mortality $\overline{\alpha}$-diversity is on average 37.621, γ-diversity 37.172 and β-diversity 1.004 (Figure A4, purple triangle).

(2) Fully isolated scenario with 100% dispersal mortality $\overline{\alpha}$-diversity is on average 11.945, γ-diversity 32.801 and β-diversity 2.876 (Figure A4, orange triangle).

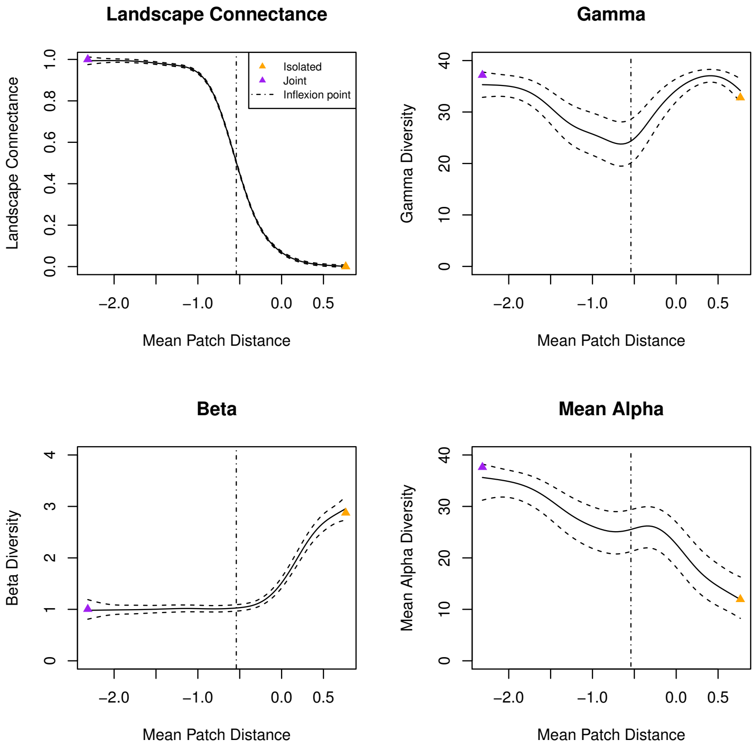

FIGURE A4: Shown are model predictions for landscapes with 40 patches across the whole gradient of the mean patch distance ($\overline{\tau}$, $\log_{10}$-transformed; x-axis). Top-left panel shows the landscape connectance averaged over all species (y-axis) as response to the mean patch distance ($\overline{\tau}$, $\log_{10}$-transformed; x-axis). Subsequent panels show γ-diversity, β-diversity and $\overline{\alpha}$-diversity (y-axes) in response to the mean patch distance ($\overline{\tau}$, $\log_{10}$-transformed; x-axis). Purple triangles represent reference points from dedicated simulations in a joint scenario and orange triangles for fully isolated scenarios (see section S7).

Sensitivity analysis

We tested the effect of randomly drawn dispersal parameters (maximum dispersal rate, a, and the shape of the dispersal function, b; Equation (A.3)) on $\overline{\alpha}$-, β- and γ-diversity for consumers and plants respectively. We used generalized additive mixed models (GAMM) from the mgcv package in R for all sensitivity analyses. To fit the model assumptions, we logit-transformed $\overline{\alpha}$-diversity, and log-transformed β- and γ-diversity.The emigration parameters were separately used as fixed effects and the ID of the food web (1 - 30) as random factor (with normal distribution for $\overline{\alpha}$- and β-diversity, and binomial distribution for γ-diversity). Both parameters show no strong effect in all tested cases (Figure A5 - A7). Only the maximum emigration rate a of consumers shows a small negative effect on $\overline{\alpha}$-diversity (Figure A5). As a higher maximum emigration rate results in an overall larger loss term due to dispersal, this fits to our general findings.

Additional sensitivity analysis for interference competition, allometric exponent for attack rates of consumer species, exponents for handling time, hill coefficient and nutrient turnover rate were omitted as they were tested thoroughly in Schneider *et al.* Schneider et al. (2016). There, the dynamics of the food web model were shown to be robust to changes in model parameters. For each of the 2073 simulation runs the parameters of the trophic interactions were independently sampled from appropriate probability distributions within ecologically reasonable limits (see Table A1). To account for the stochastic nature of the algorithm provided by Schneider *et al.* (Schneider et al., 2016) by which food web topologies are created, we generated an ensemble of 30 food webs by randomly sampling 30 sets of species body masses.

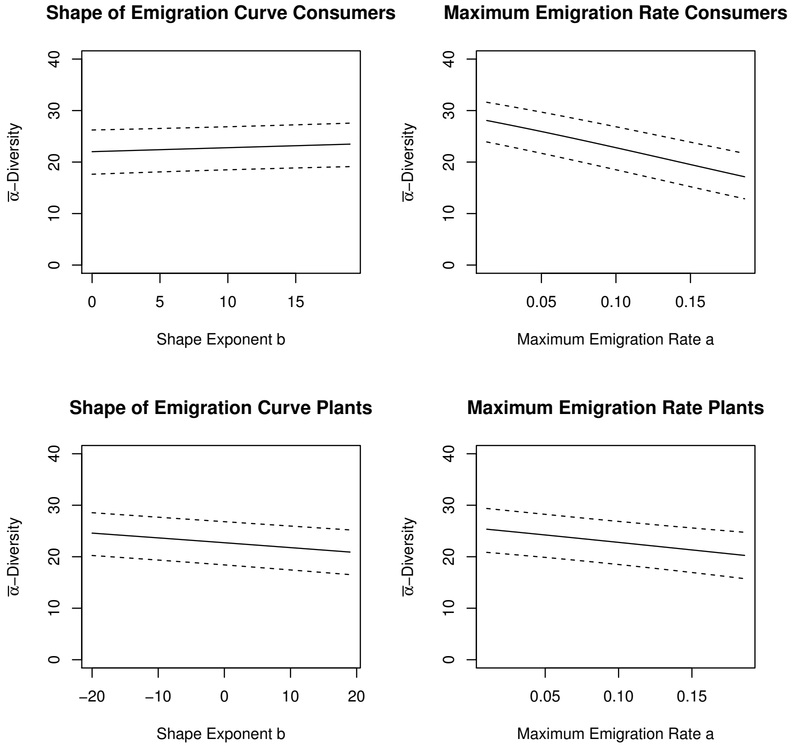

FIGURE A5: $\overline{\alpha}$-diversity (y-axes) of consumers and plants in dependence of the maximum emigration rate, *a*, and the shape of the emigration function, *b* respectively (x-axes).

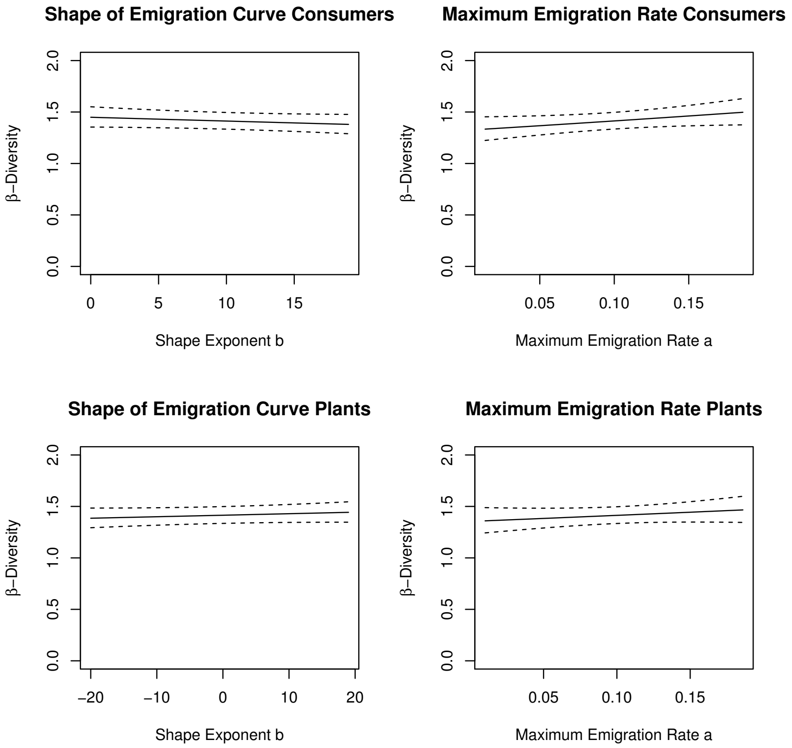

FIGURE A6: β-diversity (y-axes) of consumers and plants in dependence of the maximum emigration rate, a, and the shape of the emigration function, b respectively (x-axes).

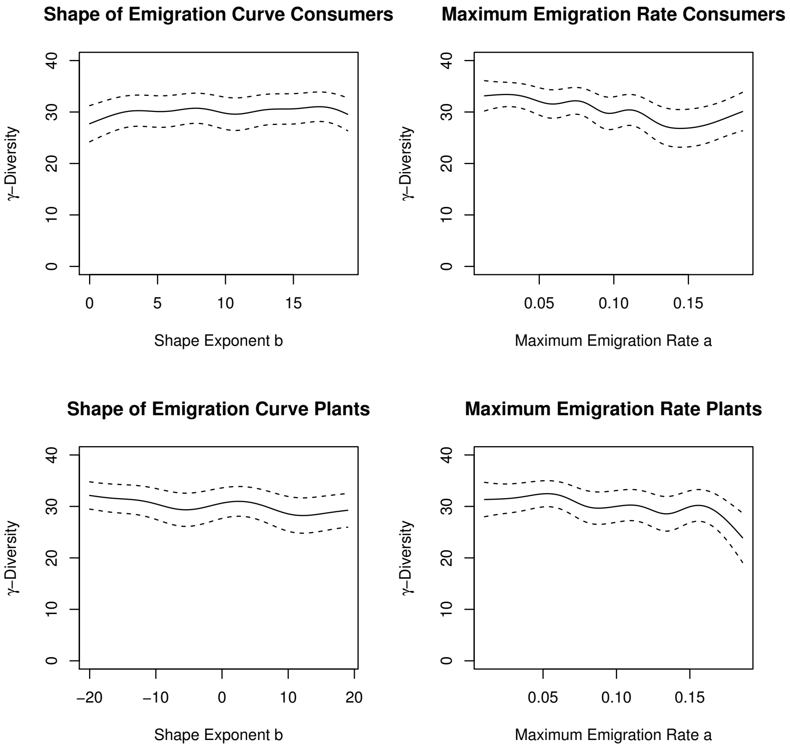

FIGURE A7: γ–diversity (y-axes) of consumers and plants in dependence of the maximum emigration rate, a, and the shape of the emigration function, b respectively (x-axes).

Initial and post-simulation β-diversity

To see how the initialised β-diversity (see section A) influenced the post-simulation β-diversity we performed a generalized additive mixed model (GAMM) from the mgcv package in R with the initial β-diversity as fixed effect and the post-simulation β-diversity as the response variable. Both were log-transformed to fit model assumptions. The post-simulation β-diversity and initial β-diversity were not correlated. This suggests that the initial β-diversity which is due to initializing the patches in the landscape with only a subset of species from the regional species pool does not influence the post-simulation β-diversity detectably (approximate p-value: 0.518) (Figure A8).

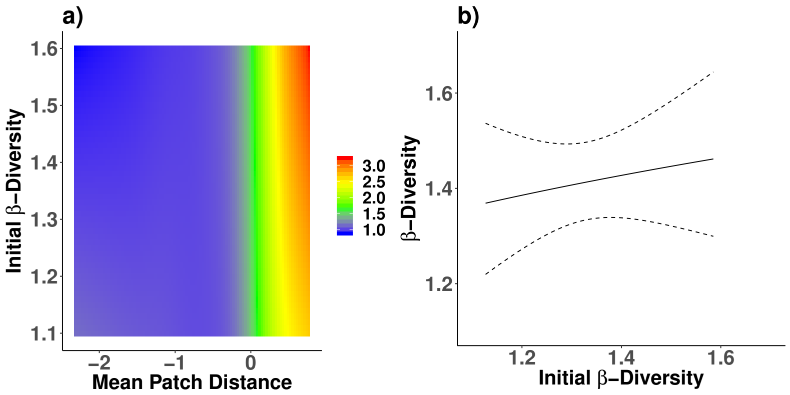

FIGURE A8: (a) Heatmap visualizing β-diversity (color-coded; z-axis) in response to habitat isolation, i.e. the mean patch distance ($\overline{\tau}$, $\log_{10}$-transformed; x-axis) and the initial β-diversity (y-axis). The heatmap was generated based on the statistical model predictions. (b) The post-simulation β-diversity (y-axis) and the initial β-diversity (x-axis) were not correlated. In strongly isolated landscapes β-diversity increases slightly with higher initial β-diversity. However, post-simulation β-diversity is higher than the initial β-diversity.

Standard errors in biomass densities

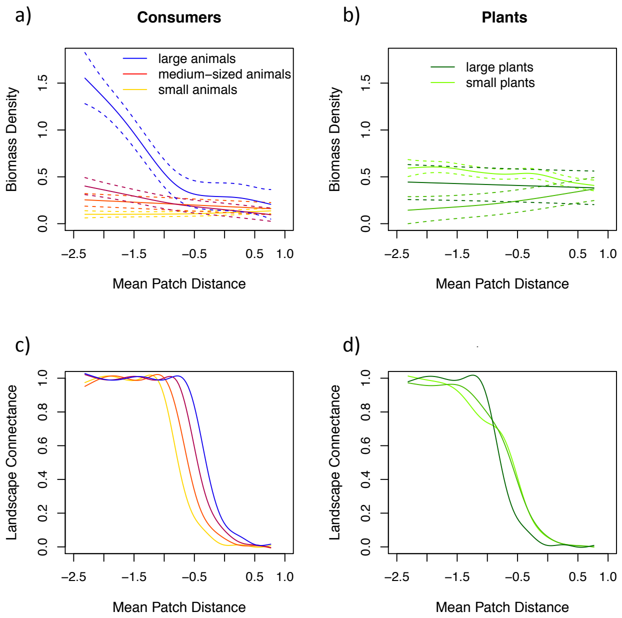

FIGURE A9: Top row: Mean biomass densities [$\log_{10}$(biomass density +1)] with standard errors [± 2*SE] for four exemplary animal consumer species (a) and three exemplary basal plant species (b) over all food webs (B_i, $\log_{10}$-transformed; y-axis) in response to habitat isolation, i.e. the mean patch distance ($\overline{\tau}$, $\log_{10}$-transformed; x-axis). Each color depicts the biomass density of species i averaged over all food webs: (a) color gradient where orange represents the smallest, red the intermediate and blue the largest consumer species; (b) color gradient where light green represents the smallest and dark green the largest plant species. Bottom row: Mean species-specific landscape connectance (ρ_i; y-axis) for consumer (c) and plant species (d) over all food webs as a function of the mean patch distance ($\overline{\tau}$, $\log_{10}$-transformed; x-axis).

Bibliography

P. A. Abrams and L. Ruokolainen. How does adaptive consumer movement affect population dynamics in consumer–resource metacommunities with homogeneous patches? *J Theor Biol*, 277(1):99 – 110, 2011. ISSN 0022-5193. doi: 10.1016/j.jtbi.2011.02.019.

P. Amarasekare. Spatial dynamics of foodwebs. *Annu Rev Ecol Evol Syst*, 39:479–500, 2008. doi: 10.1146/annurev.ecolsys.39.110707.173434.

D. E. Bowler and T. G. Benton. Causes and consequences of animal dispersal strategies: relating individual behaviour to spatial dynamics. *Biol Rev*, 80(2):205–225, 2005. doi: 10.1017/S1464793104006645.

U. Brose. Complex food webs prevent competitive exclusion among producer species. *Proc R Soc B Biol Sci*, 275(1650), 2008. doi: doi.org/10.1098/rspb.2008.0718.

U. Brose, P. Archambault, A. D. Barnes, L.-F. Bersier, T. Boy, J. Canning-Clode, E. Conti, M. Dias, C. Digel, A. Dissanayake, A. A. V. Flores, K. Fussmann, B. Gauzens, C. Gray, J. Häussler, M. R. Hirt, U. Jacob, M. Jochum, S. Kéfi, O. McLaughlin, M. M. MacPherson, E. Latz, K. Layer-Dobra, P. Legagneux, Y. Li, C. Madeira, N. D. Martinez, V. Mendonça, C. Mulder, S. A. Navarrete, E. J. O'Gorman, D. Ott, J. Paula, D. Perkins, D. Piechnik, I. Pokrovsky, D. Raffaelli, B. C. Rall, B. Rosenbaum, R. Ryser, A. Silva, E. H. Sohlström, N. Sokolova, M. S. A. Thompson, R. M. Thompson, F. Vermandele, C. Vinagre, S. Wang, J. M. Wefer, R. J. Williams, E. Wieters, G. Woodward, and A. C. Iles. Predator traits determine food-web architecture across ecosystems. *Nat Ecol Evol*, 2019. doi: 10.1038/s41559-019-0899-x.

R. B. Ehnes, B. C. Rall, and U. Brose. Phylogenetic grouping, curvature and metabolic scaling in terrestrial invertebrates. *Ecol Lett*, 14(10):993–1000, 2011. doi: 10.1111/j.1461-0248.2011.01660.x.

E. A. Fronhofer, D. Legrand, F. Altermatt, A. Ansart, S. Blanchet, D. Bonte, A. Chaine, M. Dahirel, F. De Laender, J. De Raedt, L. Di Gesu, S. Jacob, O. Kaltz, E. Laurent, C. J. Little, L. Madec, F. Manzi, S. Masier, F. Pellerin, F. Pennekamp, N. Schtickzelle, L. Therry, A. Vong, L. Winandy, and J. Cote. Bottom-up and top-down control of dispersal across major organismal groups. *Nat Ecol Evol*, 2(12):1859–1863, 2018. doi: 10.1038/s41559-018-0686-0.

A. C. Hindmarsh, P. N. Brown, K. E. Grant, S. L. Lee, R. Serban, D. E. Shumaker, and C. S. Woodward. Sundials: Suite of nonlinear and differential/algebraic equation solvers. *ACM Trans Math Soft (TOMS)*, 31(3):363–396, 2005.

M. R. Hirt, W. Jetz, B. C. Rall, and U. Brose. A general scaling law reveals why the largest animals are not the fastest. *Nat Ecol Evol*, 1:1116–1122, 2017. doi: 10.1038/s41559-017-0241-4.

R. Holt and M. Hoopes. *Food Web Dynamics in a Metacommunity Context: Modules and Beyond*. The University of Chicago Press, 2005.

R. D. Holt. Food webs in space: On the interplay of dynamic instability and spatial processes. *Ecol Res*, 17(2):261–273, 3 2002. doi: 10.1046/j.1440-1703.2002.00485.x.

R. A. Ims and H. P. Andreassen. Density-dependent dispersal and spatial population dynamics. *Proc R Soc B Biol Sci*, 272(1566):913–8, 2005. doi: 10.1098/rspb.2004.3025.

D. G. Jenkins, C. R. Brescacin, C. V. Duxbury, J. A. Elliott, J. A. Evans, K. R. Grablow, M. Hillegass, B. N. Lyon, G. A. Metzger, M. L. Olandese, D. Pepe, G. A. Silvers, H. N. Suresch, T. N. Thompson, C. M. Trexler, G. E. Williams, N. C. Williams, and S. E. Williams. Does size matter for dispersal distance? *Glob Ecol Biogeogr*, 16(4): 415–425, 2007. doi: 10.1111/j.1466-8238.2007.00312.x.

W. Jetz, C. Carbone, J. Fulford, and J. H. Brown. The scaling of animal space use. *Science (New York, N.Y.)*, 306(5694):266–8, 10 2004. doi: 10.1126/science.1102138.

G. Kalinkat, F. D. Schneider, C. Digel, C. Guill, B. C. Rall, and U. Brose. Body masses, functional responses and predator–prey stability. *Ecol Lett*, 16(9):1126–1134, 2013. doi: 10.1111/ele.12147.

B. Lang, R. B. Ehnes, U. Brose, and B. C. Rall. Temperature and consumer type dependencies of energy flows in natural communities. *Oikos*, 126(12):1717–1725, 2017. doi: 10.1111/oik.04419.

A. F. Macedo. Abiotic stress responses in plants: Metabolism to productivity. In P. Ahmad and M. Prasad, editors, *Abiotic Stress Response in Plants*, pages 41–61. Springer, New York, NY, 2012. doi: 10.1007/978-1-4614-0634-1.

Y. Miyazaki, T. Osawa, and Y. Waguchi. Resource level as a proximate factor influencing fluctuations in male flower production in cryptomeria japonica d. don. *J For Res*, 14(6):358–364, 2009. doi: 10.1007/s10310-009-0148-2.

M. Penrose. *Random Geometric Graphs*. Oxford University Press, 2003.

B. C. Rall, U. Brose, M. Hartvig, G. Kalinkat, F. Schwarzmüller, O. Vucic-Pestic, and O. L. Petchey. Universal temperature and body-mass scaling of feeding rates. *Philos Trans R Soc B Biol Sci*, 367(1605):2923–2934, 2012. doi: 10.1098/rstb.2012.0242.

J. O. Riede, U. Brose, B. Ebenman, U. Jacob, R. Thompson, C. R. Townsend, and T. Jonsson. Stepping in elton's footprints: a general scaling model for body masses and trophic levels across ecosystems. *Ecol Lett*, 14(2):169–178, 2011. doi: doi.org/10.1111/j.1461-0248.2010.01568.x.

F. D. Schneider, U. Brose, B. C. Rall, and C. Guill. Animal diversity and ecosystem functioning in dynamic food webs. *Nat Commun*, 7(12718), 2016. doi: 10.1038/ncomms12718.

T. Schnicke, B. Langenberg, and C. Krause. Eve - high-performance computing cluster, 2017. URL `https://wiki.ufz.de/eve/`.

R. C. Team. R: A language and environment for statistical computing, 2016. URL `https://www.r-project.org/`.

R. H. Whittaker. Evolution and measurement of species diversity. *Taxon*, 21(2/3): 213–251, 1972. doi: 10.2307/1218190.

R. J. Williams and N. D. Martinez. Simple rules yield complex food webs. *Nature*, 404 (6774):180 – 183, 3 2000. doi: 10.1038/35004572.

S. N. Wood. *Generalized Additive Models: An Introduction with R (wnd edition).* Chapman and Hall/CRC., wnd editio edition, 2017.

P. Yodzis and S. Innes. Body size and consumer-resource dynamics. *Am Nat*, 139(6): 1151–1175, 1992. doi: 10.2307/2462335.

Appendix B

Supplementary material to Chapter 3

Example Variability

In this section, we show illustrative time series of two species on two patches to demonstrate effects of synchronous and asynchronous dynamics on α-, β- and γ-variability (Figure B1). Frequency and amplitude of the biomass oscillations (and thus also the α-variability) are the same for both species. Perfectly asynchronous (antiphase) oscillations of species 1 result in β-variability $\rightarrow \infty$ and γ-variability approaching 0. Conversely, perfectly synchronous dynamics of species 2 result in a β-variability of 1 and γ-variability equal to the α-variability.

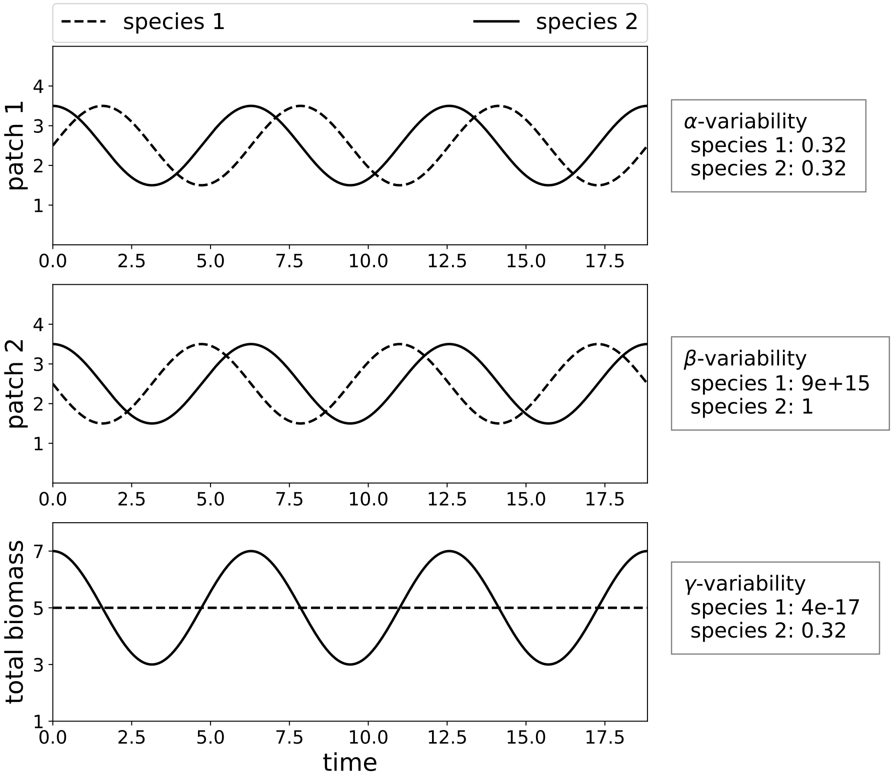

FIGURE B1: Exemplary dynamics of a system with two species on two patches. The first two panels show the time series for each species on patch 1 and 2, respectively, while the bottom panel shows the corresponding total biomasses. The boxes to the right contain the numerical values of the α-, β- and γ-variabilities.

Attack rate dependence of local biomass oscillations

We tested a broad range of combinations of consumer and predator attack rates to find suitable parameter sets for oscillatory dynamics. There are two areas in the parameter space that show oscillatory dynamics, separated by an area that leads to a stable equilibrium (Figure B2). Oscillatory behavior is indicated by an increased α-variability (CV). Mean biomasses of the species are shown to illustrate the two different trophic cascades. The change in biomass between the two cascades is most striking for the autotroph: at low attack rates (weak trophic cascade), it has relatively low biomass, as it is controlled by the consumer, which in turn is only weakly controlled by the predator, whereas its biomass is high when attack rates are also high (strong trophic cascade). Now the consumer is strongly top-down controlled by the predator and cannot control the autotroph anymore.

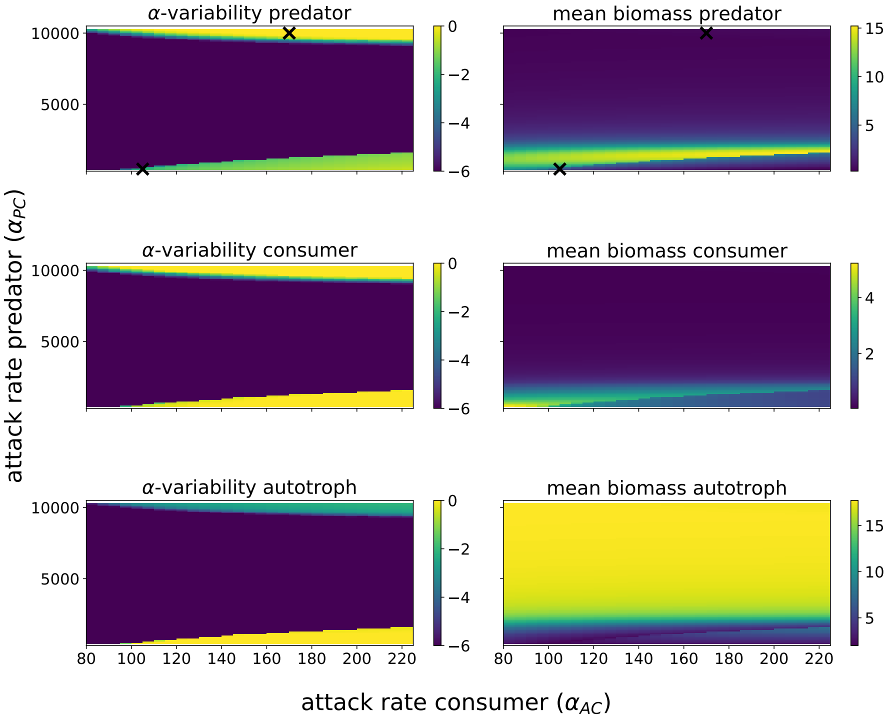

FIGURE B2: Simulation results of the food chain on a single patch for a broad range of consumer- and predator attack rates. Shown are the α-variabilities (left) on a logarithmic scale (log_{10}) and biomasses (right) of predator, consumer, and autotroph species. The black x's denote the parameter values used for the main simulations. Step size attack rate predator: 10; step size attack rate consumer: 5

Variabilities of consumer and autotroph species

To complement the results, we here show α-, β-, and γ-variabilities for the consumer (Figure B3) and the autotroph (Figure B4). The main trends for the local (α-variability), between habitat patches (β-variability) and metapopulation dynamics (γ-variability) are qualitatively the same for the consumer and the autotroph as for the predator species (Figure 3.3).

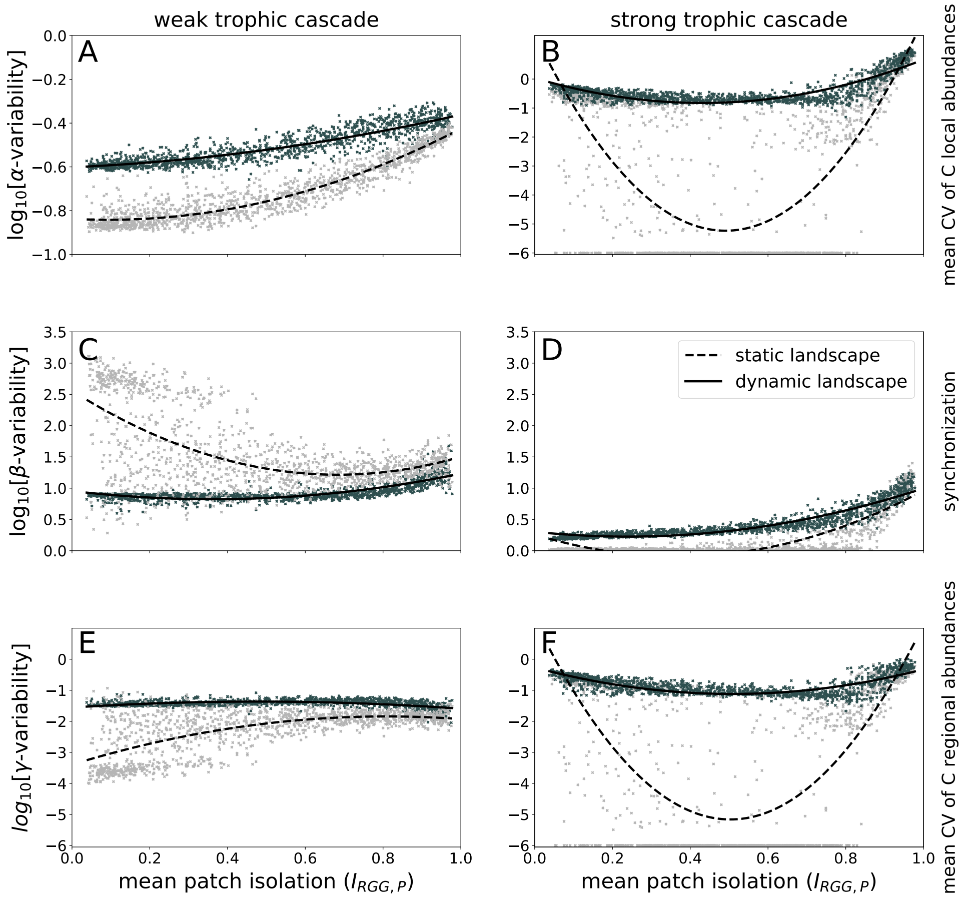

FIGURE B3: Local (α-variability, top row), between patch (β-variability, middle row) and metapopulation dynamics (γ-variability, bottom row) of the consumer for the weak (left column) and the strong trophic cascade (right column). Light gray data points and dashed trend lines (second order fit) indicate static landscapes, dark gray data points and solid trend lines indicate dynamic landscapes. Each data point represents the result of one simulation run with a unique spatial network of habitat patches. All data points where the variability is below 10^{-6} are set to 10^{-6} as differences between them provide no meaningful information that close to the fixed point.

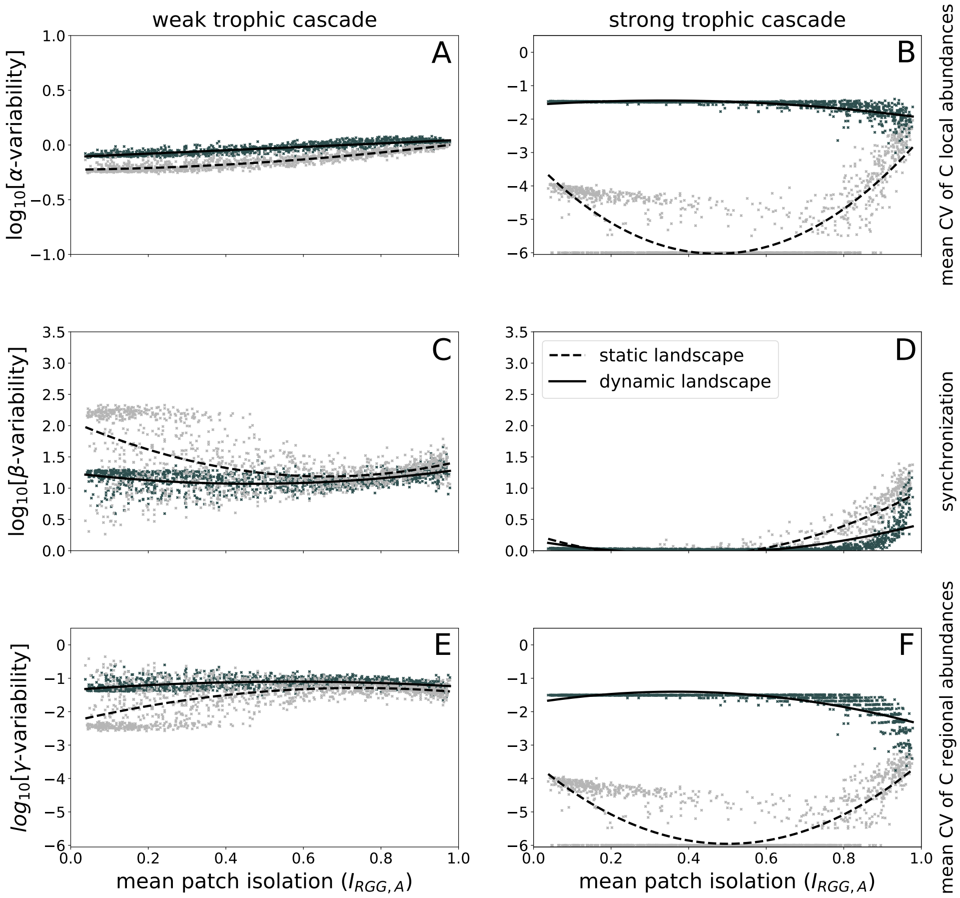

FIGURE B4: Local (α-variability, top row), between patch (β-variability, middle row) and metapopulation dynamics (γ-variability, bottom row) of the autotroph for the weak (left column) and the strong trophic cascade (right column). Light gray data points and dashed trend lines (second order fit) indicate static landscapes, dark gray data points and solid trend lines indicate dynamic landscapes. Each data point represents the result of one simulation run with a unique spatial network of habitat patches. All data points where the variability is below 10^{-6} are set to 10^{-6} as differences between them provide no meaningful information that close to the fixed point.

Alternative stable states in the weak trophic cascade

In order to establish whether the weak trophic cascade (in static landscapes) is indeed bistable, as the seemingly disconnected clouds of data points in Figure 3.3 (C and E) suggest, we performed dedicated simulations with one randomly chosen RGG (fixed patch locations) and evaluated the β-variability of the predator. The minimum dispersal distance, D_0, which controls the mean patch isolation of the RGG (the larger D_0, the lower is the mean patch isolation), was varied between 0.06 and 1.05, first from low to high values (grey points in Figure B5) and then from high to low values (black points in Figure B5). In both cases, the respective attractor the system had settled on was numerically followed, but sudden jumps in the β-variability occurred as the network structure of the RGG changed in a discontinuous way or one of the attractors lost stability. In this particular case, an asynchronous attractor (high β-variability) is present for all values of D_0, while a second attractor with more synchronous dynamics (lower β-variability) is present only for low ($D_0 < 0.4$) or high ($D_0 > 0.9$) values.

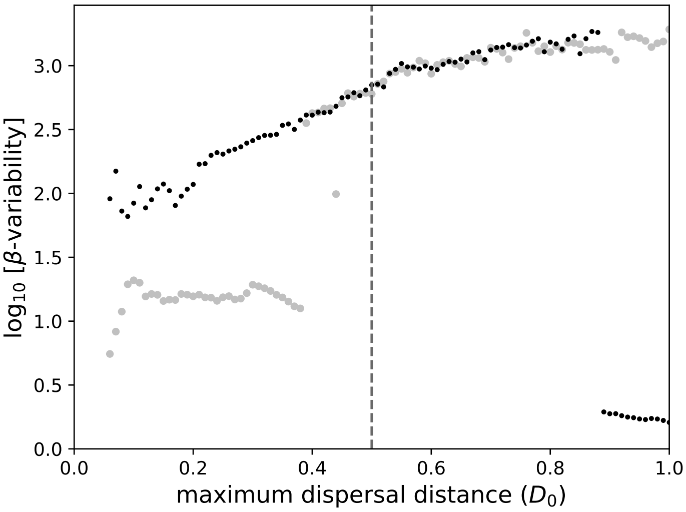

FIGURE B5: Bifurcation diagram of the β-variability of the weak trophic cascade with the minimum dispersal distance, D_0, as control parameter. Grey points: Simulations starting at low D_0 and gradually increasing it (step size: 0.01), black points: simulations starting at high D_0 and gradually decreasing it. The dashed line (D_0=0.5) denotes the maximal D_0 used for the simulations of the main results.

Mean biomasses of each species for different mean patch isolation of the landscape

Over the gradient of patch isolation, the average biomasses (per patch) of the three species in the weak trophic cascade gradually changes. The mean biomass of the predator and consumer species steadily decreases with increasing mean patch isolation, while the mean biomass of the autotroph increases.

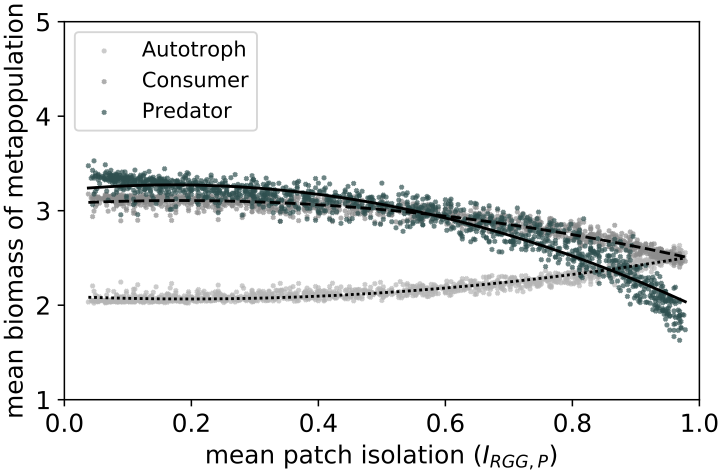

FIGURE B6: Mean biomasses (per patch) for the weak trophic cascade in static landscapes. Dotted trend line (second order fit) and dark gray data points: autotroph, dashed trend line and gray data points: consumer, solid trend line and light gray data points: predator. Each data point represents the result of one simulation run with a unique spatial network of habitat patches.

Appendix C

Supplementary material to Chapter 4

Methods

Local interactions

Our species community model is an extension of the niche model (Williams and Martinez, 2000), taking into account allometric degree distributions and empirical data on scaling relationships for the body masses and the respective trophic levels of the species (Riede et al., 2011). Each species i is characterized exclusively by its average adult body mass m_i, the key trait to describe both animal and plant species. The log_{10} body masses of animal species are randomly drawn from the inclusive interval [2,12] and the log_{10} body masses of plant species from the inclusive interval [0,6]. The body mass also determined the interaction strengths of the feeding links and the metabolic requirements of the species.

Feeding interactions and the respective interaction strength are determined through handling times h_{ij} (Eq. C.3) and through a capturing coefficient κ_{ij} (Eq. C.1), both scaled with the according species body masses m_i and m_j. The capturing of a predator species i on a prey species j is defined as

$$\kappa_{ij} = \lambda_l m_i^{\beta_i} m_j^{\beta_j} L_{ij} , \tag{C.1}$$

with the constant scaling factor λ_l which subdivide the group of consumer species into herbivore (λ_0= 40) and carnivore species (λ_1= 5000), the scaling exponent for body masses β_i and β_j sampled from a normal distribution (mean: μ_{β_i} = 0.42, s.d.:

σ_{β_i} = 0.05; mean: μ_{β_j} = 0.19, s.d.: σ_{β_j} = 0.04 (Hirt et al., 2017)) and the feeding efficiency L_{ij}. For plants as resources, $m_j^{\beta_j}$ was set to 1 (since plants do not move). From each mean body mass m_i a unimodal attack kernel defines the feeding efficiency, L_{ij}, which determines the probability of the consumer species i attacking and capturing an encountered prey species j. We model L_{ij} as an asymmetric hump-shaped Ricker function

$$L_{ij} = \left(\frac{m_i}{m_j R_{opt}} e^{1-\frac{m_i}{m_j R_{opt}}} \right)^{\gamma} , \tag{C.2}$$

maximized for an energetically optimal resource body mass (optimal consumption-resource-body mass ratio R_{opt} =100) with a scaling component $\gamma = 2$. The feeding interactions in the model are such that animal consumers feed on resources that can be both plants and other animal species smaller than themselves.

We described the other part of the feeding interactions through the handling times h_{ij} accounting for the time a consumer i needs to kill, ingest and digest:

$$h_{ij} = h_0 m_i^{\eta_i} m_j^{\eta_j} . \tag{C.3}$$

The handling times are defined by a scaling constant h_0=4 and body masses are scaled through the exponents η_i and η_j sampled from a normal distribution (mean: $\mu_{\eta_i} = -0.48$, s.d.: $\sigma_{\eta_i} = 0.03$; mean: $\mu_{\eta_j} = -0.66$, s.d.: $\sigma_{\eta_j} = 0.02$). See also Schneider et al. (2016) for more information on the allometric food web model.

Emigration

In natural ecosystems, emigration is a complex process involving various environmental factors and species characteristics. We assume that emigration depends on the net per capita growth rate $\upsilon_{i,z}$ of the species i on patch z, which reflects its current situation in this habitat. For example, if the net growth rate of an animal species is positive, the habitat offers suitable living conditions and the rate of emigration is low. However, when local environmental conditions deteriorate, species intrinsic motive to disperse in search of a better habitat increases and emigration rate increases. For plants, life history strategies are more complex and we assumed an additional scenario. For example, there are also plant species that disperse from their local habitat when they are doing well, i.e. they have a high net growth rate and they allocate more resources for reproduction, leading to higher seed formation and seed dispersal (Miyazaki et al., 2009). As for animal species, there are also examples where plants tend to disperse largely when they are in a poor state and reallocate resources to reproduction (Macedo, 2012), we assume both scenarios (see Figure C1).

Figure C1 shows exemplarily how the dispersal rate (Eq. 4.5) is changing depending on the net growth rate of a species for plant and animal species:

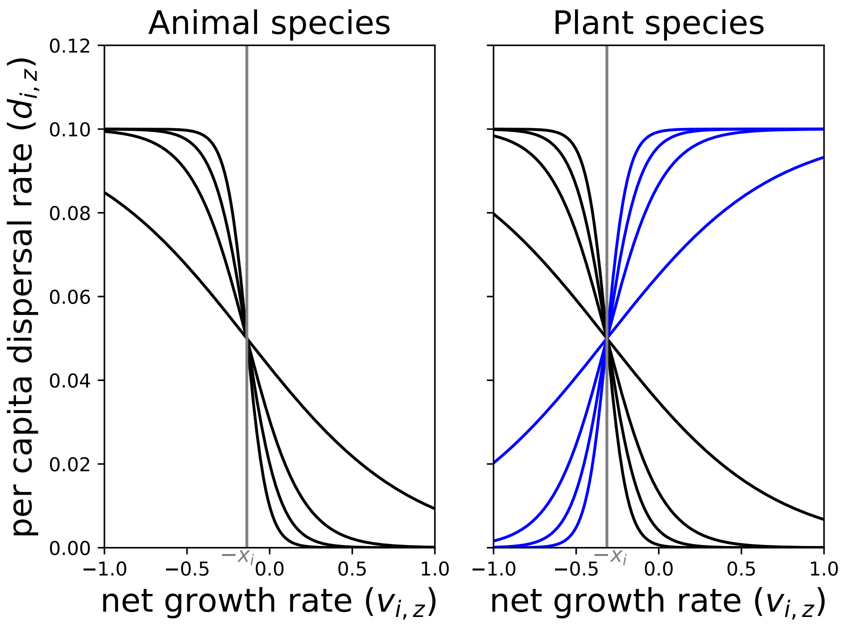

FIGURE C1: Emigration function (see Eq. 4.6 in main manuscript) for animal and plant species, with selected values for the shape b, a fixed maximum emigration rate a and x_i the metabolic demands defining the point of inflection. The black color shows examples of a positive value for b and the blue color a negative value.

Data analysis

GAM- Generalized additive model Generalized additive models are a statistical model approach that uses smooth functions $f(x)$ of input variables to fit an output y. The advantage of the statistical approach is that they capture nonlinear relationships (in contrast to a linear model) and can also account for multiple input variables. The model uses a general form of

$$y = \beta_0 + \sum_p f_p(x_p) \tag{C.4}$$

with y_i the additive function, x_p the different input variables used for the model and the constant factor β_0. For implementation, we used the mgcv package in R (Wood, 2011) and selected a Gaussian model with the use of five basis functions (k=5) and penalized splines for predictions of $\bar{\alpha}$-diversity and six basis functions (k=6) for predictions of β-diversity. The number of basis functions determines how many functions are used in the fitting process. For verification of the goodness and reliability of the fit we compared the resulting pseudo-R^2 with the OOB score of the RF model (see Table C2).

To select predictor variables for the full model and best model we used the following stepwise selection procedure based on the full dataset. To avoid confounding effects between the input variables we first checked the correlation (cor) between predictor variables and selected between those below a threshold of cor < 0.75. This selection provides the basic set of predictor variables for the full model with 11 predictor variables. In a next step, we used the GAM model to select the predictors that are significant for $\bar{\alpha}$- and β-diversity (p-value < 0.05), respectively. A final selection is done based on the lowest AIC value for the GAM, giving our best model.

RF- Random forest Random forest models are a machine learning approach commonly applied for data analysis (Ref) with the advantage of a simple model structure and high versatility. The model utilizes multiple regression trees to make an aggregated prediction for an output variable across the trees. Each tree consist of multiple nodes where each node corresponds to a decision for the strongest associated predictor variable based on a randomly chosen subset of the full data set.

We used the random forest model to (1.) compare the best model fit with the least number of predictor variables and the full model fit for $\bar{\alpha}$-diversity and β-diversity via relative importances and out-of-bag predictions (OOB), and (2.) to visualize the partial effects of each predictor variable on the diversity.

1. The out-of-bag prediction is an error estimation calculated from the remaining data set not used in the subset for the calculation of the tree. The accuracy is

   $$OOB = 1 - \frac{MSE}{\sigma_y}\,, \tag{C.5}$$

   with σ_y as the variance of the output variable y and MSE the mean squared error of the OOB predictions comparing the mean prediction y of OOB and the true value. Thus it can be interpreted as a measure of a pseudo R^2 with an upper bound of 1, where in this case (pseudo $R^2 = 1$) the model predicts a perfect model outcome.

   Derived from these error estimation, we can also evaluate the importance for each variable we used for predicting the output value y. It is quantified by permuting the predictor value across all trees used in the random forest model and quantifying its change in accuracy. If the accuracy of a predictor variable changes to a larger extent, this indicates that the corresponding predictor is more important for model prediction. Based on the relative importances, a low correlation between predictors and the AIC of the GAM model, the best model with the least necessary parameters and a large OOB-score was chosen.

   The random forest model was implemented in Python through the Scikit-learn library (Pedregosa et al., 2011). For each variable, the random forest model was trained with 2500 tress.

2. The partial effects of each input predictor on the output variable can be visualized in a partial dependence plot. Through the training data set we obtained a RF model prediction, our target function, and plot the trends for the different predictor variables of interest. Each prediction g for an input predictor variable x_i with j numbers of input variables can be defined as follows:

   $$g(x_j) = \frac{1}{n} \sum_{m=1}^{n} g(x_{m,1}), ..., f(x_{m,j}))\,, \tag{C.6}$$

   with m data points for each variable j (Hastie et al., 2009). We take the median value of n predictions, calculated by the RF model, for each data point to derive the trend line. In addition we calculate a confidence interval (99 %) from the mean and standard deviation $\frac{3 \cdot \sigma}{s}$ for the sample size s.

Other output variables For comparison of the random forest models we used a so called full model, which we compared to the best model fit. In this full model we used 11 predictor variables, predictors 1-6 are described in the main manuscript (Table 4.2) and predictors 7-11 are described in Table C1. Each predictor is standardized between 0 and 1 to avoid scaling problems. The calculations of the regional predictors: transitivity and mean closeness centrality were calculated through the python package networkx (Hagberg et al., 2008).

Calculation of robustness For the calculation of the robustness we used an additional set of simulations. The robustness of the food webs was calculated for each food web separately by assuming two extreme scenarios on a single habitat patch. In the first scenario we ignored dispersal and evaluated the resulting species richness depending only on local food web dynamics. In the second scenario we accounted for dispersal, but emigrating biomass was completely lost to the matrix. For each scenario we simulated 20 replicates and took the mean of both scenario as measure for the robustness (mean species richness) of a single food web. The standard deviation of the robustness is the parameter R_{SD} (Table 4.2 in the main manuscript) used in the model.

TABLE C1: Other output variables (predictors 7-11) with ecological interpretation used in the full model

Parameter	Description and interpretation of output variables	Definition
	Local predictors	
μ_q, σ_q	mean and standard deviation of **Hill coefficient** - the coefficient in the functional response term (see Eq. 4.5 in manuscript) that determines whether the shape of the response is more like a functional type II or type III response. We assumed a normal distribution with a lower and upper bound of 1 and 2, respectively. The Hill coefficient reveals different strategies where type III indicates more selective feeding response and type II a more generalist feeding response and contributes to stabilize dynamics for a low coefficient.	1.5, 0.2
	Regional predictors	
a	**Maximum emigration rate of plant and animal species** given by mean and standard deviation from a normal distribution. The larger the emigration rate on a habitat patch, the larger the potential biomass loss through dispersal. Thus it can be an estimator for the potential amount of mean dispersal loss. Parameter range is defined in the methods of the main manuscript.	μ_a,σ_a
Θ	**Transitivity** - The relative number of triangles in the graph, compared to total number of connected triples of nodes present in the RGG, where patches are the nodes and dispersal connections correspond to the edges. It is a measure for the relative frequency of triangles and is closely related to the clustering coefficient, a measure to what extent habitat clustering occurs in the landscape or not.	$\frac{3\,x \text{ number of triangles}}{\text{number of connected triples of nodes}}$
Δ_{mc}	**Mean closeness centrality** - the centrality of a patch n is the reciprocal of the average shortest path distance ($\delta_{v,n}$) to n over all z-1 reachable patches. Thus it gives us a measure how central on average patches are in the landscape.	$\frac{z-1}{\sum_{v=1}^{z-1} \delta_{v,n}}$

Results

We replicated the results of Ryser et al. (2019), which qualitatively show the same results of diversity patterns. An increase of mean patch isolation led to an decrease in $\overline{\alpha}$-diversity (local species richness), an increase in β-diversity (compositional differences between the local communities), and no significant trend in γ-diversity (diversity of metacommunity) for the selected range of mean patch isolation (Figure C2).

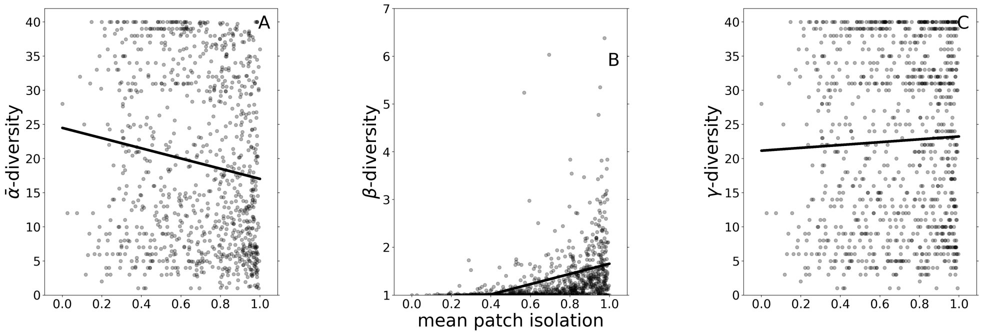

FIGURE C2: The full dataset showing $\overline{\alpha}$-, β- and γ-diversity in response to a changing mean patch isolation of the landscapes. The trend line is a linear fit of the data.

TABLE C2: Overview of model results for random forest approach in comparison to generalized additive model (GAM).

Model	**pseudo R^2 (GAM)**	**OOB (Random Forest)**
local $\bar{\alpha}$-diversity - full data set, best model - five predictors	0.89	0.89
local $\bar{\alpha}$-diversity - full data set, all - eleven predictors	0.89	0.90
local $\bar{\alpha}$-diversity - subset - five predictors	0.93	0.99
β-diversity - full data set, best model - four predictors	0.27	0.496
β-diversity - full data set, all - eleven predictors	0.27	0.52
β-diversity - subset - four predictors	0.49	0.84

A comparison of the generalized additive model approach, and the random forest approach shows very congruent results for local $\bar{\alpha}$-diversity while the explained variance for β-diversity in the random forest approach almost doubles for each selected model compared to the GAM (see Table C2).

When comparing the trends between the two model approaches (RF vs. GAM), they show qualitatively the same shape. Minor differences can nevertheless be identified. Especially when there is a lower amount of data points available or towards the end of an axis, the GAM model has problems with the fit (see e.g. Figure C4 C,D & C5 C). However, this probably does not completely explain the large differences in the explained variance between the approaches.

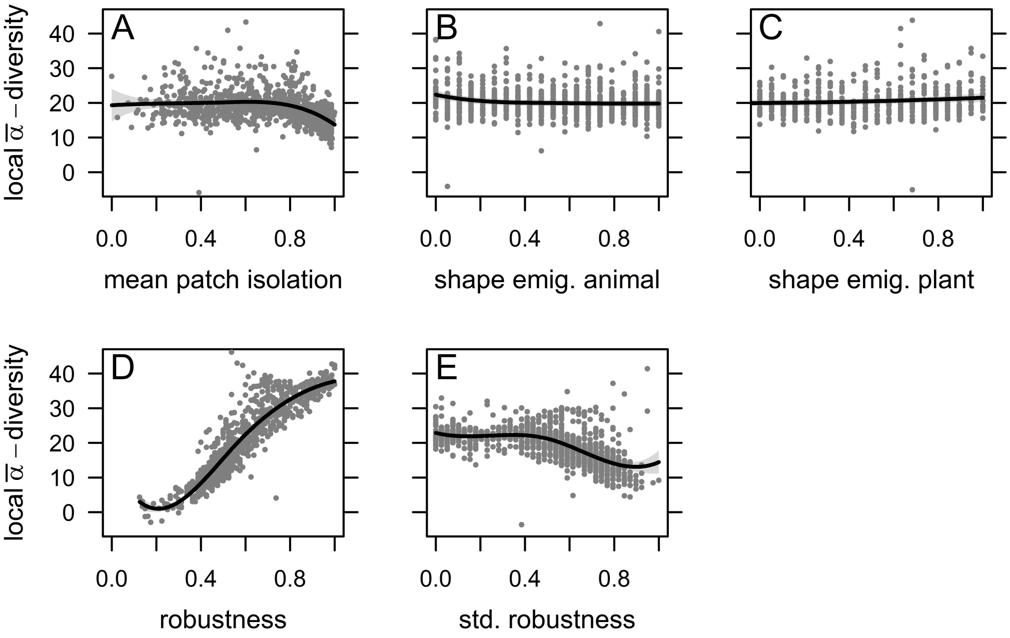

FIGURE C3: Model predictions of generalized additive model for $\overline{\alpha}$-diversity and five selected predictors. Two local predictors are the robustness (d.f.: 4, p-value: $< 2 \cdot 10^{-16}$) and variance of robustness (d.f.: 4, p-value: $< 2 \cdot 10^{-16}$) as well as three regional predictors, the mean patch isolation (d.f.: 4, p-value: $< 2 \cdot 10^{-16}$), shape of emigration function for basal (d.f.: 3.8, p-value: 0.019) and for plant species (d.f.: 4, p-value: 0.00011).

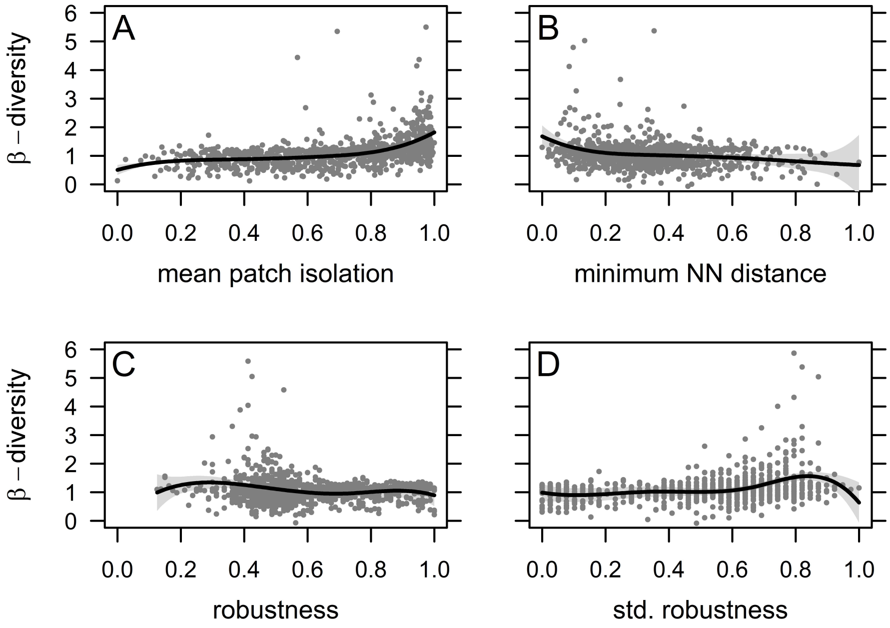

FIGURE C4: Best model predictions of generalized additive model for β-diversity for four selected predictors. Two regional predictors, the mean patch isolation (d.f.: 5, p-value: $< 2 \cdot 10^{-16}$) and minimum nearest neighbor distance (d.f.: 5, p-value: $1.86 \cdot 10^{-6}$) as well as two local predictors, the robustness (d.f.: 5, p-value: 0.0006) and standard deviation of robustness (d.f.: 5, p-value: $2.5 \cdot 10^{-10}$).

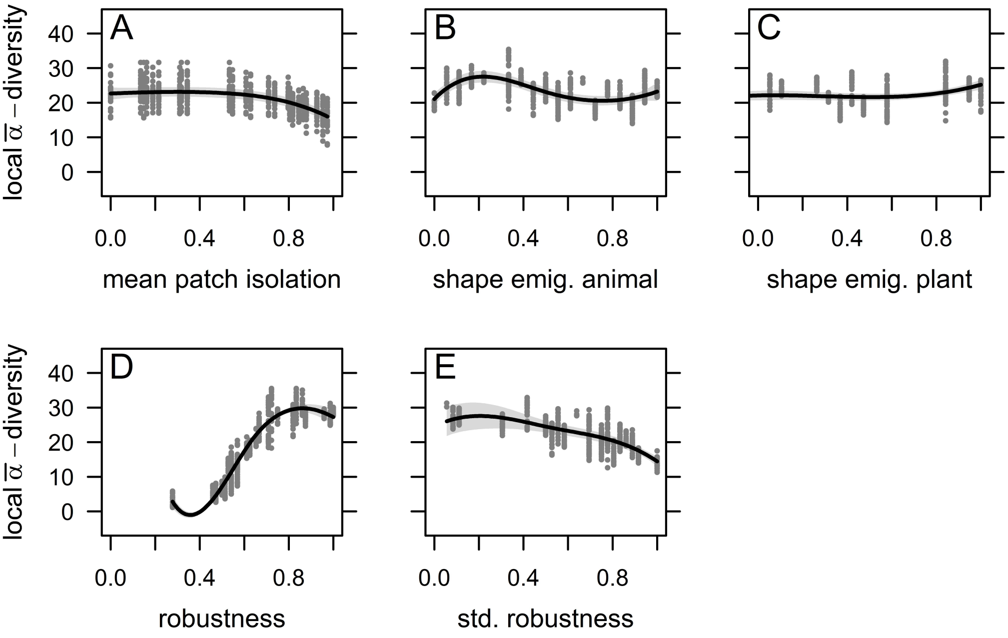

FIGURE C5: Model predictions of generalized additive model for $\overline{\alpha}$-diversity and five selected predictors of the subset. The two local predictors are the robustness (d.f.: 4, p-value: $< 2 \cdot 10^{-16}$) and variance of robustness (d.f.: 4, p-value: $< 2 \cdot 10^{-16}$) as well as three regional predictors, the mean patch isolation (d.f.: 4, p-value: $< 2 \cdot 10^{-16}$), the shape of emigration function for plant (d.f.: 4, p-value: $< 8.3 \cdot 10^{-15}$) and for animal species (d.f.: 4, p-value: $< 2 \cdot 10^{-16}$).

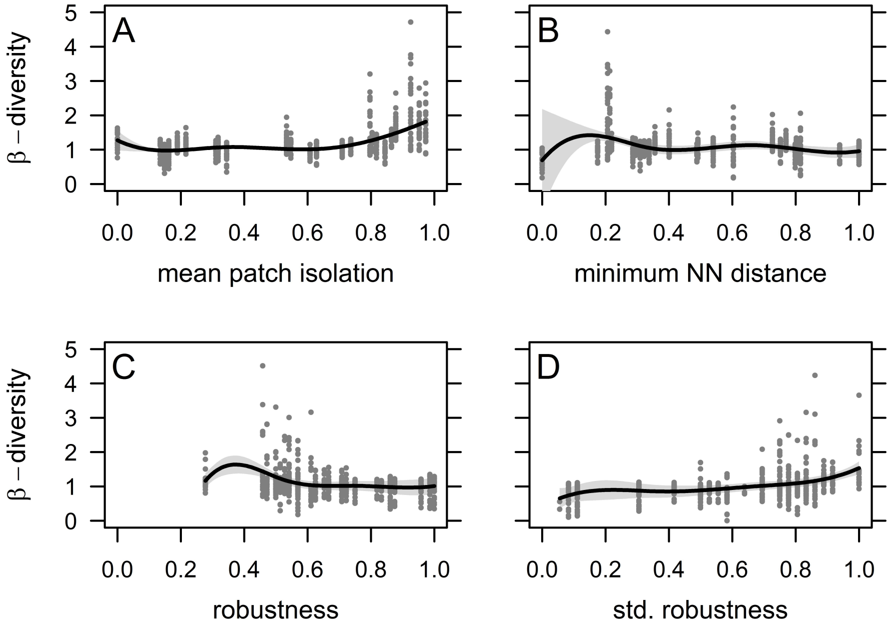

FIGURE C6: Subset model predictions of generalized additive model for β-diversity and four selected predictors. Two are regional predictors, the mean patch isolation (d.f.: 5, p-value: $< 2 \cdot 10^{-16}$) and minimum nearest neighbor distance (d.f.: 5, p-value: $< 9.8 \cdot 10^{-12}$) as well as two local predictors, the robustness (d.f.: 5, p-value: $3 \cdot 10^{-7}$) and standard deviation of robustness (d.f.: 5, p-value: $3.2 \cdot 10^{-9}$).

TABLE C3: Results for linear colinearity between the 11 predictors used in the model all and the clustering coefficient. The predictors are, the robustness, standard deviation of robustness, Hill coefficient, mean patch isolation, shape of emigration function for animal and plant species, minimum nearest neighbor distance, maximum emigration rate for animal and plant species, transitivity, mean closeness centrality and mean clustering coefficient.

predictors	**pred. 1**	**pred. 2**	**pred. 3**	**pred. 4**	**pred. 5**	**pred. 6**	**pred. 7**	**pred. 8**	**pred. 9**	**pred. 10**	**pred. 11**	**cluster. coeff.**
robustness (1)	1	-0.709	0.090	-0.028	0.069	-0.057	0.014	-0.104	-0.062	0.050	-0.045	0.046
std. robustness (2)	-0.709	1	-0.017	0.0135	-0.138	0.112	-0.001	0.153	0.099	-0.024	0.031	-0.022
Hill coefficient (3)	0.090	-0.017	1	0.014	0.004	-0.028	-0.024	0.005	0.034	0.044	0.003	0.029
mean patch isolation (4)	-0.028	0.013	0.014	1	-0.001	0.019	-0.001	-0.009	-0.014	-0.416	0.870	-0.854
shape emig. animal (5)	0.069	-0.138	0.004	-0.001	1	-0.028	0.068	0.011	-0.014	-0.027	-0.009	0.004
shape emig. plant (6)	-0.057	0.112	-0.028	0.019	-0.028	1	0.055	0.011	-0.035	-0.082	0.032	-0.033
minimum NN distance (7)	0.014	-0.001	0.024	-0.001	0.068	0.055	1	0.028	-0.036	-0.148	-0.002	-0.053
max. emig. rate animal (8)	-0.104	0.153	0.005	-0.008	0.011	0.011	0.029	1	0.015	0.005	-0.003	-0.001
max. emig. rate plant (9)	-0.062	0.099	0.034	-0.014	-0.014	-0.035	-0.036	0.015	1	0.013	-0.013	0.002
transitivity (10)	0.051	-0.024	0.044	-0.416	-0.027	-0.082	-0.148	0.005	0.012	1	-0.467	0.600
mean closeness centrality (11)	-0.045	0.031	0.003	0.870	-0.009	0.032	-0.002	-0.003	-0.013	-0.467	1	-0.924
clustering coefficient	0.046	-0.022	0.029	-0.854	0.004	-0.034	-0.053	-0.001	0.002	0.600	-0.924	1

Bibliography

A. A. Hagberg, D. A. Schult, and P. J. Swart. Exploring network structure, dynamics, and function using networkx. In G. Varoquaux, T. Vaught, and J. Millman, editors, *Proceedings of the 7th Python in Science Conference*, pages 11 – 15, Pasadena, CA USA, 2008.

T. Hastie, R. Tibshirani, and J. Friedman. *The Elements of Statistical Learning: Data Mining, Inference, and Prediction.* Springer-Verlag New York, 2009. doi: 10.1007/978-0-387-84858-7.

M. R. Hirt, W. Jetz, B. C. Rall, and U. Brose. A general scaling law reveals why the largest animals are not the fastest. *Nat Ecol Evol*, 1:1116–1122, 2017. doi: 10.1038/s41559-017-0241-4.

A. F. Macedo. Abiotic stress responses in plants: Metabolism to productivity. In P. Ahmad and M. Prasad, editors, *Abiotic Stress Response in Plants*, pages 41–61. Springer, New York, NY, 2012. doi: 10.1007/978-1-4614-0634-1.

Y. Miyazaki, T. Osawa, and Y. Waguchi. Resource level as a proximate factor influencing fluctuations in male flower production in cryptomeria japonica d. don. *J For Res*, 14(6):358–364, 2009. doi: 10.1007/s10310-009-0148-2.

F. Pedregosa, G. Varoquaux, A. Gramfort, V. Michel, B. Thirion, O. Grisel, M. Blondel, P. Prettenhofer, R. Weiss, V. Dubourg, J. Vanderplas, A. Passos, D. Cournapeau, M. Brucher, M. Perrot, and E. Duchesnay. Scikit-learn: Machine learning in python. *J Mach Learn Res*, 12(null):2825–2830, Nov. 2011. ISSN 1532-4435.

J. O. Riede, U. Brose, B. Ebenman, U. Jacob, R. Thompson, C. R. Townsend, and T. Jonsson. Stepping in elton's footprints: a general scaling model for body masses and trophic levels across ecosystems. *Ecol Lett*, 14(2):169–178, 2011. doi: doi.org/10.1111/j.1461-0248.2010.01568.x.

R. Ryser, J. Häussler, M. Stark, U. Brose, B. C. Rall, and C. Guill. The biggest losers: habitat isolation deconstructs complex food webs from top to bottom. *Proc R Soc B Biol Sci*, 286(1908):20191177, 2019. doi: 10.1098/rspb.2019.1177.

F. D. Schneider, U. Brose, B. C. Rall, and C. Guill. Animal diversity and ecosystem functioning in dynamic food webs. *Nat Commun*, 7(12718), 2016. doi: 10.1038/ncomms12718.

R. J. Williams and N. D. Martinez. Simple rules yield complex food webs. *Nature*, 404 (6774):180 – 183, 3 2000. doi: 10.1038/35004572.

S. N. Wood. Fast stable restricted maximum likelihood and marginal likelihood estimation of semiparametric generalized linear models. *J R Stat Soc (B)*, 73(1):3–36, 2011.

Declaration of Authorship

I, Markus STARK , declare that this thesis titled, “Implications of local and regional processes on the stability of metacommunities
in diverse ecosystems” and the work presented in it are my own. I confirm that:

- This work was done wholly or mainly while in candidature for a research degree at this University.
- Where any part of this thesis has previously been submitted for a degree or any other qualification at this University or any other institution, this has been clearly stated.
- Where I have consulted the published work of others, this is always clearly attributed.
- Where I have quoted from the work of others, the source is always given. With the exception of such quotations, this thesis is entirely my own work.
- I have acknowledged all main sources of help.
- Where the thesis is based on work done by myself jointly with others, I have made clear exactly what was done by others and what I have contributed myself.

Signed:

Date: